الجـــــــــــــــــــــــمهـوريـــــــة الجـــــــــــــــزائـريـة الديمـــــــقـراطيـة الشـــــــــعبيـة

DEMOCRATIC AND POPULAR REPUBLIC OF ALGERIA.

وزارة التـــــــــــــــــــــــــــــعليـم العـــــــالي و البـــــــــــحث العـــــلـمـــي

Ministry of Higher Education and Scientific Research.

جـــــــــــــــامعة أبي بكـــر بـلـقـايد – تـلمســـــــــــــــان –

University of Abou Bekr Belkaid – Tlemcen –

Faculty of TECHNOLOGY

THESE

Presented for the attainment of the **Doctorate** Degree, **3rd Cycle**.

In: Mechanical Engineering.

Specialization: Energetics.

By : HACHEMI Houssem

Topic

Valorization of Sig diatomite for thermal insulation in buildings.

Publicly defended on 09/06/2024, in front of the jury composed of:

M. Rachid SAIM	Pr.	Univ. Tlemcen	President
M. Chakib SELADJI	Pr.	Univ. Tlemcen	Thesis supervisor
M. Abdel Illah Nabil KORTI	Pr.	Univ. Tlemcen	Examine 1
M. Ahmed Soufiane BENOSMAN	Pr.	ESSAT	Examine 3
M. Hocine GUELLIL	MCA	Univ. Tlemcen	Examine 2

Academic year: 2023-2024

Dedication

I dedicate this work

To the man of my life, my eternal role model, my moral support, a source of joy and happiness, the one who has always sacrificed himself to see me succeed. May God bless and keep you for me, My Father.

In the light of my days, the source of my efforts, and the flame in my heart, my life and my happiness: my beloved mother.

To my brothers Yacine, Mounir, and Nadir, as well as to my sisters in life: Wissam Latrache, Chems Houda Rabhi, Sabrina Taieb Bouderbal, and my fiancee Nasima Bensaber.

To all the people who have always helped and encouraged me, who have always been by my side and accompanied me during my higher education studies, to my dear friends, my fellow students: Ilyes Boucheta, Sid Ahmed Belkadi, Ilyes Marouf, Ilyes Helhouli, Houssem Saim Mamoune, AbdelHadi Haddouche, and Reda, Bilal Benotman, Chakib Malti, Abd Elghani Jdid, Zakaria Bouhamama, and Mohamed, Amrani nassim and mostafa.

Furthermore, to all the members of the Hachemi and Benotmane families.

Thanks

This work was carried out at the laboratory of Energy and Thermal Applied (ETAP) of the University of Tlemcen.

Firstly, I would like to thank the Almighty God, who has helped us and given us patience and courage during these long years of study.

I would like to express my heartfelt gratitude to Mr. Chakib Seladji, a professor at the University of Tlemcen, who supervised this thesis. Thank you for encouraging and guiding me throughout these years. I also thank him for his availability at all times, as well as for his indispensable advice. I would also like to express my sincere thanks to all my professors in the Mechanical Engineering Department.

I express my gratitude to all the members of the jury, M. Rachid Saim, M. GUELLIL Hocine ,M. KORTI Abdel Illah Nabil, professors at the University of Tlemcen, and M. BENOSMAN Ahmed Soufiane, a professor at the Higher School of Sciences Applied Sciences (ESSAT), for agreeing to examine this work and providing the necessary feedback for the final formatting of this thesis.

I would also like to thank Mr. Houti Farid Ibrahim, a teacher in the Civil Engineering Department, as well as Mr. Fraine Youssef, my former master's co-director.

I also want to express my deep gratitude to my parents for their invaluable sacrifice and support during all my studies.

Finally, my thanks also go to all my friends and colleagues at the ETAP laboratory, as well as to all those who helped, directly or indirectly, in the realization of this modest work.

Abstract

Phase change materials (PCMs) combined with hygroscopic materials are considered an appropriate solution for improving the indoor environment of building envelopes in the construction sector, by providing a technique for storing heat or cold during environmental changes. In this thesis, a phase change humidity control material (PCHCM) derived from diatomite extracted from the Sig mine located in northwestern Algeria was used as a final coating in buildings to experimentally analyze its performance using a dedicated thermal chamber. The experiment involved exposing three hollow refractory brick walls with different insulating coatings (mortar, Algerian diatomite, and PCHCM) to specific temperatures and humidity levels. A wall is placed in the thermal chamber dividing it into two compartments: in the first, temperature and humidity is controlled by a ZL-7918A control unit; in the second, a TESTO890 infrared camera measures temperature and humidity fluctuations on the wall surface, while the ZL-7918A control unit measures these fluctuations in the compartment every 30 minutes according to the experimental operating conditions. After the experiment, two sets of experimental results were distinguished based on operating conditions: the PCHCM showed better performance at a constant temperature equal to or higher than the PCM's melting point, while diatomite alone showed more significant results at a temperature below the PCM's melting point. An in-depth study was conducted to evaluate the performance of effective composite phase change heat storage materials (PCHCM) in thermal insulation applications. In addition to experimental analysis, numerical analysis was used to illustrate the results more accurately, showing good agreement between experimental results and numerical analysis, and highlighting the accuracy of the methods used and the validity of the conclusions drawn. Special attention was paid to the impact of PCHCM material quality on their performance in thermal insulation applications, by analyzing two types of PCHCM: the first containing a PCM with a melting point of 28°C, and the second composed of two PCMs with different melting points (28°C and 22°C). The results showed that using the second type of PCHCM further improves temperatures and humidity on the inner face of the wall compared to the first type, indicating the additional benefits of using multiple PCM compositions in thermal insulation applications, thus contributing to improving energy efficiency and environmental comfort in various buildings and structures.

Keywords

Porous medium; Coupled heat and moisture transfer; Diatomite; PCHCM; Mortar.

ملخص

تعتبر المواد المتغيرة الطور (PCM) المدمجة مع المواد الاسترطابية حلاً مناسباً لتحسين البيئة الداخلية لغلاف المبنى في مجال البناء، حيث توفر تقنية تخزين الحرارة أو البرودة خلال التغيرات البيئية. في هذه الأطروحة، تم استخدام مادة تحكم بالرطوبة متغيرة الطور (PCHCM) المشتقة من الدياتومايت المستخرج من منجم سيق الواقع في شمال غرب الجزائر كطبقات نهائية في المباني بهدف تحليل أدائها تجريبياً من خلال غرفة حرارية مخصصة. تضمنت التجربة تعريض ثلاثة جدران مكونة من الطوب المجوف الملبد بطبقات عزل مختلفة (الملاط، دياتومايت الجزائر، وPCHCM) لدرجات حرارة ورطوبة محددة. عند وضع جدار داخل الغرفة الحرارية تنقسم هذه الغرفة إلى حجرتين: الأولى تم التحكم في درجات الحرارة والرطوبة بواسطة وحدة التحكم ZL-7918A، والثانية استخدمت كاميرا الأشعة تحت الحمراء TESTO890 لقياس تقلبات درجة الحرارة والرطوبة على سطح الجدار، بالإضافة إلى وحدة التحكم ZL-7918A لقياس تقلبات درجة الحرارة والرطوبة في الحجرة كل 30 دقيقة وفقاً لظروف التشغيل التجريبية. بعد إتمام التجربة، تم تمييز مجموعتين من النتائج التجريبية استنادًا إلى ظروف التشغيل، حيث أظهرت المادة PCHCM أداءً أفضل عند درجة حرارة ثابتة تعادل أو تزيد عن درجة انصهار PCM، في حين أظهر الدياتوميت وحده نتائج أكثر أهمية عند درجة حرارة أقل من درجة انصهار PCM. تم إجراء دراسة متعمقة لتقييم أداء مواد تخزين الحرارة ذات التغيُّر المركب الفعال (PCHCM) في تطبيقات العزل الحراري، بالإضافة إلى التحليل التجريبي، فقد تم استخدام التحليل العددي لتوضيح النتائج بدقة أكبر، وأظهرت النتائج توافقًا جيدًا بين النتائج التجريبية والتحليل العددي مما يبرز دقة الأساليب المستخدمة وصحة الاستنتاجات المستندة إليها. تم توجيه اهتمام إضافي نحو تأثير نوعية مواد PCHCM على أدائها في تطبيقات العزل الحراري، حيث تم تحليل نوعين من PCHCM: الأول يحتوي على PCM واحد بدرجة انصهار C°28، بينما الثاني يتألف من اثنين من PCMs بدرجات انصهار مختلفة (C°28 وC°22). أظهرت النتائج أن استخدام النوع الثاني من PCHCM يؤدي إلى تحسين درجات الحرارة والرطوبة على الجانب الداخلي من الجدار بشكل أفضل مقارنة بالنوع الأول، مما يشير إلى الفوائد الإضافية لاستخدام تركيبات متعددة PCM في تطبيقات العزل الحراري، ويمكن أن يساهم في تحسين كفاءة الطاقة وراحة البيئة في المباني والهياكل المختلفة.

الكلمات مفتاحية

وسط مسامي ؛ انتقال الحرارة والرطوبة المقترن؛ الدياتوميت؛PCHCM؛ الملاط.

Résumé

Les matériaux à changement de phase (PCM) combinés avec des matériaux hygroscopiques sont considérés comme une solution appropriée pour améliorer l'environnement intérieur de l'enveloppe du bâtiment dans le domaine de la construction, en fournissant une technique de stockage de chaleur ou de froid pendant les variations environnementales. Dans cette thèse, un matériau de contrôle de l'humidité à changement de phase (PCHCM) dérivé de diatomite extraite de la mine de Sig située au nord-ouest de l'Algérie a été utilisé comme revêtement final dans les bâtiments afin d'analyser ses performances expérimentalement à l'aide d'une chambre thermique dédiée. L'expérience a consisté à exposer trois murs en briques creuses réfractaires avec différents revêtements isolants (mortier, diatomite algérienne, et PCHCM) à des températures et humidités spécifiques. Lorsqu'un mur était placé dans la chambre thermique, celle-ci était divisée en deux compartiments : dans le premier, la température et l'humidité étaient contrôlées par une unité de contrôle ZL-7918A ; dans le second, une caméra infrarouge TESTO890 mesurait les fluctuations de température et d'humidité à la surface du mur, tandis que l'unité de contrôle ZL-7918A mesurait ces fluctuations dans le compartiment toutes les 30 minutes selon les conditions d'exploitation expérimentales. Après l'expérience, deux ensembles de résultats expérimentaux ont été distingués en fonction des conditions d'exploitation : le PCHCM a montré une meilleure performance à une température constante égale ou supérieure au point de fusion du PCM, tandis que la diatomite seule a donné des résultats plus significatifs à une température inférieure au point de fusion du PCM. Une étude approfondie a été menée pour évaluer les performances des matériaux de stockage de chaleur à changement de phase composite efficace (PCHCM) dans les applications d'isolation thermique. En plus de l'analyse expérimentale, une analyse numérique a été utilisée pour illustrer les résultats avec plus de précision, montrant une bonne concordance entre les résultats expérimentaux et l'analyse numérique, soulignant la précision des méthodes utilisées et la validité des conclusions en découlant. Une attention particulière a été portée à l'impact de la qualité des matériaux PCHCM sur leurs performances dans les applications d'isolation thermique, en analysant deux types de PCHCM : le premier contenant un PCM avec un point de fusion à 28°C, et le second composé de deux PCMs avec des points de fusion différents (28°C et 22°C). Les résultats ont montré que l'utilisation du second type de PCHCM améliore davantage les températures et l'humidité sur la face intérieure du mur comparativement au premier type, indiquant les avantages supplémentaires de l'utilisation de compositions PCM multiples dans les applications d'isolation thermique, pouvant ainsi contribuer à améliorer l'efficacité énergétique et le confort environnemental des bâtiments et structures divers.

Mots clés

Milieu poreux ; Transfert couplé de chaleur et d'humidité; diatomite; PCHCM ; Mortier

Table of contents

List of Figures

List of tables

Nomenclature

Acronyms		
EPS	Expanded polystyrene	
HBCD	Hexabromocyclododecane	
POP	Persistent Organic Pollutant	
PCHCM	Phase Change Humidity Control Material	
PCM	Phase Change Materials	
HVAC	Heating, Ventilation, Air conditioning	
HCM	Humidity control materials	
PCMM	Phase Change Material Microcapsules	
PEG	Polyethylene Glycol	
APREU	Agency for the Promotion and Rationalization of Energy Use	
NEEP	National Energy Efficiency Program	
REDC	Renewable Energy Development Center	
Toe	Ton of Oil Equivalent	
M-Toe	Miga- Ton of Oil Equivalent	
LPG	Liquefied Petroleum Gas	
ASHARE	American Society of Heating, Refrigerating and Air Conditioning Engineers	
PMV	Predicted Mean Vote	
PPD	Predicted Percentage Dissatisfied	
FS IOS	French Standard, International Organization for Standardization	
FS ES	French standard, European standard	
BET	Brunauer, Emmett and Teller	
GAB	Guggenhein-Anderson-de Boer	
EPSF	Expanded Polystyrene Foam	
EXPF	Extruded Polystyrene Foam	
REV	Representative Elementary Volume	
WUFI	Wärme und Feuchte Instationär	
IBP	Institut Bauphysik	
FSPCM	Form Stabilized Phase Change Materials	
HPCM	Hygroscopic Phase Change Materials	
TES	Thermal Energy Storage	
ALA	Artificial Lightweight Aggregates	
SM	Support material	
EG	Expanded Graphite	
xGnP	Exfoliated Graphite Nano Platelets	
SDC	Scanning Differential Calorimetry	
SEM	Scanning Electron Microscope	
PW	Paraffin Wax Blend	
LP	Liquid Paraffin	
PDE	Partial Differential Equation	
FEM	Finite element method	
TGA	Thermogravimetric analysis	
FTIS	Fourier Transform Infrared Spectroscopy	
HAM	Heat, Air and Moisture	
HAMSTAD	Heat, Air and Moisture Standards Development	
T_ext,	Outside air temperature	°C
T_int,	Interior air temperature	°C
RFCHT	Reduced Total Heat Flow	
Greek letters		
Φ	Relative humidity	%

Γ	surface tension of water	N/m
P	Density	kg/m^3
Θ	Contact angle	°
∂	Area portion	
M	Water vapor resistance factor	-
T	Water adsorption rate (constant)	
δ_v	Water vapor diffusion coefficient in porous materials	m^2/s
δ_p	Water vapor permeability	$kg/(Pa{\cdot}m{\cdot}s)$
H	Viscosity	$\mathrm{kg}/(\mathrm{m}{\cdot}\mathrm{s})$
Λ	Thermal conductivity	$W/(m{\cdot}K)$
λ_0	Thermal conductivity of dry building material	$W/(m.K)$
ϵ	Report	–
δ_s	Thermal diffusion coefficient	–
λ_h	Hydraulic conductivity of the material	$kg/(m{\cdot}s{\cdot}Pa)$
Σ	Boltzmann constant	$W/(m^2{\cdot}K^4)$
ε	Material emissivity	–
$\frac{\partial\omega}{\partial\varphi}$	Slope of the adsorption isotherm curve	–
ω	moisture content	kg/m^3
ω_{sat}	Moisture content at saturation	kg/m^3
ω_{cr}	Critical moisture content	kg/m^3
δ	Water vapor diffusion coefficient in the air	$kg/(m.s.Pa)$
ξ	Moisture storage capacity	kg/m^3
ρ_s	Bulk density of dry building material	kg/m^3
θ_d	Volume fraction of diatomite	–
ρ_l	Density of pure water	kg/m^3
κ	Solar absorption coefficient	–
Ψ_j	Basic functions	
β	Mass transfer coefficient	s/m
Latin letters		
t	Time	s
P_v	Vapor pressure	Pa
$P_{v,sat}$	Saturated vapor pressure	Pa
T	Absolute temperature	K
M	the molar mass of water vapor	Kg/mol
u	Mass moisture content	kg/kg
m	Wet sample mass	kg
m_0	Mass of dry sample	kg
V	Sample volume	m^3
u_{cap}	Mass moisture content at capillary saturation	kg/kg
P_c	Capillary pressure	Pa
P	Pression	Pa
r	Capillary ray	m
R	Perfect gas constant	$J/(K{\cdot}\,mol)$
M_ω	Molar mass of water	kg/mol
N_{ads}	Number of additional molecules adsorbed	-
N_{des}	Number of molecules already adsorbed	-
N_m	Number of molecules in a complete layer	-
p_1	Probability of a bound molecule hitting the surface	-
p_2	Probability of an adsorbed molecule	-
q_{ad}	Amount of water adsorbed	kg/m^3
c	Constant	-
A	Constant	-

Q_{cd}	Condensed heat	kJ
Q_{ad}	Heat adsorbed from the first layer	kJ
F	Correction factor	-
Q_T	Total adsorbent heat	kJ
g_a	Density of vapor transported	$kg/(m^2 \cdot s)$
D_a	Water vapor diffusion coefficient in stagnant air	m^2/s
v	Volumetric moisture content	m^3/m^3
P_0	Standard atmospheric pressure	Pa
R_v	Water vapor gas constant	$J/(kg \cdot K)$
$g_{T,V}$	Non-isothermal vapor density	$kg/(m^2 \cdot s)$
$D_{T,V}$	Non-isothermal vapor diffusion coefficient	$kg/(K \cdot m \cdot s)$
g_v	Water vapor flux density	$kg/(m^2 \cdot s)$
g_l	Flow density of liquid water	$kg/(m^2 \cdot s)$
k_p	Perméabilité	m^2
g_{s-l}	Surface Diffusion Flux Density	$kg/(m^2 \cdot s)$
$D_{s,l}$	Surface diffusion coefficient	m^2/s
D_φ	Liquid conduction coefficient	$kg/(m \cdot s)$
$g_{T,l}$	Thermal Moisture Flux Density	$kg/(m^2 \cdot s)$
$D_{T,l}$	non-isothermal liquid transport coefficient	$kg/(K \cdot m \cdot s)$
D_T	Thermal diffusivity	$kg/(K \cdot m \cdot s)$
D_ω	Moisture diffusivity	m^2/s
Ra_l	Rayleigh number	-
k	Thermal conductivity of air	$W/(m \cdot K)$
g	Total Moisture Flux Density	$kg/(m^2 \cdot s)$
S	Moisture source term	-
H_s	Enthalpy of a dry building material	J
C_p	Specific heat	$J/(kg \cdot K)$
S_h	Heat source due to condensation or evaporation	$J/(s \cdot m^3)$
$h_{l,v}$	Latent heat of phase change	J/kg
D_m	Total diffusion coefficient	m^2/s
l_v	Latent heat of vaporization	J/kg
H	Total material enthalpy	J
S_e	Radiation at the outer surface of the wall	W/m^2
S_{dir}	Direct radiation	W/m^2
S_{dif}	Diffuse radiation	W/m^2
$\dot{m}$	Phase change rate	-
S_i	Radiation at the inner surface of the wall	W/m^2
Q_{conv}	Thermal convective flow	$J/(m^2 \cdot s)$
h_c	Heat convection coefficient	$W/(m^2 \cdot K)$
h_n	Heat transfer coefficient in the chamber.	$W/(m^2 \cdot K)$
H_{conv}	Mass convective flux	$kg/(m^2 \cdot s)$
h_m	Mass exchange coefficient	$kg/(m^2 \cdot s \cdot Pa)$
a_p	Absorptivity coefficient to precipitation.	-
r_s	Driving rain coefficient by specific site	s/m
v	wind speed	m/s
S_ω	Source term	$kg/(m^3 \cdot s)$
S_T	Source term	W/m^3
u_i	Functions	
Indices		
T	Temperature	
m	Massive	
conv	Convectif	

s	dry	
i	Interior	
Dif	Diffusive	
Dir	Direct	
e	Exterior	
l	Liquid	
v	Vapor	
a	Air	
Ad	Absorbed	
Cd	Condensed	
c	Capillary	
sat	Saturation	
d	Diatomite	
eff	Effective	
cr	Critical	
occ	Busy	
des	Desorbed	
surf	Surface	
Int	Interior	
ext	Exterior	

General Introduction

General Introduction

Energy consumption and production significantly impact climate change, as they contribute significantly to the atmospheric CO2 emissions from fossil fuels. This has been acknowledged by the United Nations Framework Convention on Climate Change, which was established during the Rio Conference in 1992, as well as the Kyoto Protocol of 1997. Climate change is now recognized as a critical global challenge. In recent years, there has been a growing emphasis on limiting global warming, with the Paris Agreement at COP 21 in December 2015 representing a major milestone in global climate change negotiations. Mitigation strategies such as energy efficiency and reducing energy demand have been highlighted in numerous reports as essential measures in the fight against climate change [1].

Particularly in developing nations like Algeria, where the construction sector contributes significantly, accounting for over 45% of total energy consumption, the imperative to address energy inefficiency in buildings is urgent [2]. Currently, buildings in Algeria typically fall within the D to E energy efficiency classes, indicating subpar performance with energy consumption exceeding 151 kWh/m² annually for various purposes such as heating, cooling, hot water, and lighting [3,4]. These inefficiencies not only drive up energy usage but also escalate greenhouse gas emissions and environmental degradation. To confront these challenges, Algeria has initiated measures to promote sustainable building practices, notably by banning polystyrene as an insulating material following the ratification of the Stockholm Convention [2]. This prohibition aims to curtail environmental harm and spur the adoption of alternative, eco-friendly insulation materials. The transition towards these alternatives is pivotal for enhancing building energy efficiency and mitigating environmental impact. Among the sustainable alternatives, natural and bio-based materials emerge as promising options, offering superior insulation properties, lower embodied energy, and reduced carbon footprint compared to conventional materials. Recent research has concentrated on innovative alternatives, with phase change materials (PCMs) emerging as a standout solution for regulating indoor temperatures effectively [5,6]. Integrating PCMs within building structures facilitates energy efficiency by absorbing and releasing thermal energy as needed, thereby moderating temperature fluctuations [7-11]. This process aids in preventing overheating during the day and reducing the need for cooling systems, while also providing natural insulation during cooler periods [12]. The integration of PCMs as a thermal regulation strategy presents numerous benefits, including enhanced energy efficiency, improved occupant comfort through stable indoor environments, and decreased reliance on conventional heating and cooling systems, thus reducing greenhouse gas emissions [6].

Furthermore, managing relative humidity is vital for preserving building integrity, ensuring optimal storage conditions, and minimizing energy consumption [13-15]. Humidity control materials (HCM) offer a solution by regulating humidity and temperature without requiring external power or mechanical equipment. Incorporating HCM into construction or strategic locations within buildings enables effective humidity management, thereby safeguarding structural integrity [13,16-18]. Additionally, HCM plays a crucial role in preserving goods by preventing moisture-related damage and spoilage, offering an energy-efficient alternative to traditional methods and reducing associated costs. In summary, HCM presents a holistic solution for humidity control, benefiting building longevity, storage conditions, and overall energy efficiency.

In recent years, several approaches have been explored to enhance the hygrothermal performance of building envelopes by developing passive materials. One such approach involves the integration of porous materials such as PCM and HCM to create new endothermic hygroscopic materials that can regulate both temperature and humidity within indoor environments [2]. Karaman et al. [19] revolutionized thermal energy storage with their development of a stable shape-stabilized Phase Change Material (SSPCM) composite. By blending polyethylene glycol (PEG) with diatomite, they achieved a composite with excellent thermal stability. The key innovation lay in securely retaining PEG within the pores of diatomite matrices, ensuring no leakage even under varying conditions. This breakthrough holds significant promise for applications requiring reliable and long-term thermal energy storage solutions. JL. Shang [20] expanded the application horizon of PCM composites by exploring their potential within porous sepiolite matrices. Through meticulous experimentation with various combinations such as Na_2SO_4, $10H_2O$/sepiolite, paraffin/sepiolite, and dodecanol/sepiolite, Shang uncovered the moisture-regulating gel's remarkable efficacy, especially when augmented with LiCl. The composite exhibited an impressive moisture storage capacity, offering potential solutions for moisture regulation in diverse environments. M. Qin et al. [21] ventured into the realm of Phase Change Moisture Control Materials (PCHCMs), leveraging PCM microcapsules enveloped in SiO_2 shells alongside hygroscopic materials like vésuvianite, sepiolite, and zeolite. Their study yielded valuable insights, with the PCM shell/vésuvianite composite emerging as a standout performer in terms of hygrothermal performance. This finding opens avenues for developing advanced materials capable of efficiently managing both heat and moisture in various applications. Building upon these advancements, Wu et al. [22] and Chen et al. [5] further refined PCM composite technologies. Wu's team developed a PCM/diatomite composite boasting a 12.9% encapsulated PCM rate, highlighting its potential for effective thermal storage. Meanwhile, Chen's research explored the impact of different mass ratios of encapsulated PCM in SiO_2 shell/diatomite composites, emphasizing the crucial role of the shell in reducing supercooling and preventing leaks. These findings lay the foundation for scalable and practical solutions for thermal management and humidity control in

diverse settings. Fraine et al. [2] showcased the versatility of PCM/diatomite composites by integrating them into hollow bricks, effectively remolding their cavities. Their study demonstrated the composite's ability to significantly reduce indoor temperature and relative humidity fluctuations, thereby curbing total heat flux by an impressive 50%. This application holds promise for enhancing the energy efficiency and comfort levels of buildings, ultimately contributing to sustainable and resilient construction practices. Hasan et al. [23] examined incorporating diatomite earth (DE) as a substitute for cement in high-strength concrete formulations. Their study, ranging from 0% to 15% DE replacement levels, assessed surface morphology alterations, mass loss, and degradation of compressive strength at elevated temperatures. Mona and al. [24] employed wollastonite powder to significantly augment the flexural and compressive strengths, as well as the initial setting time and resistance to drying shrinkage in mortar mixes. This innovative approach not only enhanced the mechanical properties of the mortar but also contributed to its durability and performance over time. Ergün [25], the investigation focused on the utilization of diatomite and waste marble powder (WMP) as partial substitutes for cement in concrete. The inclusion of these materials aimed to improve the mechanical properties of the resulting concrete mixes. Through experimentation, it was found that concrete formulations incorporating specific combinations of diatomite and WMP exhibited notable enhancements in compressive and flexural strengths. Specifically, concrete mixes containing 10% diatomite, 5% WMP, and a combination of 5% WMP with 10% diatomite replacements were identified as yielding the highest levels of compressive and flexural strengths. This indicates the potential for optimizing the proportion of these materials to achieve desired performance characteristics in concrete structures. Hamidi et al. [26] conducted a study where they integrated phase change materials (PCM) into the structure of hollow brick walls, aiming to enhance energy efficiency specifically in Mediterranean climates. Their findings emphasized the significant influence of climate on the performance of PCM in storing and releasing energy. In North-East Mediterranean cities, employing a PCM with a melting temperature of 26°C led to notable energy savings of up to 56%. However, in South-East cities, no discernible energy savings were observed. Abbas et al. [27] undertook an experimental and computational exploration focusing on PCM capsules utilized as insulation components within hollow brick walls. Their results showcased that embedding PCM within the wall structure could bring about several benefits. These included a decrease in inner surface wall and room temperatures by approximately 4.7°C, an extension of the time lag by 2 hours, a reduction in temperature fluctuation by 23.84%, and the attainment of a decrement factor of 0.7.

This doctoral work aims to explore the potential of using Algerian diatomite, optimized PCHCM diatomite, and diatomite infused with two different PCMs as substitutes for traditional mortar in order to decrease energy consumption in buildings. The approach involves conducting 3D numerical simulations on brick walls with various finishes, including mortar, diatomite, and PCM/diatomite

combinations. These simulations integrate a coupled model of heat and moisture transfer to accurately represent the behavior of the building envelope. In addition to the numerical simulations, experimental validation is a key aspect of this research. To achieve this, an experimental test bench is developed in the laboratory of the University of Tlemcen. The experimental setup is designed to mimic real-world conditions and allows for the comparison of experimental results with those obtained from the numerical simulations. This manuscript is organized around 4 chapters.

The first chapter provides some information on energy consumption in the Algerian construction sector, the main disturbances caused by moisture in buildings, and the resulting damages. This chapter also introduces some concepts on the properties of porous media to help us understand the phenomenon of heat and moisture transfer in porous building materials.

The second chapter provides definitions and information on phase change materials (PCM) and environmentally friendly moisture control hygroscopic materials (MCHM). Furthermore, it explores the possibility of combining diatomite with PCM and its use in the construction field.

The third chapter describes our experiment in detail, along with an explanation of the mathematical modeling.

The fourth chapter is dedicated to analyzing the various results obtained through the experiment and numerical model, using numerous insulation materials.

Finally, a general conclusion summarizes the work done in this thesis, including perspectives to be considered in future research.

Chapter I

Hygrothermal Transfer State of the Art: Building Envelope and Energy Efficiency

I.1 Introduction

Reducing energy consumption in buildings presents significant ecological and economic challenges, as the building sector is one of the most energy-intensive sectors. To address this issue, many laboratories and research institutions are studying building physics, energy performance, and the quality of living spaces, with the aim of minimizing the environmental impacts associated with buildings.

Measures taken to lower a building's energy bill typically involve strong insulation with reduced infiltration and indoor air renewal. However, these solutions can increase the likelihood of pathologies caused by excessive humidity, whether in the habitable environment or in the building envelope. To accurately predict degradation risks related to humidity, physical models that describe a building's hygrothermal behavior with maximum precision need to be developed [28].

The transfer of heat and moisture in building envelopes and construction materials is a complex process involving multiple mechanisms. This area of study has garnered the attention of many researchers due to the numerous theories and models involved. However, there are still some aspects that require further research in order to better understand the challenges associated with heat transfer [29]. Adding to the complexity is the fact that construction materials are porous media with a complex structure. Pores within these materials can contain both moisture and dry air, and the transfer of heat and moisture within these porous media is coupled, multiphase, and multicomponent [30].

This chapter provides an overview of energy consumption in Algeria, followed by a state-of-the-art review of degradation caused by humidity, including the primary factors contributing to these pathologies. It also discusses the main quantities characterizing porous materials and the various phenomena involved in heat and mass transfer and storage in construction materials. Additionally, the chapter presents the primary models of coupled heat, humidity, and air transfer in building envelopes, classified according to their types of thermal and hydraulic transfer engines.

I.2 Energy consumption in Algeria in the building sector

In recent years, the building sector in Algeria has experienced significant growth, driven by substantial investments from the government. As a result, there has been a corresponding increase in energy consumption, particularly in the residential sector. This underscores the urgent need for sustainable practices and innovative solutions to promote energy efficiency and reduce energy consumption in the building sector.

Figure I.1 : Residential construction in Algeria [30].

In Algeria, the building sector is the primary consumer of energy, accounting for a staggering 41% of the country's total final energy consumption, according to the National Agency for the Promotion and Rationalization of Energy Use (NAPREU) [30]. Unfortunately, energy and environmental considerations are not taken into account during the construction of most buildings in Algeria, regardless of whether they are old or new. This lack of attention results in a heightened dependence on ventilation, heating, and air conditioning (HVAC) systems to regulate the indoor environment of the building envelope, leading to a marked increase in electricity and gas consumption. Addressing this issue is critical to promoting sustainability and reducing energy consumption in the Algerian building sector.

According to the 2019 National Energy Balance [31], natural gas dominates the structure of national energy consumption in Algeria, accounting for 33.8%, followed by petroleum products at 32.1%, and electricity at 28.4%, as illustrated in the following figure. It is essential to note that reducing energy consumption in the building sector will not only help Algeria to meet its environmental commitments but also contribute to the diversification of the national energy mix and promote energy security.

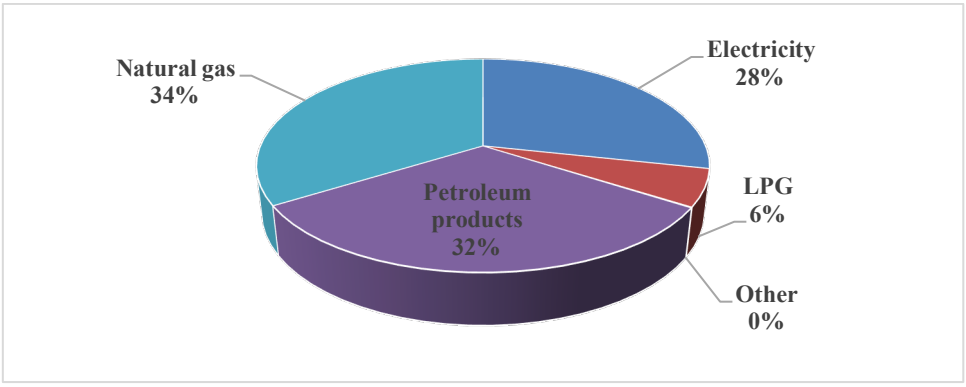

Figure I.2 : Structure of final energy consumption by product [31].

The most recent report indicates that final energy consumption in Algeria increased from 48.1 million tons of oil equivalent (Mtoe) in 2018 to 50.359 Mtoe in 2019, reflecting a 2.2 Mtoe or (+4.6%) increase. This growth was driven by higher consumption of natural gas, electricity, and LPG, which more than compensated for the decline in petroleum products. The changes in final energy consumption by product between 2018 and 2019 are presented in detail in the following table:

Product	2018 [K Toe]	2019 [K Toe]	Evolution	
			Quantity	%
Petroleum products	15 517	16 153	636	4,1
Natural gas	16 024	17 002	978	6,1
Electricity	13 926	14 299	373	2,7
LPG	2 588	2 838	250	9,6

Table I.1 : Final consumption by product [31].

The increase in natural gas consumption by a rate of 6.1% is explained by the increase in the total number of Sonelgaz subscribers, which reached 6 million in 2019, as well as the growing needs of high (+15.2%), medium (+5.0%) and low pressure (+3.8%) customers. The increase in electricity consumption (2.7%) to reach 14.3 Mtoe is due to the increase in demand from Sonelgaz customers, especially households (7.3%), whose total number of subscribers reached nearly 10 million at the end of 2019, up 4.6% compared to 2018.

The evolution of final consumption by sector of activity showed an increase in the consumption of the industrial and building sector by 9.3%, from 10.45 Mtoe to 11.424 Mtoe, due to the increase in consumption of the Buildings and Public Works subsector (+83.5%). The evolution of final energy consumption by sector between 2018 and 2019 (industry and construction sector) is detailed in the following table:

Unit: K Toe	2018	2019	Evolution	
			Quantity	(%)
Industry and BPW, including:	10 450	11 424	974	9,3
Construction materials	4 659	4 888	229	4,9
SEMME	1 283	1 805	522	40,7
BPW	486	892	406	83,5
Manufacturing Industries:	1 122	1 167	45	4,0
(Of which: Agrifood)	1 011	1 048	37	3,7
Chemistry	541	483	-58	-10,8
Other industries	2 359	2 189	-170	-7,2

Table I.2 : Final consumption of the 2 sectors industry and construction [31].

I.3 Moisture-related disorders in buildings

The building envelope plays the most crucial role in maintaining the necessary level of comfort in the living environment. It serves as the site of heat, air, and moisture transfers that influence the internal temperature and humidity of the building. In addition, according to Rousseau [32] a good building design relies on understanding moisture transfer and storage mechanisms in building materials and mastering moisture management techniques in the building envelope. Regardless of its origin, excessive moisture in the building represents the source of several pathologies. It is generally considered the most significant threat to the durability and long-term performance of the housing stock [28,33]. The disturbances caused by moisture in buildings can be classified into four categories:

Moisture-induced modifications: Moisture transfer through the building envelope can significantly impact the thermo-physical properties of building materials. Such changes in characteristics can alter their performance, leading to potential degradation. For instance, a material's conductivity may differ significantly when it is at 0% humidity compared to when it is at 90% humidity. Therefore, it is crucial to understand the impact of moisture transfer on building materials and to take appropriate measures to mitigate any adverse effects on their longevity and efficiency.

Moisture-induced modifications: Moisture can penetrate a material through its pores and undergo continuous dynamic variations, leading to moisture migration. Such moisture migration can cause material degradation through a freezing action. Therefore, it is essential to comprehend the impact of moisture migration on materials, including the potential for freezing action, and to take measures to prevent any adverse effects on the material's longevity and performance.

Moisture-induced modifications in a humid environment: Elevated humidity levels can lead to the corrosion of metallic elements in buildings, as well as the growth of molds, bacteria, algae, and lichens. These can pose a significant risk to human health, making it crucial to address and control high humidity levels within buildings.

Degradation of indoor environments: Moisture plays a crucial role in determining the quality of indoor environments in buildings. It can have both direct and indirect impacts on indoor air quality, such as respiratory difficulties and the development of harmful agents that can cause allergic reactions [34]. Figure I.3 provides several examples of damages caused by moisture to building materials, emphasizing the need to control and mitigate moisture-related issues in buildings to maintain a healthy indoor environment.

Figure I.3 : Examples of problems caused by moisture.

I.3.1 Health problems related to humidity

Exposure to mold can lead to various health issues, including but not limited to:

- ✓ Respiratory problems, such as breathing difficulties and nasal/sinus congestion.
- ✓ Burning and watery eyes.
- ✓ Dry and persistent cough.
- ✓ Sore throat and irritation of the nose and throat.
- ✓ Shortness of breath.
- ✓ Skin irritation.
- ✓ Mood disturbances.

It is essential to control and mitigate mold growth in buildings to prevent these health issues and maintain a healthy indoor environment [30].

I.4 Porous media

In building physics, construction materials are considered as porous media with a complex shape due to their heterogeneous and anisotropic nature at the macroscopic scale. Various phenomena of mass and heat transfer and exchange occur in these materials. A porous material comprises three distinct phases: the solid phase, which forms a porous network of capillary pores, the liquid phase composed of pure water, and the gaseous phase, consisting of humid air [28, 34]. Understanding the complex nature of porous materials is crucial in predicting and mitigating moisture-related issues in building envelopes.

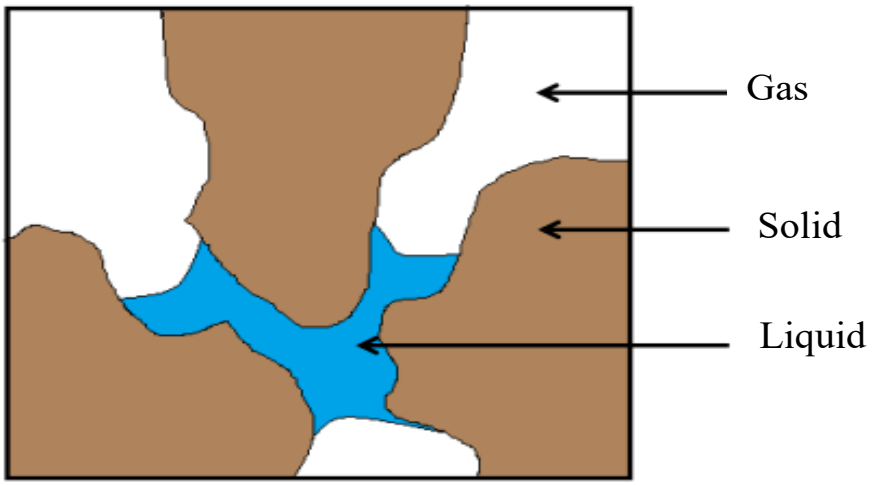

Figure I.4 : Schematic representation of a porous medium [28].

Characteristic quantities that describe the properties of a porous medium include porosity, pore distribution, tortuosity, and connectivity. These quantities provide information on the available pore space and its geometry, which are essential in understanding and predicting various phenomena related to heat and mass transfer in porous materials.

I.4.1 Intrinsic properties of a porous medium.

Hygroscopicity: A material is referred to as hygroscopic when it can effectively absorb and retain a considerable amount of moisture from the surrounding air.

Relative humidity: it is the ratio of the water vapor content of the air to its maximum capacity to hold water vapor under those conditions.

$$RH = \varphi = \frac{V}{V_{sat}} = \frac{P_V}{P_{v,sat}} \quad (I.1)$$

The saturated vapor pressure ($P_{v,sat}$) depends on temperature and can be described empirically. This relationship has been validated for temperatures ranging from 0 to 80 °C with an accuracy of ±0.15% (Peuhkuri, 2003).

$$P_{v,sat} = e^{23.5771-\frac{4042.9}{T-87.58}} \quad (I.2)$$

Water content: Water content refers to the amount of water present in a material, which is typically measured as the ratio of the weight of water to the weight of the dry material.

$$u = \frac{m-m_0}{m_0} \quad (I.3) \qquad w = \frac{m-m_0}{V} \quad (I.4)$$

The capillary saturation degree is a measure used to assess the moisture content of porous building materials. It can be expressed as follows:

$$S_{cap} = \frac{U}{U_{cap}} \quad (I.5)$$

Porosity: This parameter describes the internal geometry of the material and ranges from 0% to 100%. There are two types of porosity: total and open.

Specific surface area: It is the surface accessible to molecules per unit mass of the material. A high value of specific surface area leads to a particularly significant adsorption capacity of the material.

Tortuosity: Tortuosity is a fundamental concept that describes the complexity and sinuosity of the path taken by a fluid particle through a porous medium. It is defined as the ratio of the effective length of the average fluid path to the apparent length of the porous medium.

Laplace's law, Kelvin's law: At the microscopic scale, the interface between liquid water and water vapor is subject to the phenomenon of surface tension. This liquid-gas interface forms an angle with the surface of the solid matrix called the contact angle θ acute on the wetting fluid side (Figure I.6). If θ= 0, the wetting is total. If $0 < \theta < 90$, the wetting is partial, and if $\theta > 90$, the fluid is non-wetting and seeks to minimize its contact surface with the solid.

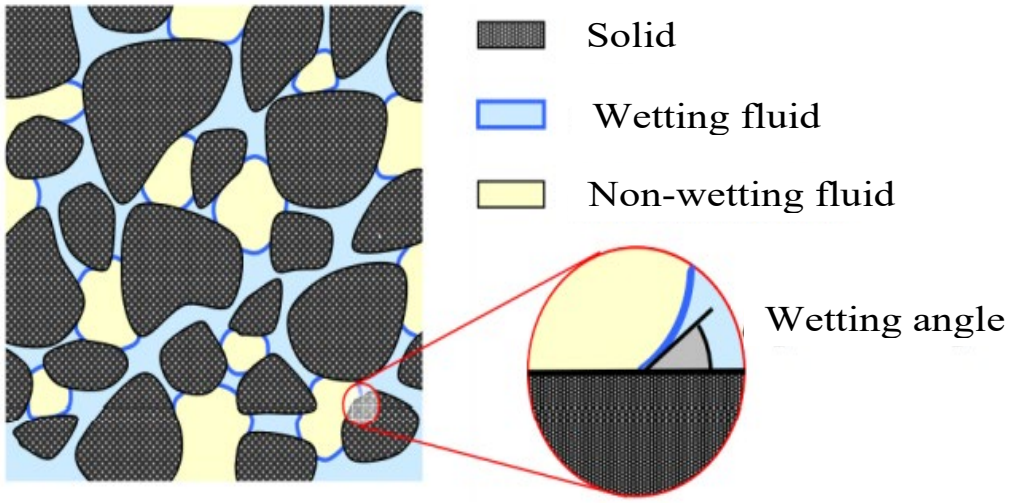

Figure I.5 : Diphasic occupancy of the pore space [28].

The curvature of the interface between two immiscible fluids results in pressure differences between the two sides of the interface, with the interface behaving like a tension membrane. Laplace's law expresses the equilibrium at the liquid-gas interface, where the capillary pressure represents the difference between the total pressure (P) and the liquid pressure (Pl).

$$P_c = P - P_l = \frac{2\gamma\cos\theta}{r} \quad (I.6)$$

The relationship between capillary pressure and the radius of a liquid meniscus can be described by fundamental principles of thermodynamics, such as Kelvin's law. This relationship indicates that the water pressure at the meniscus is lower than the air pressure, and this effect is particularly pronounced for small values of the radius [28,30].

$$P_c = \frac{R.T\rho_\omega}{M_\omega} \ln\left(\frac{\omega}{\omega_s}\right) \quad (I.7)$$

I.5 Mechanisms of heat and mass transfer in porous media

I.5.1 Heat transfer and storage in porous media

I.5.1.1 Heat transfer in building materials

The most dominant heat transfer mode in a porous medium is thermal conduction, determined by Fourier's law. The heat flux $\overrightarrow{dQ_{cond}}$ crossing a surface ds is proportional to the temperature gradient T.

$$\overrightarrow{\mathrm{dQ_{cond}}} = -\lambda\overrightarrow{\mathrm{grad}}(\mathrm{T}).\,\mathrm{ds} = \overrightarrow{\mathrm{q_{cond}}}.\,\mathrm{ds} \tag{I.8}$$

The moisture-dependent thermal conductivity λ (ω) of mineral building materials is given by:

$$\lambda\,(\omega) = \lambda_0\left(1 + \frac{b.\omega}{\rho_s}\right) \tag{I.9}$$

The symbol "b" represents a percentage ratio that indicates the increase in thermal conductivity of a material with respect to its moisture content. This value is specific to the type of construction material, but for hygroscopic materials, it is largely independent of their apparent density. [28, 30].

I.5.1.2 Energy storage in building materials

Enthalpy is a measure of the amount of heat that a material contains under isobaric conditions. In the construction industry, where temperatures typically range from -20°C to 40°C, there is a roughly linear relationship between a material's enthalpy and its temperature. The enthalpy of a dry construction material can be described by the following equation, I.12 [30].

$$\mathrm{H_s} = \rho.\,\mathrm{C_p}.\,\mathrm{T} \tag{I.10}$$

It is necessary to add to this enthalpy the enthalpy of water contained in the building material. The enthalpy of water depends on its physical state (gas, liquid, solid), which is difficult to identify accurately in fine pores. The following equation can be used to determine the enthalpy of water in the building material:

$$H_s = \left[(\omega - \omega_e)c_\omega + \omega_e c_e - h_e\frac{d\omega_e}{dt}\right]t \tag{I.11}$$

I.5.1.3 Heat flux with phase change

The phase change of building materials can greatly affect heat transfer, particularly when the materials are exposed to significant moisture and a temperature gradient. Research by HM Künzel [35] has shown that under certain high humidity conditions, the heat flux can double due to vapor diffusion through the insulation layer. Therefore, it is important to account for these enthalpy fluxes in a separate equation. In general, the relationship between vapor diffusion and phase change can be expressed as a source term in the thermal balance equation:

$$S_h = h_{l,v}\,\nabla g_v \tag{I.12}$$

I.5.2 Transfer and storage of moisture in porous media

I.5.2.1 Diffusion

The moisture transfer phenomena in a material depend mainly on the nature of its porous structure. The mechanisms of water vapor diffusion can vary depending on the pore size. Under isothermal conditions, moisture transfer in porous building materials occurs through three different modes depending on the pore diameter:

- **Pores with a diameter greater than 10^{-6} m:** Under most conditions, the primary mechanism of water vapor transfer in building materials is through molecular diffusion, also known as Fick's diffusion. This process is driven by collisions between individual molecules and does not involve interaction with the solid matrix of the material (see Figure I.11). The diffusion coefficient in this case can be calculated using the equation proposed by Philip and De Vries [36], as shown in Equation I.4.

$$D_a = c\ (\frac{P_0}{P})\ (\frac{T}{T_0})^n \tag{I.13}$$

  Where the reference pressure and temperature take the following values:
  P_0 = 1.01325× 10^{-5} $[Pa]$, T_0 = 273.15 $[K]$, c = 2.17× 10^{-5} $[m^2/s]$ et n = 1.88.

- **Pores with a diameter smaller than 10^{-8} m:** When the diameter of pores is less than 10^{-8} m, the phenomena of Knudsen diffusion or effusion occur. In this case, water molecules are transferred through collisions with the pore wall as the pore diameter is smaller than the mean free path (see Figure I.11). The pore wall is considered to be rough, creating obstacles on the diffusion path, leading to different tortuosities. The Knudsen diffusion coefficient, denoted as D_k, can be defined using the following relationship:

$$D_k = 9.7 \times 10^3 \sqrt{\frac{T}{M}} \tag{I.14}$$

- **Surface diffusion**: The phenomenon described corresponds to the motion of water vapor molecules that become adsorbed and held at the surface of pores. When a certain activation energy is present, these molecules can be released and jump from one adsorption site to another (refer to Figure I.6).

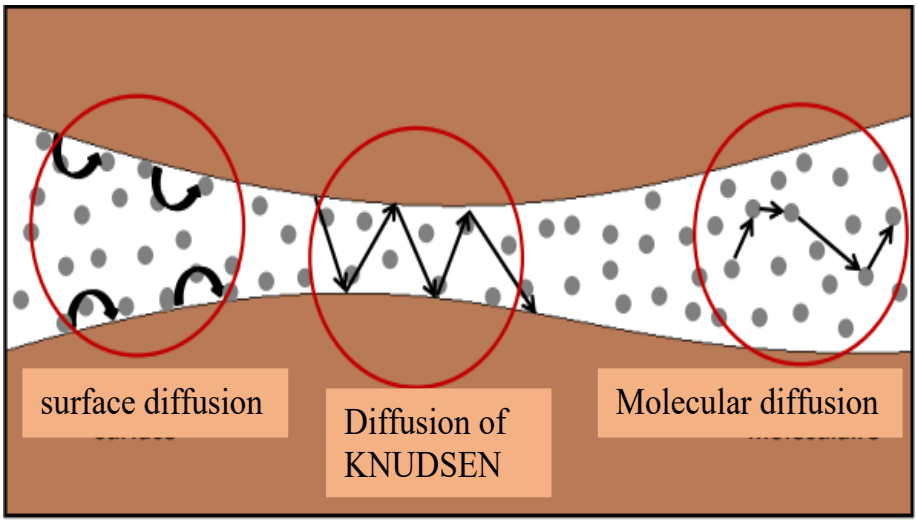

Figure I.6: Illustration of the different modes of water vapor diffusion in a pore [28].

If non-isothermal conditions occur, another mode of water vapor transfer in the porous medium may occur, caused by a temperature difference. This mode of moisture transfer is known as thermal diffusion and is based on the difference between the density of dry air and that of water vapor molecules. This density difference causes a movement of vapor particles from cold to warm air [28].

I.5.2.2 Moisture storage mechanism

Adsorption is a process where molecules from a fluid phase adhere to and accumulate on the surface of a solid. This phenomenon takes place when the concentration of the fluid near the surface of the solid increases. There are two types of adsorption: physical adsorption, also known as van der Waals adsorption, and chemical adsorption, also referred to as activated adsorption.

- **Physical adsorption:** it is a reversible phenomenon that arises from the intermolecular forces of attraction between the molecules of the solid and those of the adsorbed fluid. This type of adsorption is multimolecular, meaning that it involves the accumulation of multiple layers of molecules, and it does not exhibit specific sites of adsorption.
- **Chemical adsorption:** An irreversible phenomenon can alter the nature of the solid material. It results from a chemical interaction that involves the transfer of electrons between the solid and the adsorbed fluid, leading to the formation of a compound on the surface of the solid [28].

I.5.3 Effect of coupling between heat and mass transfer

To accurately represent the hygrothermal behavior of wet building materials, it is necessary to consider the coupling of energy and mass transfers. The thermal and hydric conditions of a material directly affect the kinetics of hygrothermal transfers, which can be summarized as follows:

- ✓ Temperature and humidity significantly impact the main thermal and hydric properties. For instance, the hydric state, in particular, affects thermal properties such as specific heat and thermal conductivity, as noted by researchers such as Jerman and al. [37].
- ✓ A moisture movement can be induced by a temperature gradient, referred to as the "Soret effect." Temperature changes the relative humidity, which, in turn, affects the moisture content locally, leading to moisture redistribution within the porous material.
- ✓ Mass transfer in a porous medium generates energy transfer by advection. In a humid porous medium, an additional specific heat of water intervenes in the overall enthalpy. This enthalpy of water depends on its state. Its exact determination can only be possible if the pore distribution and humidity storage function are well defined [35].
- ✓ In a building material exposed to high humidities under a temperature gradient, the phase change phenomenon inside the porous material has a significant effect on thermal transfer. Künzel [35] showed that the phase change phenomenon can double the thermal flux in some insulating materials exposed to high relative humidities [10].

I.6 Modeling coupled heat, air, and moisture transfers in multilayered building walls.

Research on moisture-related pathologies and deterioration, especially in building envelopes, has highlighted that precise prediction of these issues necessitates detailed modeling of coupled heat, air, and moisture transfers. Accurate modeling is crucial for predicting the energy performance of buildings and the level of comfort that they provide to their occupants [28].

I.6.1 Main physical models of coupled heat and moisture transfer in building materials

The choice of transfer mechanisms depends on the approach used to model hygrothermal transfer in porous media. In the literature, two main approaches are distinguished for modeling coupled heat and moisture transfer: a homogenization approach and scale change from micro- to macro-scale, and a macroscopic phenomenological approach. Several models have been proposed in each of these approaches to describe hygrothermal transfer in porous building materials.

I.6.1.1 Modeling by homogenization

Describing the physical phenomena of construction materials in a heterogeneous porous medium is very complex, if not impossible, if all the heterogeneities are taken into account. Homogenization methods are commonly used approaches to overcome this difficulty. They allow for the representation of a highly heterogeneous porous medium at the macroscale by a continuous homogeneous medium with a similar behavior on average at the macroscale.

Indeed, homogenization modeling allows for obtaining a macroscale physical behavior of porous media by taking into account a microscopic description of the associated physical phenomena.

- Homogenization approaches are grouped into three types of methods: homogenization by averaging, where physical phenomena are modeled at the pore scale, and a representative elementary volume (REV) is subsequently considered to obtain an equivalent fictitious medium (see Figure I.7), by expressing an average of macroscopic variable fields in a representative spatial domain [30].

  The REV method is widely used in the field of hygrothermal transfer, as well as in the field of flows and transfers in porous media.

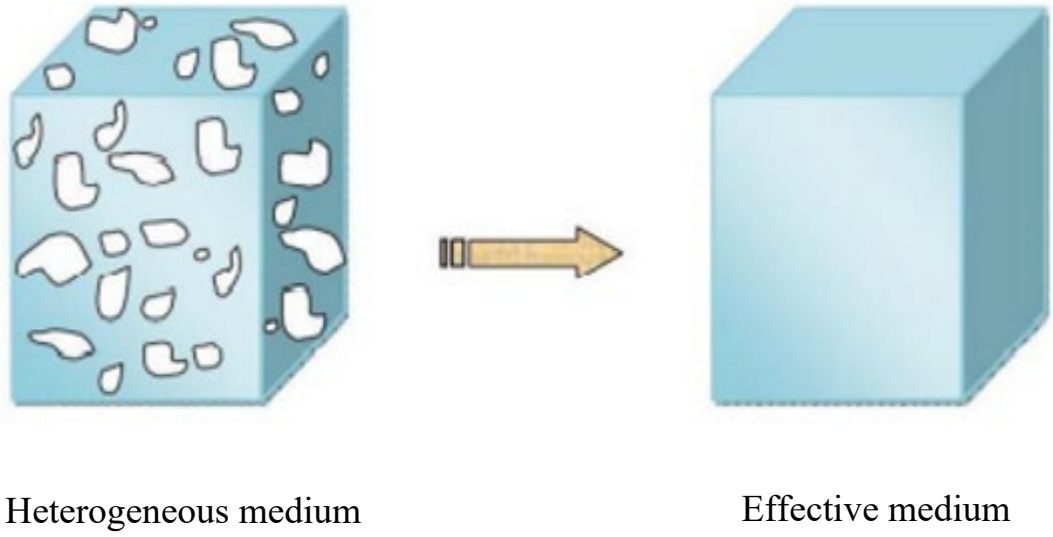

Figure I.7 : Homogenization by volume averaging [28].

- Periodic homogenization consists of assuming that the microscopic structure of the macroscopic domain is assimilated to a periodic repetition of an elementary cell defined as a basic cell (see Figure I.8) [38-40].

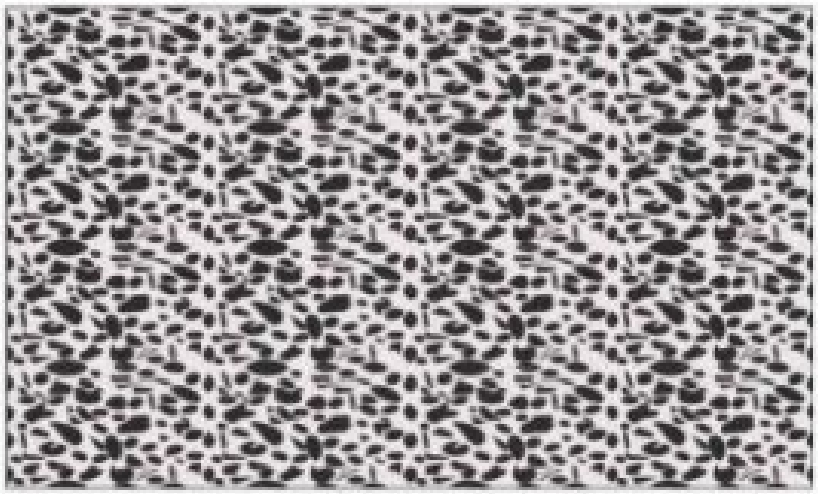

Figure I.8: Microstructure consisting of the periodic distribution of the cell [41].

This approach is relatively less used in the field of hygrothermal transfer compared to the VER method. However, several studies have been carried out in this direction. Bouddour et al. [42] established several models of hygrothermal transfers by periodic homogenization for different physical configurations (predominant heat convection, predominant steam diffusion, etc.). Lewandowska et al. [43] used periodic homogenization approach in the case of water transfer in a double porosity medium. Bennai [34] applied the periodic homogenization approach to study coupled heat, air, and moisture transfer and understand the influence of geometric parameters of envelope eco-materials such as hemp concrete on hygrothermal transfer mechanisms.

- Other homogenization approaches can be found through the use of statistical methods applied to randomly or disorderly microstructured media, as developed by researchers such as Maghous et al., Snahuja et al., and Zhu et al. [44-46].

I.6.1.2 Phenomenological modeling

Generally, modeling of coupled heat, air and moisture transfers in building envelopes is based on a phenomenological approach inspired by the work of Luikov [47], where the porous medium is considered as a homogeneous medium, allowing to establish hygrothermal transfer equations from the fundamental principles of thermodynamics. The energy and mass balances are expressed using measurable transfer drivers (temperature, water content, vapor pressure, etc.) and coefficients explicitly linked to the macroscopic properties of the materials (thermal conductivity, specific heat, water vapor permeability, etc.) determined experimentally [28]. There are several models with different moisture transfer drivers.

- Luikov Model [47]: This model highlights the phenomenon of thermo-diffusion, where the diffusion of water in the form of vapor and liquid is considered dependent on gradients of mass water content, temperature, and total pressure. Moisture can move in vapor form due to a gradient in vapor concentration, while liquid water can move by a capillary gradient.

$$\begin{cases} g_v = -D_v \rho_s \nabla u - D_{v,T} \rho_s \nabla T \\ g_l = -D_l \rho_s \nabla u - D_{l,T} \rho_s \nabla T \end{cases} \quad \text{(I.15)}$$

An additional parameter appears in this model, the phase change rate $\dot{m}$ defined by:

$$\dot{m} = \epsilon \rho_s \frac{\partial u}{\partial t} \quad \text{(I.16)}$$

ϵ represents the ratio between the water vapor flux and the total mass flux, if $\epsilon = 1$, moisture transfer occurs in the form of vapor, and if $\epsilon = 0$, it occurs in the liquid form.

The system of partial differential equations of the AV. Luikov model is given as:"

$$\begin{cases} \frac{\partial u}{\partial t} = div\ (D_m\ (grad\ u + \delta_s\ grad\ T)) \\ \rho_s C_p \frac{\partial T}{\partial t} = div\ (D_T\ grad\ T) + L_v \epsilon \rho_s \frac{\partial u}{\partial t} \end{cases} \quad \text{(I.17)}$$

- **Philip and al. [36]:** This model is more classical, as the two researchers developed a theory that describes hygrothermal transfer as a function of volumetric water content and temperature. They considered that heat transfer is described only by pure conduction and transfer related to phase change. Thermal advection related to gradients of vapor pressure and total pressure is not considered. The transport of water vapor is a diffusion process governed by Fick's law. They used the Darcy's law to express the flux in the liquid phase:

$$\begin{cases} g_v = -\rho_l (D_{v,e} \nabla v - D_{v,T} \nabla T) \\ g_l = -\rho_l (D_{l,e} \nabla v - D_{l,T} \nabla T - \lambda_h) \end{cases} \quad \text{(I.18)}$$

The system of equations describing the mass and energy balances is represented in the equation:

$$\begin{cases} \frac{\partial v}{\partial t} = \nabla (D_T \nabla T) + \nabla (D_v \nabla v) + \nabla \lambda_h \\ \rho\ C \frac{\partial T}{\partial t} = div\ (\lambda\ grad\ T) + L_v\ div (D_{v,e}\ grad\ v) \end{cases} \quad \text{(I.19)}$$

- **Pedersen Model [48]:** In this model, the hydric transfer is decomposed into two equations for liquid and vapor transport. Vapor pressure is chosen as the driving force for vapor transport, while capillary pressure is chosen for liquid phase, in order to ensure continuity of capillary transfer for multi-layer wall components. The mass balance is expressed as follows:

$$\frac{\partial v}{\partial t} = \text{div}\left(\delta_p\ \text{grad}\ P_v - \lambda_h\ P_c\ grad(ln P_c)\right) \quad \text{(I.20)}$$

- **Künzel Model [35]:** This model considers temperature and relative humidity as drivers of hygrothermal transfer. The transfer of the vapor phase is ensured by the effect of a vapor pressure gradient, while the transfer of the liquid phase is ensured by capillary forces between fluids and thus between the fluid and solid phases. The system of differential equations for this model is written as follows:

$$\begin{cases} \frac{\partial \omega}{\partial \varphi} \frac{\partial \varphi}{\partial t} = div\ (D_\omega grad\ \varphi + \delta_p grad\left(\varphi P_{v,s}\right)) \\ \frac{\partial H}{\partial t} \frac{\partial T}{\partial t} = div (\lambda\ grad\ T) + L_v div\ (\delta_p grad\left(\varphi P_{v,s}\right)) \end{cases} \quad \text{(I.21)}$$

The Künzel model (1995) [35] is widely used for coupled heat and moisture transfer modeling in 1D and 2D. It is implemented in the software WUFI, which is one of the most commonly

used commercial tools for simulating hygrothermal transfers. Additionally, this model has also been integrated into the COMSOL Multiphysics software [30].

I.7 Heat and Moisture Transfer at Interfaces in Buildings

Two types of boundary conditions are distinguished in macroscopic modeling of heat and moisture transfer in multilayer walls. The first type pertains to the interface between the building envelope and the environment, while the second type is associated with the interface between two adjacent layers of dissimilar materials within a multilayer wall.

I.7.1 Interaction between the building envelope and the environment

In the modeling of heat and moisture transfer for multilayered walls, two distinct types of boundary conditions are identified. The first type occurs at the interface between the building envelope and the external environment, while the second type occurs at the interface between successive layers of different materials within a multilayered wall. The wall has two sides that are exposed to different environments: the external climatic environment and the indoor living environment. The external environment affects the wall through temperature and relative humidity variations, long- and short-wave radiation, forced convection caused by wind, and the impact of rain. The indoor environment also affects the wall through temperature and relative humidity variations, long-wave radiation, and natural or forced convection, depending on the ventilation strategy employed.

- **Radiation**

  Radiative heat exchange is composed of long-wave and short-wave radiation. The radiation at the exterior surface of the wall is expressed as follows [49]:

$$S_e = k\left(S_{dir} + S_{dif}\right) + \sigma\, \varepsilon\, [F_{floor}\left(T_{floor}^4 - T_e^4\right) + F_{sky}\left(T_{sky}^4 - T_e^4\right)] \quad \text{(I.22)}$$

  The radiation at the interior surface is due to the long-wave radiation exchange between the interior surface of the wall at temperature (T_{si} $[K]$) and the other walls of the room at temperature (T_{wall} $[K]$). It is determined by Equation I.23:

$$S_i = \frac{\sigma(T_{si}^4 - T_{wall}^4)}{\left(\frac{1-\varepsilon_{surf}}{\varepsilon_{surf}\cdot S_{surf}} + \frac{1}{F_{surf-wall}\cdot S_{surf}} + \frac{1-\varepsilon_{wall}}{\varepsilon_{wall}\cdot S_{wall}}\right)} \quad \text{(I.23)}$$

- **Convection**

  Convection in building physics consists of two types, thermal convection and mass convection due to the exchange of heat and water vapor between the surface of the wall and the air (either

exterior or interior), respectively. These exchanges are expressed by convective heat and mass transfer coefficients as follows:

$$\begin{cases} Q_{conv} = h_c(T_{air} - T_{surf}) \\ H_{conv} = h_m(P_{v,air} - P_{v,surf}) \end{cases} \quad \text{(I.24)}$$

The values of convective heat and mass transfer coefficients depend on the environment (interior or exterior).

- **Rain**

The calculation of rain or rain infiltration is rarely considered in the modeling of exterior boundary conditions. Künzel (1995) expressed rain infiltration as a liquid water flux, as follows:

$$g_{l,infiltrated\,rain} = a_p . g_{l,rain} \quad \text{(I.25)}$$

I.7.2 Interaction between two layers of the wall

Building walls are composed of several layers of materials that possess diverse hygrothermal properties. The boundary conditions at the interfaces between successive layers are established depending on the type of contact between them. In a study conducted by VP. De Freitas et al. [50], three types of contact were proposed for the layers of a wall: natural contact, hydraulic contact, or an air gap between the two layers (see Figure I.9).

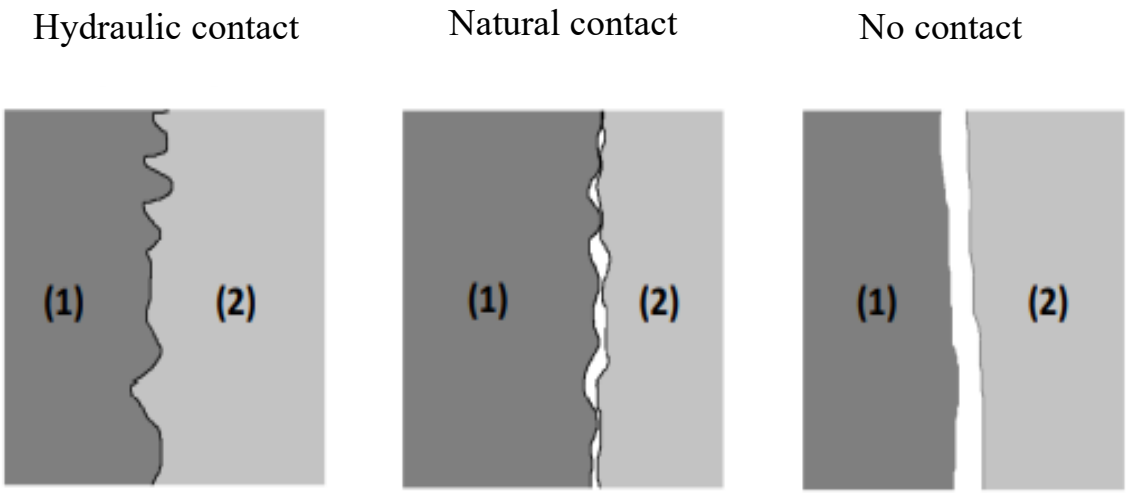

Figure I.9: Possible types of contact between two materials [30].

For hydraulic contact, continuity is assumed to be ensured for thermal and hydraulic fluxes at the interface, and therefore the boundary conditions can be expressed as follows:

$$\begin{cases} T_1^{interface} = T_2^{interface} \\ P_{v,1}^{interface} = P_{v,2}^{interface} \end{cases} \quad \text{(I.26)}$$

Regarding natural contact, the density of the hydraulic flux at the interface is expressed by Equation I.27 [28].

$$g_{interface} = \frac{-HR_1^{interface} - HR_2^{interface}}{R_{hydrique}} \quad \text{(I.27)}$$

When an air gap is assumed to exist between the two materials, continuity is no longer ensured for either thermal or hydraulic transfer. The hydraulic flux is expressed using Equation I.57 as described above, while a thermal resistance is imposed when writing the density of the thermal flux at the interface, as shown in Equation I.28.

$$Q_{interface} = \frac{-T_1^{interface} - T_2^{interface}}{R_{thermal}} \quad \text{(I.28)}$$

When modeling hygrothermal transfers in multi-layer building walls, the assumption of hydraulic continuity is often adopted [28, 51, 52]. However, this assumption is not valid when using water content as the driving force for hydraulic transfer [53, 54]. Indeed, water content is a variable that strongly depends on the nature of the material and its porous structure, and therefore a discontinuity in hydraulic flux is observed at the interface between two materials with different microstructures. To overcome this issue, hydraulic transfer is described using state variables that are not dependent on the material's microstructure, such as water vapor pressure, capillary pressure, or relative humidity [28].

I.8 Conclusion

The study conducted in this chapter provides an overview of energy consumption in Algerian buildings and the risks associated with moisture in terms of degradation of indoor air quality and structural deterioration of the building envelope. A thorough understanding of the hygrothermal behavior of porous building materials enables better prediction of moisture-related risks and optimization of energy consumption. Furthermore, this chapter includes a section dedicated to describing the porous medium and its primary characteristic parameters, as well as the physical phenomena involved in the transfer and storage of heat and mass in building materials. The chapter also presents a synthesis of various coupled heat, air, and moisture transfer models in building walls to select the appropriate model for the work to be carried out, such as the HM Künzel model based on a phenomenological approach.

Chapter II

Hygroscopic Phase Change Materials in Buildings

II.1 Introduction

Algeria's population growth is causing a significant increase in energy demand, necessitating the exploration of various methods to provide it. Thermal storage is one of the solutions that has been considered. This chapter presents a critical review of the literature on different forms of thermal energy storage. By comparing the three types of energy storage, this chapter aims to demonstrate why latent heat storage was chosen as one of the best storage methods for building materials. Moreover, this chapter pays special attention to the potential use of a natural and eco-friendly material known as "diatomite" which has high hygroscopicity and low thermal conductivity, as a hygrothermal insulation material in building construction. Finally, this chapter reports that incorporating PCHM into porous building materials has significant effects on improving their capacity to control temperature and humidity in the indoor environment.

II.2 Thermal storage

Thermal energy storage involves storing a quantity of energy in a specific location when it is abundant and available at low cost, and retrieving it later when it becomes scarce or expensive [55]. Heat can be stored in several forms: sensible heat, latent heat, and chemical reactions.

- **Sensible heat storage** is the oldest method of storing energy over short or long periods of time. It uses a heat source to raise the temperature of a material without a change in state. At constant pressure, for the temperature increase from T_1 to T_2 of a body with mass m and specific heat capacity C(T), the stored energy is given by the change in enthalpy:

$$Q_{2-1} = \int_{T_1}^{T_2} m\, C(T) dT \quad \text{(II.1)}$$

- **Latent heat storage:** Latent heat storage involves storing energy as latent heat within a narrow range of constant temperature that corresponds to a phase change range. The literature refers to the materials used in latent storage systems as PCMs. These materials undergo a phase change at specific temperatures or within a limited temperature range. On average, PCMs can store ten times more energy per unit volume than sensible heat storage systems. The specific energy stored between the initial temperature T_1 and the final temperature T_2 can be calculated as follows:

$$Q_{2-1} = \int_{T_1}^{T_f} m\, C_s dT + L_f + \int_{T_f}^{T_2} m C_l\, dT \quad \text{(II.2)}$$

- **Thermochemical storage:** The term thermochemical storage encompasses two phenomena: sorption and chemical reaction. Heat storage by sorption is interesting for low-temperature storage (T ≈ 80 °C) while for concentrated solar applications (T ≈ 200 to 1000 °C), chemical synthesis reactions appear to be the most suitable [56].

To select the type of storage, you must check the application that you will implement.

II.2.1 Types of PCMs

Researcher A. Abhat [57] proposed a general classification of PCMs in 1983, which has been widely adopted by the latent storage scientific community. This classification is depicted in Figure II.1.

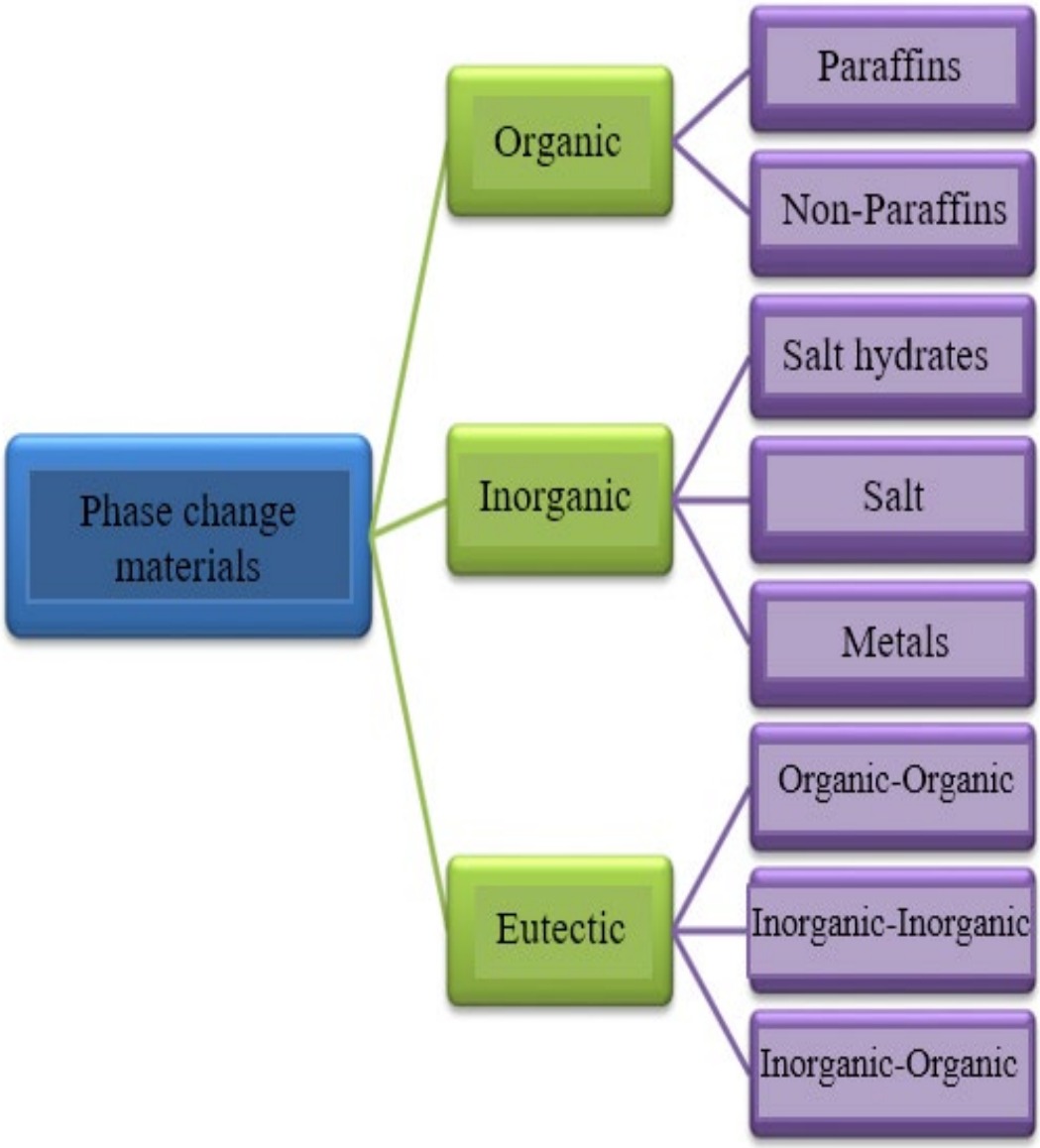

Figure II.1 : Classification of PCMs [57].

This research primarily focuses on paraffins, which are commonly used in building construction due to their variable phase change temperatures and latent heat that depends on molar mass. The table below provides examples of paraffins and their corresponding physical properties:

Name	"C" No. Atoms	Fusion point (°C)	Density (kg/m^3)	Thermal conductivity (W/m.K)	Latent Heat of Fusion (kJ/kg)
n-Dodecane	12	-12	750	0.21^S	n.d
n-Tridecane	13	-6	756		n.d
n-Tetradecane	14	4.5-5.6	771		231
n-Pentadecane	15	10	768	0.17	207
n-Hexadecane	16	18.2	774	0.21^S	238
n-Heptadecane	17	22	778		215
n-Octadecane	18	28.2	814^S, 775^L	0.35^S, 0.149^L	245
n-Nonadecane	19	31.9	912^S, 769^L	0.21^S	222
n-Eicosane	20	37			247
n-Heneicosane	21	41			215
n-Docosane	22	44			249
n-Tricosane	23	47			234
n-Tetracosane	24	51			255
n-Pentacosane	25	54			238
Paraffin Wax	n.d	32	785^S	0.514^S, 0.224^L	251
n-Hexacosane	26	56	770	0.21^S	257
n-Heptacosane	27	59	773		236
n-Octacosane	28	61	910^S, 765^L		255
n-Nonacosane	29	64			240
n-Triacontane	30	65			252
n-Hentriacontane	31	n.d	930^S, 830^L		n.d
n-Dotricontane	32	70			n.d
n-Tritricontane	33	71			189

S: solid; L: liquid; n.d: not available

Table II.1 : Physical properties of different paraffins [58].

II.3 Thermal storage by latent heat in the construction of the building

In recent years, there has been growing interest in the use of phase change materials (PCMs) for thermal energy storage in building construction. PCM-based storage systems can store energy as both sensible and latent heat, with the latter providing a much higher storage capacity. Such systems

involve the absorption or release of heat as the PCM changes phase (e.g., from solid to liquid or liquid to solid). By incorporating PCMs in building envelopes and other components, it is possible to reduce the reliance on HVAC systems and minimize temperature fluctuations inside buildings [30].

II.4 Application of PCMs to building thermal management

In response to the energy crisis, a plethora of studies since the 1980s have been dedicated to the development of PCMs, covering areas such as configurations, geometry, enhancement techniques, mathematical modeling, preparation and characterization, heat transfer, and various applications. The majority of these studies have demonstrated that PCMs' thermal storage performance has a beneficial impact on building thermal management. As shown in Figure II.2, PCMs have been utilized in various building applications.

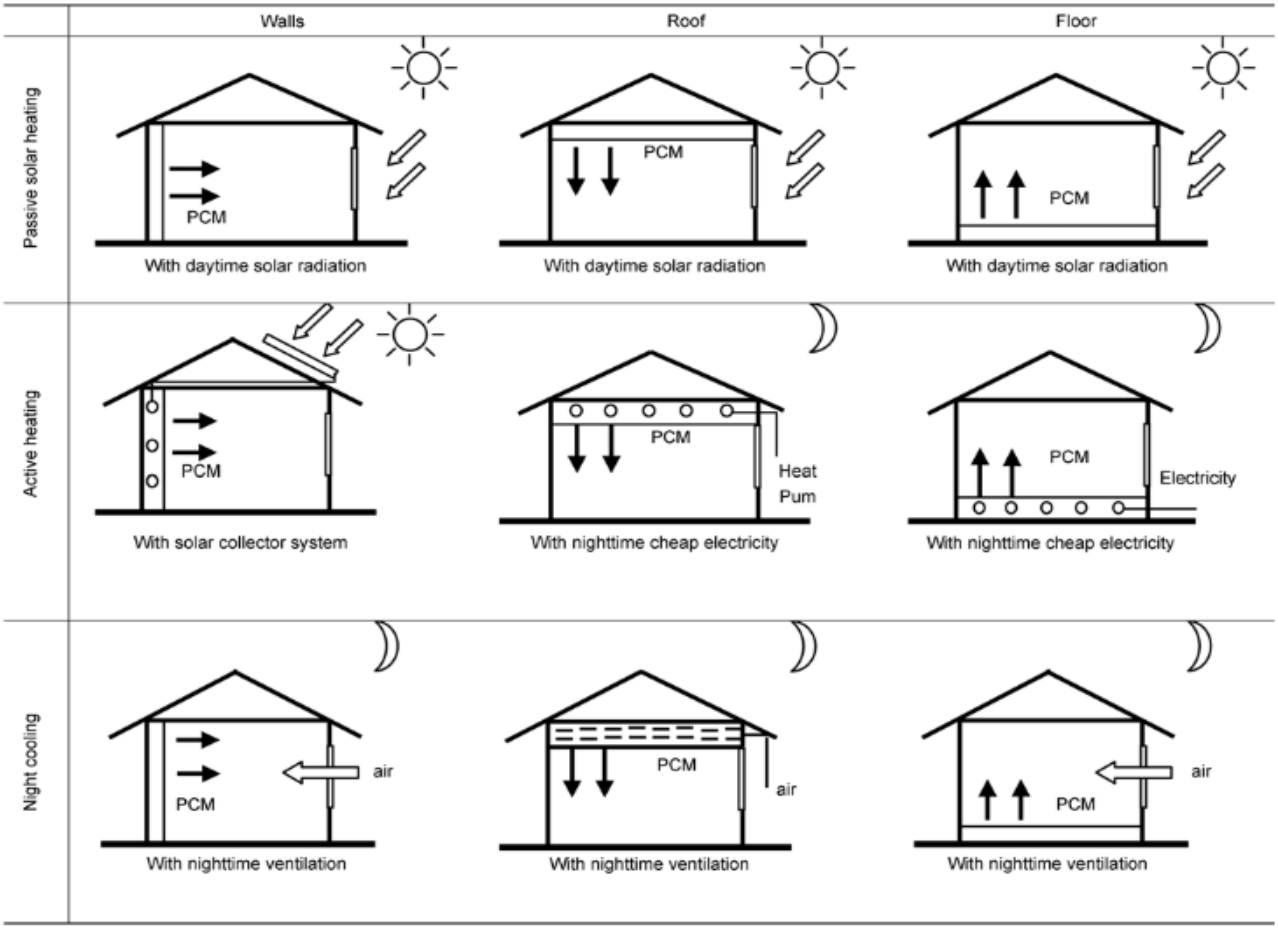

Figure II.2 : PCM applications/building envelopes [59].

Numerous studies have confirmed the positive impact of phase change materials (PCMs) on building thermal management. To achieve efficient thermal management, PCMs with an appropriate melting temperature range should be chosen, typically between 20 and 32°C. Table II.2 provides an overview of possible PCMs with their melting point and latent heat within this temperature range [1]. PCM selection criteria for indoor thermal management also include availability in large quantities at low

cost, high latent heat, specific heat and thermal conductivity, low volume variations during phase transition, no undercooling during freezing, stability, and being non-toxic, non-flammable, and non-explosive. Furthermore, the local climate conditions of the building's surroundings, such as solar radiation and temperature fluctuations between day and night, should be taken into consideration.

PCM's	Fusion point (°C)	Latent heat (kJ/kg)
Propyl palmitate	16–19	186
Acetic acid	16.7	184
Capric/lauric acid	17–21	143
Dodecanol	17.5–23.3	188.8
Butyl stearate/butyl palmitate	18–22	140
Butyl stearate	18–23	140
Potassium fluoride tetrahydrate Capric/lauricacid	18.5–19 19.1–20.4	231 147
Capric/lauric acid Paraffin C_{13} –C_{24}	19.1 20–24	132 152–189
Polyethylene glycol 600	20–25	146
Iron bromide hexahydrate Dimethylsabacate	21.0 21	105 120
Capric/myrstic Polyglycol E 600	21.4 22	152 127.2
Capric/palmitate	22.1	153
Tech. grade octadecane	22.5–26.2	205.1
RT20/montmorillonite	23	79.25
Salt hydrate from climator	23/24	148/216
Peg1000/Peg600	23–26	150.5

Myristic acid, acetic acid octylester	24	147.7
Manganese nitrate hexahydrate Calcium chloride hexahydrate,magnesium chloride hexahydrate Calcium chloride, magnesium chloride hexahydrate	25.8 25 25	125.9 127 95
1-Dodecanol d-Lactic acid RT25 RT30	26 26 26.6	200 184 232.0
Capric-stearate	26.8	160
Calcium chloride, sodium chloride Potassium chloride, water Vinyl stearate	26.8 27–29	188 122
Organic PCM/silicon dioxide	27–30	77
Calcium chloride hexahydrate Gallium–gallium antimony eutectic	29.7 29.8	171 –

Table II.2 : Potential PCMs can be used in construction [30].

II.5 Hygroscopic materials

Buildings located in coastal cities often experience high indoor air humidity levels, especially during the summer, which can negatively impact the building's construction, indoor furniture, and wooden structures. This problem is particularly prevalent in new buildings and can lead to increased heating and cooling costs and mold growth. Studies have shown that the average humidity levels range from 55 to 70% at night in wooden houses and roundwood rooms, 38 to 78% in some rooms of reinforced concrete buildings, and 57 to 72% when certain air conditioners are used. It is important to control the relative humidity inside buildings to maintain indoor air quality, energy efficiency, and building envelope durability. To this end, many researchers have focused on developing moisture control materials, such as PCMs, for thermal management.

Indoor temperature and humidity can be controlled with PCMs and the building itself, respectively. Research has demonstrated that the application of hygroscopic materials with well-controlled HVAC systems can reduce indoor energy consumption for heating and cooling by up to 5% and 30%, respectively. Humidity control materials are capable of automatically absorbing or releasing moisture without the need for a power supply or mechanical equipment due to their sensitivity to changes in relative humidity and ambient temperature. These materials can absorb and desorb moisture or remain wet due to moisture when humidity fluctuates greatly. Table II.3 provides a summary of the applications of humidity control materials in buildings and their key findings.

Material	Preparation method	Main conclusions
Kaolinite	Prepared by selective leaching and combustion.	Water absorption significantly increases when the relative humidity is between 50% and 75%.
Polyacrylic acid fibers	The relationship between B-values and moisture content was discussed.	Moisture content reaches about 40% when the B-value is 0/°C at a vapor density of 15.0 g/V.
Polyacrylic acid fibers	Discussed the relationship between B-values and moisture sorption/desorption isotherm	Fiber products with the desired B-value can be designed from the sorption and desorption of moisture.
Sepiolite and activated carbon	Mixed with sepiolite and activated carbon	Adsorbent with better moisture control properties in the medium and high relative humidity range (89–39%)
Cement, polymer gel	Mixed with a saline solution, such as CaCl2 or Li solution	The absorption and desorption rates of the hygroscopic panel are 10 to 13 times higher than those of the conventional concrete block.
Porous silica gel	Glass of water in the presence of poly (acrylic acid)	The amount of adsorption water at equilibrium was 0.7 g per gram of silica.

Porous ceramic	Mixture of volcanic ash, weathered volcanic ash and waste glass.	The absorbed water volume of GA: 255 g/m^2; GM: 55g/m^2
Sepiolite	Mixed with phosphate, alumina and fibrin as additives.	Can adsorb or desorb 1.2g/g water at 25°C
Zeolite	The conversion is carried out under sub-saturated water vapor conditions	The new method of synthesis of zeolites could be applied in a general way
silica-n Meso-structured	Synthesized using fumed silica and quaternary alkylammonium surfactant	The maximum content of adsorbed water is between 40 and 90%.
Porous composite	Composed of zeolite, diatomite, sepiolite, nano-titanium dioxide	The amount of adsorbed water content was 5–6%
Zeolitic tuff	Ground and reacted with 50% by mass of ordinary Portland cement.	Pore volume was the amount of water vapor adsorption and desorption.
Charcoal	Prepared by carbonizing kenaf (Deccan hemp) at 400–1000°C	The moisture control abilities were much greater than those of common charcoal.
Allophane, silica gel and gibbsite	Slab sample prepared by mixing gibbsite and clay.	The mixture was suitable for interior wall materials and showed superior performance.
Acrylate-based copolymer emulsion	Prepared by emulsion polymerization using main monomers and functional monomers.	Showed high water absorption capacity (27.4%)

Activated carbons (in bamboo)	Prepared by chemical activation with K_2CO_3 or by physical activation with CO_2	The highest moisture control capability was prepared at 873 K with a soak rate of 1.0.
Carboxymethylcell ulose, sepiolite, acrylic acid/acrylamide copolymer	Mix all the components at room temperature.	Maintains a relative humidity between 57 and 60.5% at 25 ° C; the equilibrium moisture adsorption amount is 78.6%; for NO2 and SO2, 227 mg g-1 and 288 mg g-1
Polymer resin, inorganic material	A mixed composite of polymer resin and inorganic material.	The composite showed shorter hygroscopic time and could maintain constant relative humidity (43%)
Silicon carbide, frozen skim milk	Simulate by infinite difference	Drying time was 33.1% shorter than ordinary microwave freeze drying under typical operating conditions
silica gel, calcium chloride	Comparison of silica gel, calcium chloride and composite desiccant.	The composite showed superior hygroscopic ability and a remarkable increase in moisture removal
Japanese cedar wood	Blended with cedar flat grain wood and porous ceramic wall materials	Changing the rate of temperature change over a period strongly affected the value of Cb.

Table II.3 : Application of moisture control materials in the building [30].

The B-value was defined based on the degree of control of the surrounding humidity. Meanwhile, the C_b value was defined as the ratio of the humidity amplitude inside the steel box filled with material to that in the empty steel box.

II.6 Different methods of incorporating PCMs into building materials

The incorporation of phase change materials (PCMs) into building construction elements is of great interest to researchers. There is a wide range of materials such as plasterboards, bricks, concrete, mortar, and diatomite. Here are some principles for PCM conditioning:

- ✓ The storage container material and the PCM must be compatible.
- ✓ The storage container must provide rigidity, corrosion resistance, flexibility, thermal stability, reversibility over a large number of cycles, and tightness to prevent any leakage of PCM in case it becomes liquid.
- ✓ Phase change produces a volume change; therefore, the container must be adapted to absorb these volume changes.

There are many techniques for conditioning PCMs:

II.6.1 Direct incorporation

The direct incorporation process involves adding PCM (in solid or liquid form) directly to the mix of building materials during their production, making it a relatively simple process. A study by Feldman et al. demonstrated the production of energy storage gypsum panels with 22% PCM through direct incorporation. The energy storage capacity of the PCM gypsum plasterboard was compared to that of a regular plasterboard, showing a ten-fold improvement. The physical and mechanical properties of both types of plasterboards were also compared [60].

II.6.2 Immersion

The immersion technique is a method in which porous building materials like blocks, gypsum boards, and wood are immersed in a container filled with melted PCM. The PCM is absorbed by capillary action, and the time required for effective absorption depends on the absorption capacity of the building materials, temperature, and viscosity of the PCM. The immersion process typically takes several hours [61]. Lee et al. [62] incorporated butyl stearate and paraffin into regular and autoclaved concrete blocks. However, they observed that during thermal cycling, some of the paraffin had flowed out, leaving a thin film of paraffin on the surface of the regular concrete blocks. Hawes et al. studied the absorption capacity of autoclaved and regular concrete blocks for PCM at a temperature of 80°C. The time required to completely impregnate autoclaved blocks with butyl stearate and paraffin ranged from 40 minutes to 1 hour, while regular concrete blocks took 6 hours of immersion to become completely saturated with paraffin. The study concluded that autoclaved blocks are better suited for immersion due to their porosity and high absorption rate [63].

II.6.3 Vacuum impregnation

In the vacuum impregnation process, porous aggregates are first subjected to a vacuum to remove air. They are then soaked in a liquid PCM under vacuum. Zhang et al. conducted a study on the vacuum impregnation of PCM into a granular material that can be added to construction materials such as concrete. Figure II.3 provides a schematic of the vacuum impregnation setup [64].

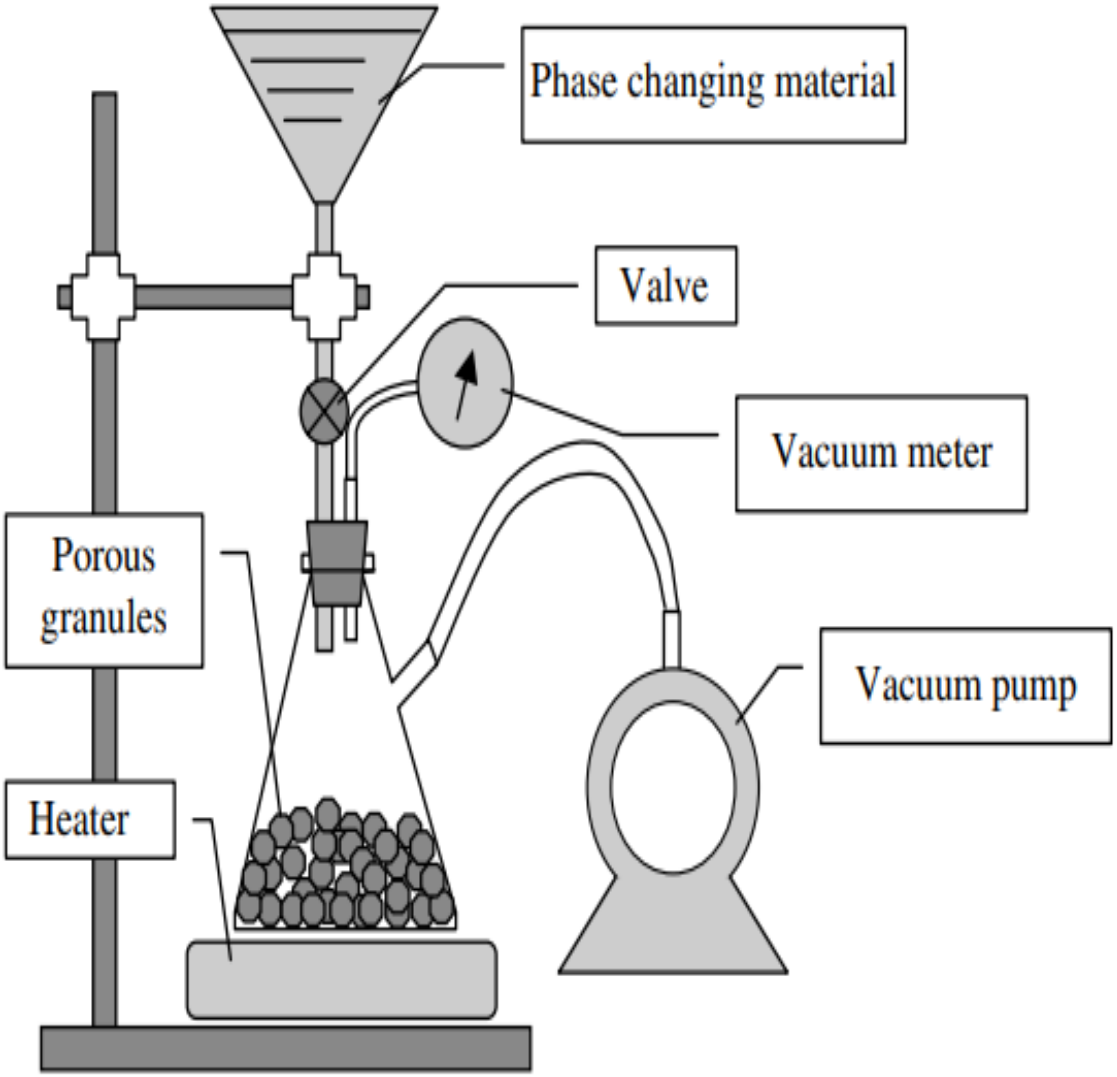

Figure II.3 : Vacuum impregnation scheme [64].

II.6.4 Encapsulation of phase change materials

Phase change materials can be encapsulated prior to incorporation into construction elements. There are two forms of encapsulation:

- **Macro-encapsulation:** In this case, the phase change materials are packed into containers such as tubes, spheres, or panels that have dimensions larger than 10 mm in diameter/thickness

according to researchers Cabeza et al. [65]. These various containers are illustrated in Figure II.4. The geometric and thermal parameters of the container have a direct influence on the heat transfer characteristics of the PCM. Therefore, the capsule must be designed to optimize the speed of heat transfer while also eliminating leaks, corrosion, and problems related to the volume variation of the PCM [60].

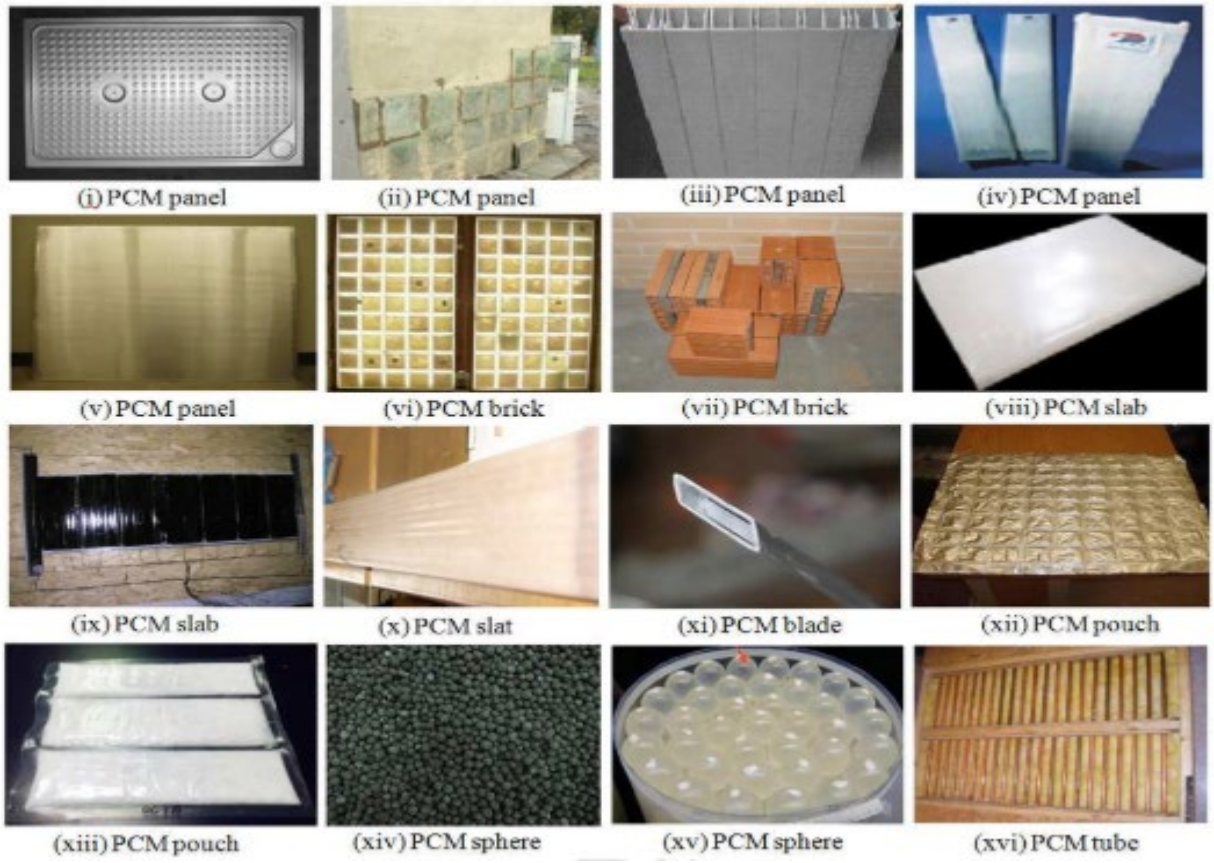

Figure II.4: Example of macro-encapsulation technique of PCM [66].

- **Micro-encapsulation:** One commonly used method for incorporating PCMs into construction materials is micro-encapsulation, where small PCM particles ranging from 1 µm to 1000 µm are enclosed in a thin solid shell made from natural and synthetic polymers. These microcapsules can be in powder form or dispersed in a liquid. Figure II.5 illustrates the various forms of micro-encapsulation [56]. The microcapsules can then be directly added to construction materials such as concrete, plaster, diatomite, or mortar during their manufacturing process. This method allows for the PCM composite to cover a large surface area, thus providing better heat transfer per unit volume. Additionally, the capsules prevent leakage and resist volume changes during phase transitions.

Figure II.5: Different forms of encapsulation [56].

II.6.5 Stabilized form method

Due to the potential risks of PCM leakage in the melted phase and their impact on the environment, several researchers have proposed a new type of PCM material called Stabilized Shape Composite PCM (PCMSS). This stabilization is achieved by using a support material (SM), such as high-density polyethylene, styrene, or butadiene, to manufacture stabilized shape composites. The shape stabilization of PCMs, such as micro-encapsulation, not only prevents leakage but also improves the thermal behavior of the phase change composite during melting/freezing cycles. The choice of SM and the fabrication technique for PCMSS is a crucial factor that influences its thermal properties. Several materials have been used as SM for PCMSS manufacturing, as shown in Table II.4. In addition, three main methods are used to manufacture PCMSS: direct absorption, vacuum impregnation, and the sol-gel method [67].

PCM	support material	Combination method
CA-PA	xGnP	Direct absorption
n-Heptadecane	xGnP	Direct absorption
n-Hexadecane, n-octadecane	xGnP and Na-MMT	Vacuum impregnation method
PEG	Expanded graphite (EG)	Direct absorption

Paraffin	Expanded graphite (EG)	Direct absorption
n-Octadecane	Expanded graphite (EG)	Direct absorption
Hexadecane	xGnP	Vacuum impregnation method
Bio-based PCM	silica smoke and xGnP	Vacuum impregnation method
Hexadecane, octadecane	silica smoke	Vacuum impregnation method
PEG	SiO 2	Sol-gel
PEG	Diatomite and Expanded Graphite	Vacuum impregnation method
Paraffin RT21	Nano-silica	Direct absorption
Octadecane	xGnP	Vacuum impregnation method
Stearic acid	silica smoke	Vacuum impregnation method
Paraffin RT21	Diatomite	Direct absorption
CA, PEG, dodecanol, and heptadecane	Bentonite	Vacuum impregnation method

Table II.4 : Different support materials used for manufacturing PCMSS [67].

Addition of SM can modify the thermo-physical properties of PCM. Therefore, characterization of the manufactured PCMSS composites is of great importance. Additionally, the effects of PCMSS on the thermal and mechanical properties of the host building materials must be experimentally evaluated [30].

II.7 Algerian diatomite as a moisture control and thermal insulation material

II.7.1 Origin and geographical location

Diatomite deposits are found in two different contexts: lacustrine deposits in a volcanic context, and marine deposits in areas where cold currents rise. Diatomite deposits are derived from chemical or biochemical sedimentary rocks formed under exogenous conditions. These rocks are formed in marine environments by the accumulation of organic products, including the siliceous shells of diatoms, which are unicellular algae found in all bodies of water and in the sands of the hottest deserts. The Talahait diatomite deposit, shown in Figure II.6, is located 5 km southeast of the city of Sig, 50 km from the city of Oran, and 40 km from the city of Mascara.

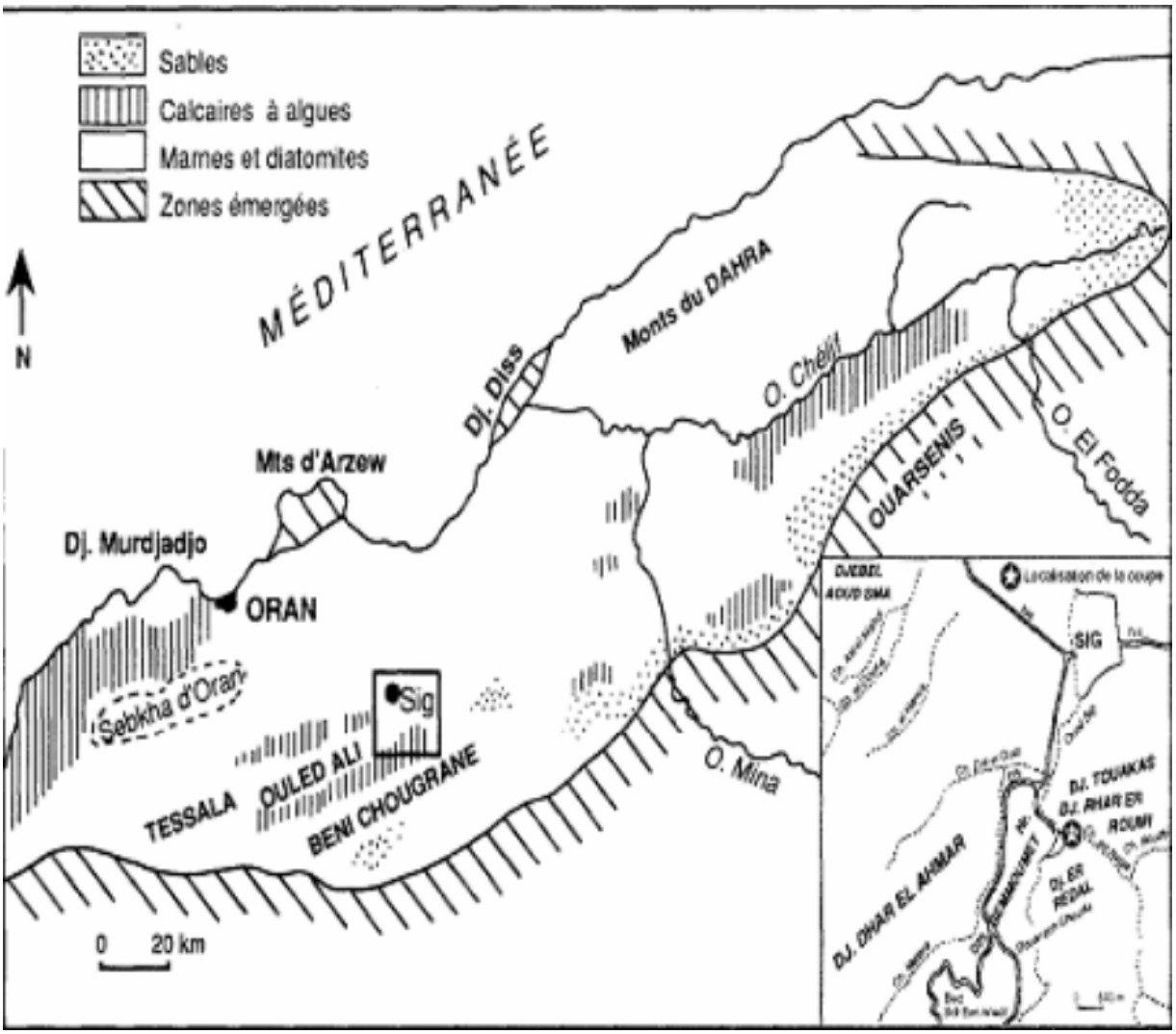

Figure II.6 : Geological map of the western region with the main deposits [68].

The main diatomite deposits of Algeria - West region are shown in Table 1.

Deposit (province)	Service access	Geology	composition, quality	Uses (Production)	Reserves, deposit conditions
Noumene (Tlemcen)	W108: 4km Port: Ghazaouet 40km	diatomite with marls (Miocene)	Al_2O_3 6,0% SiO_2 57,5% Fe_2O_3 2,3% CaO 13,34% MgO 2,3% K_2O 0,87%	Filler and adsorbents	Very important, low recovery
Grimez-sectors chadlia and Tahalait-(Mascara)	Near. RN4-RN6 Factory: 16 km Port: Ghazaouet 50km	Late Miocene	Al_2O_3 3,32% SiO_2 59,86% Fe_2O_3 1,5% CaO 12,8% MgO 4,73%	Filtration, filler and adsorbents (DIATAL production)	1 Mt exploitable geological reserves: 6Mt (5 to 7 layers 0.5 to 4 m thick)
Cadeau (mascara)	Near. RN13	Late Miocene	Medium quality	filler, cement	8 layers from 0.4 to 4.5m thick, deposit to be reassessed
AbdelMalek Ramdane (ex Ouillis) Mostaganem	Near, RN11 Port: Mostaganem 35km	Late Miocene	$SiO_2 > 80\%$ Little carbonated	Filler, adsorbent, cement. Operation stopped	Approximately 15 layers of 0.2 to 1m over 20m thick Deposit to be reassessed.
Beni zagouani (Mostaganem)	Near. RN11	Late Miocene		Filler, adsorbent, cement	Reserves 0.36 Mt
Djebel Meni (Mostaganem)	Near. RN11	Miocene	Little carbonated	Filler, adsorbent, cement	Layer 1.5m thick
Guellal (Mostaganem et Relizane)	Near.W8A	Late Miocene	Al_2O_3 3,5% SiO_2 61,6% Fe_2O_3 2% CaO 13,3% MgO 0,96% K_2O 0,6%	Filler, adsorbent, cement	Layers from 0.5 m to 2 m thick

Table II.5: Main deposits of diatomite in Algeria [69].

II.7.2 Definition

Our thesis focuses on a local material abundant in Algeria called diatomite. Geological reserves of this material are estimated at 6,500,000 [T] in the city of Mascara, specifically in Sig [70]. Diatomite, also known as kieselguhr, is receiving special attention today due to its exceptional physical and chemical properties, such as its high porosity (80% to 90%), high permeability, lightweight, small particle size, large specific surface area, low thermal conductivity, chemical inertness, and well-developed micro-cellular pores [71, 72].

Figure II.7: Diatomite from Sig (ENOF 2020).

Figure II.8: Deposit of Sig town of Mascara (ENOF 2020).

II.7.3 Algerian production of diatomite

According to ENOF 2005, 3000 tons per year of significant diatomite deposits at TAHALAIT (Sig, Mascara province) are being exploited by the state-owned company DIATAL, providing 300

years of reserves at this rate of exploitation. The raw diatomite earth goes through various processing stages, including crushing, drying and grinding, selection, and calcination, as part of an installation [73].

II.7.4 Fields of use of diatomite

The diatomaceous earth can be used in the treatment of drinking water as a filtering material or as an absorbent for pesticides in porous media. It is mainly used in industry as an additive in the filtration of various liquids, especially food, juice clarification, sugar refining, construction and insulation, antibiotics, and some pharmaceutical syrups [74-78].

Diatomite communities have many qualities that make them suitable as bio-indicators. Crushed frustules have been used as an insecticide by their action on protective waxes, promoting a loss of fluids that results in dehydration and death of the insect [79-82].

The use of diatomite in forensic medicine has been the subject of numerous studies and controversies over the decades. In France, it is used by the Institute of Legal Medicine in Strasbourg. The diagnosis of death by drowning is always difficult to reveal for forensic physicians. Diatoms transported in the body by water reach the bloodstream, lungs, marrow, etc. The study of the presence of these algae in these different tissues allows for a more precise diagnosis. It also shows whether or not there has been a displacement of the body [83, 84].

Diatomaceous earth is also used in cosmetics for its abrasive properties as well as its absorbent power, but mainly in industry for its resistance to high temperatures, inertness to acids and bases, and absorbent power. Diatomaceous earth is therefore used in the manufacture of paints, papers, concretes, varnishes, tires, matches, etc. It can be used as an abrasive, filter, insulator, or stabilizer [85].

Figure II.9 : Some field of use of diatomite [86-89].

The diatomite used in this study is raw Algerian diatomite from the TAHLAIT ENOF Sig deposit located southeast of the city of SIG in the Wilaya of Mascara. It is a white-colored diatomite.

II.7.5 Diatomite processing steps

The diatomite is processed in five steps:

- ✓ Extraction;
- ✓ Crushing;
- ✓ Grinding;
- ✓ Purification;
- ✓ Calcination.

Depending on the type of treatment, kieselguhr can be classified into three classes:

- ✓ Dry diatomite: Depending on the climatic conditions of the deposit location, transportation and storage conditions, the moisture content may vary from 30 to 65%. This moisture can be removed by drying in ovens.
- ✓ Calcined diatomite: To change the grain size, heating is carried out at temperatures between 800 and 1000 °C. The degree of consolidation of the particles depends on this temperature and the processing time.
- ✓ Activated diatomite: Diatomite is calcined with the addition of alkali such as sodium carbonate (1 to 6%). The two compounds are well mixed and then treated at temperatures of 1000 to 1200 °C.

  The addition of carbonate leads to the formation of sodium silicate, a necessary flux for agglomerating the grains.

The treatment steps for different types of diatomite are presented in figure II.11:

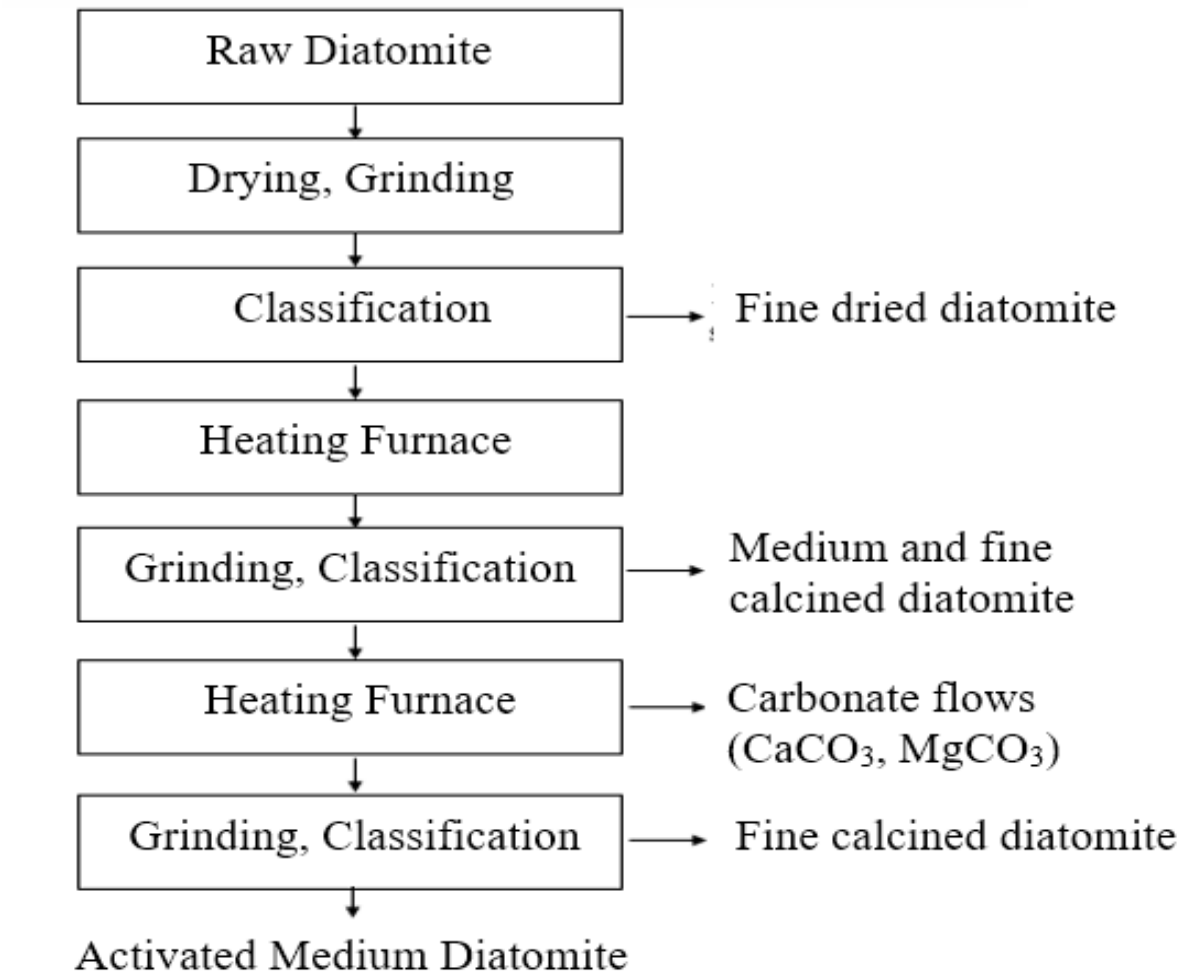

Figure II.10 : Processing steps of different type of diatomite [69].

Knowledge of the physical properties of raw materials is of paramount importance for any forming process as they control the elaboration, microstructure, and properties of the final product. It is also necessary to qualitatively and quantitatively understand the chemical composition of the raw material and the phases present in order to comprehend the physical or chemical transformations or reactions that may occur within the material due to temperature or an external agent [89].

II.7.6 Physical and chemical characteristics of diatomite

Diatomite is mainly composed of silica and impurities (organic compounds, sand, clay, calcium and magnesium carbonate, salts, etc.). The average chemical composition of diatomite from different regions is presented in Table II.6:

Component %	California	Nevada	France	Germany	Algeria
SiO_2	88.9	83.13	86	89.5	78.65
Al_2O_3	3	4.6	2.8	4.1	4.86
C_aO	0.53	2.5	0.6	0.5	4.88
M_gO	0.56	0.64	-	-	1.05
Fe_2O_3	1.69	2	4.7	1.6	1.46
Na_2O	1.44	1.6	0.7	3.6	-
K_2O	1.44	1.6	0.7	3.6	0.78
V_2O_5	0.11	0.05	-	-	-
TiO_2	3.60	5.3	-	-	0.34
Fire loss	0.14	0.18	0.3	0.2	-

Table II.6 : Chemical composition of Diatomite from different regions of the world [69,90].

II.7.7 Classification of diatomites according to KARPOV

The Russian standards have classified diatomites based on their content of main minerals, as well as moisture and bulk density, as follows:

Components	1st quality	2nd quality	3rd quality
SiO_2 not less than	80%	62%	51%
C_aO not more than	9%	11%	17%
H_2O not more than	25%	_	_
Volume weight (kg/m^3)	730	_	_

Table II.7 : Classification of Diatomite according to Russian standards (KARPOV, 1979).

II.7.8 Raw and Calcined Diatomites

The amorphous nature and highly porous structure of diatomite result in strong phonon diffusion and low thermal conductivity. These properties define its application in thermal insulation. Figure II.12 shows micrographs of raw and calcined diatomites taken with a scanning electron microscope (SEM) [91].

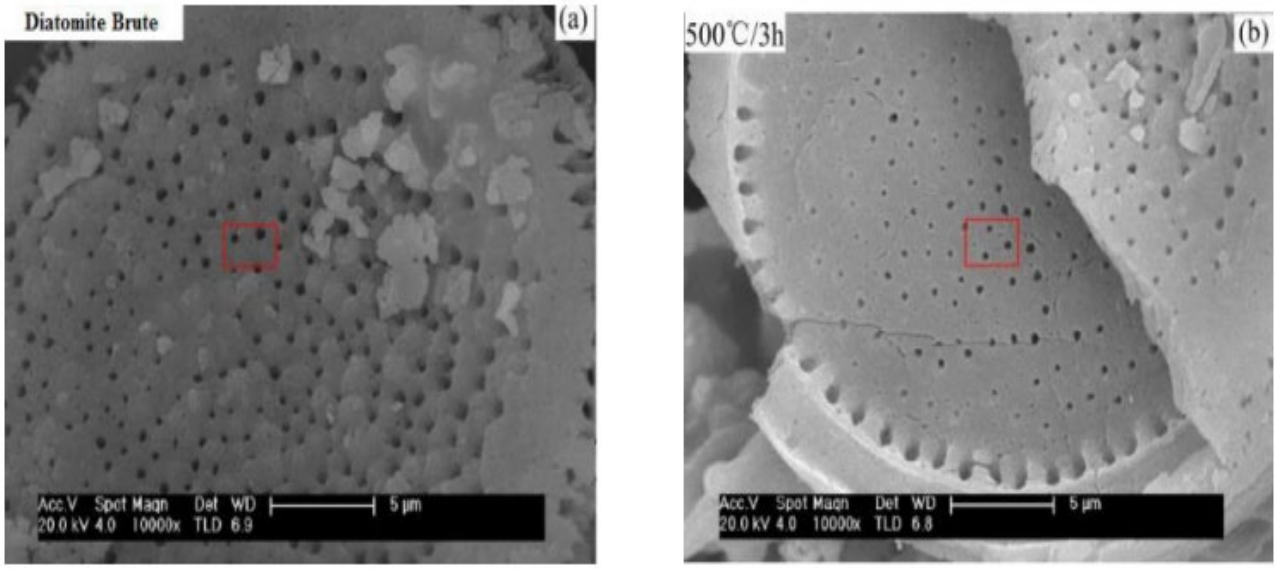

Figure II.11 : SEM of raw (a) and calcined (b) diatomite.

The raw diatomite has a round plate structure with uniform pore size and distribution as shown in Figure II.12 (a). According to Figure II.12 (b), it can be observed that the morphology of the diatomite's micropores changes after calcination at 500 °C for 3 hours. The number of small pores increases and the pores become smaller, with a minimum diameter of approximately 50 nm. Calcined diatomite can enhance moisture control performance due to its small and dense pores compared to raw diatomite. Figure 7 presents a comparative study of sorption and desorption performances between raw and calcined diatomite conducted by J. Zheng et al. [92].

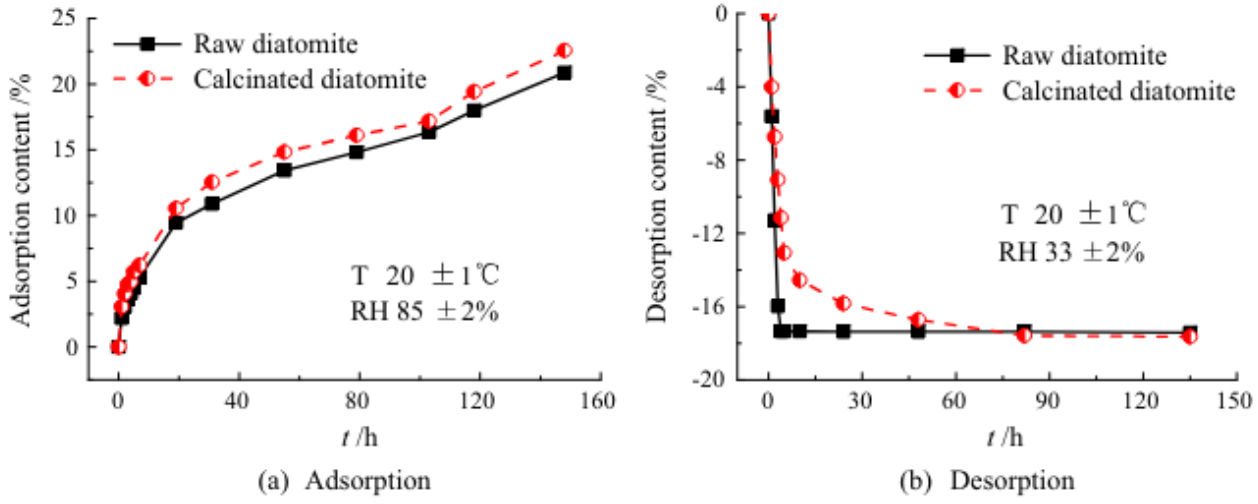

Figure II.12 : Content of adsorption and desorption of raw and calcined diatomite [91].

Figure II.13 illustrates that calcination can enhance the adsorption and desorption performance of raw diatomite. The adsorption capacity of calcined diatomite is superior to that of raw diatomite, suggesting that calcined diatomite has denser pores, which generate higher capillary forces and make

it more effective at controlling indoor relative humidity. Moreover, calcined diatomite exhibits slower moisture release, as its small and compact pores facilitate water retention.

A study by S. Benayache et al. [91] investigated the chemical composition of Algerian raw diatomite and compared it with diatomite calcined at 1100°C for two hours. As indicated in Table II.8, the calcined diatomite had a significantly higher silica content compared to the raw diatomite, as highlighted in Table II.8.

Constitute	S_iO_2	C_aO	M_gO	Al_2O_3	M_nO	T_iO_2	K_2O	Fe_2O_3	L.O.I
Raw Diatomite (%)	60.71	16.25	0.40	7.90	0.04	0.25	1.05	1.17	14.65
Calcined Diatomite (%)	73.14	15.72	0.36	8.08	0.04	0.16	1.37	1.45	-

Table II.8 : Chemical compositions of raw and calcined Algerian diatomite, [30]

II.8 Application of the composite (Diatomite /PCM) as construction material

In recent years, there has been a growing use of PCMs in the construction industry, owing to the availability of various PCM types. However, PCM leakage during melting and freezing cycles has been a concern, leading to the development of different incorporation methods that need to be carefully selected based on the intended application of PCM in the host construction material. The efficacy of PCM-fiber composite systems (PCMSS) is largely dependent on the support material and impregnation process used. Diatomite, known for its hygroscopic properties, has emerged as a key support material for PCMSS composites.

For instance, Karaman et al. [19] successfully developed a stable shape phase change material (PCM) composite by incorporating polyethylene glycol (PEG) into the pores of diatomite. This method involved carefully infusing PEG into the porous structure of diatomite, ensuring that the PCM was effectively retained within the material matrix. The composite demonstrated excellent thermal energy storage characteristics, with PEG being retained at 50% by weight within the diatomite pores without any leakage of molten PEG. This indicates that the composite can withstand multiple thermal cycles without degradation, making it a reliable material for thermal energy storage applications. The integration of PEG into diatomite not only utilized the high latent heat capacity of PEG but also leveraged the structural stability of diatomite to prevent leakage and improve durability. Wu et al.

[22] prepared a PCM/diatomite composite with an encapsulated PCM ratio of 12.9%. The preparation involved thoroughly mixing the PCM with diatomite and ensuring uniform encapsulation to achieve the desired ratio. This composite was particularly effective in regulating indoor temperature and relative humidity, crucial factors for maintaining thermal comfort and energy efficiency in buildings. When tested in a building environment, the composite led to potential energy savings of up to 18%. The study highlighted the superior hygrothermal performance of this PCM-hygroscopic composite compared to a simple combination of two separate layers of PCM and hygroscopic materials. This superiority is attributed to the integrated approach, which enhances thermal storage and moisture absorption simultaneously, thereby improving the overall energy efficiency and indoor climate control. Other studies have explored the use of various hygroscopic materials to create PCM storage systems (PCMSS) composites. Qin et al. [21] investigated PCMSS composites using microencapsulated PCMs with SiO_2 as the shell and different hygroscopic materials such as vesuvianite, sepiolite, and zeolite. The microencapsulation process involved coating the PCM with a silica shell, which provided a robust barrier against leakage and improved thermal stability. The study found that the SiO_2-PCM/vesuvianite composite demonstrated better hygrothermal performance compared to the other two composites. Vesuvianite, with its high moisture absorption capacity and thermal stability, outperformed sepiolite and zeolite in maintaining a stable indoor environment. This finding suggests that vesuvianite is particularly effective in applications requiring both moisture regulation and thermal energy storage. Benayache et al. [91] studied the impregnation of Algerian raw and calcined diatomite with a mixture of paraffin wax (PW) and liquid paraffin (LP) to create PCM composites. This process involved soaking the diatomite in a paraffin mixture to ensure deep penetration and uniform distribution of the PCM within the pores. These composites were designed to have a melting temperature below 30°C and appropriate latent heat properties to suit various thermal management applications. The resulting PCM composites based on paraffin and calcined diatomite had a melting temperature of 28.44°C and a latent heat of about 56.40 J/g. These thermal properties are ideal for applications in regions with moderate temperature variations, enabling efficient thermal energy storage and release during daily temperature cycles. Chen et al. [5] developed a PCMSS composite with different mass ratios of PCM encapsulation using SiO_2 as the shell and diatomite as the hygroscopic material. The preparation involved optimizing the mass ratios to balance thermal storage and moisture absorption capabilities. The SiO_2 shell effectively reduced the degree of supercooling of molten PCM masses, preventing PCM leakage while maintaining the hygroscopic properties of diatomite. This dual functionality enhances both the thermal and moisture-regulating capabilities of the composite, making it a versatile material for building energy efficiency. The reduced supercooling effect also ensures that the PCM transitions occur at more predictable

temperatures, enhancing the reliability of the thermal storage system. Fraine et al. [2] also developed a PCM/diatomite composite with an encapsulated PCM ratio of 12.9%, which was used to remodel the cavities of hollow bricks. The implementation involved integrating the composite material into building elements, such as bricks, to enhance their thermal performance. The use of this composite in building materials significantly reduced fluctuations in indoor temperature and relative humidity, resulting in a 50% reduction in total heat flux. This indicates that the composite has a high capacity for improving the energy efficiency and thermal comfort of buildings. By embedding PCM composites directly into structural elements, the overall thermal inertia of the building is increased, leading to more stable indoor temperatures and reduced energy consumption for heating and cooling.

II.9 Conclusion

The investigation described in the second chapter revealed that utilizing moisture control materials with latent heat storage has numerous benefits in terms of reducing energy consumption and ensuring human hygrothermal comfort.

In the initial part, we provided an initial explanation of thermal energy storage using phase change materials (PCMs) and concluded that latent heat storage is more favorable due to its ability to store larger amounts of energy with minimal changes in mass and temperature. We also discussed recent research on incorporating PCMs in building materials, examining the advantages and drawbacks of this technique. One significant challenge associated with PCM use is the possibility of leakage, which can negatively impact the mechanical, thermal, and durability properties of building materials. To overcome these concerns, researchers have proposed solutions.

In the second part, we presented the various deposits of diatomite found in Algeria and explored the possibility of using Algerian diatomite and the PCHCM composite as insulation materials in the building sector. Diatomite is environmentally friendly and characterized by its high hygrothermal capacity, which promotes optimal comfort conditions.

In conclusion, diatomite is an insulation material that can be used for both interior and exterior building insulation, and will be further discussed in the following chapter.

Chapter III

Overview of Experimental Procedure and Numerical Problem Analysis

III.1 Introduction

Due to their high energy and natural resource consumption, buildings have a significant impact on the environment, which leads to a significant increase in toxic emissions. To mitigate these effects, the use of environmentally friendly insulation materials in construction, such as diatomite, is necessary. This solution not only reduces energy consumption but also improves the hygrothermal comfort of occupants. This chapter describes the different stages of experimentation that we conducted at the Abou Bekr Belkaid University of Tlemcen to study thermal insulation based on diatomite and PCHCM on a brick wall commonly used in Algerian buildings. We also present the various stages that were followed in a numerical simulation to validate our experiments.

III.2 Description of experimental protocol available at the University of Tlemcen

In the experiment, three brick walls were built, with different finishing layers.




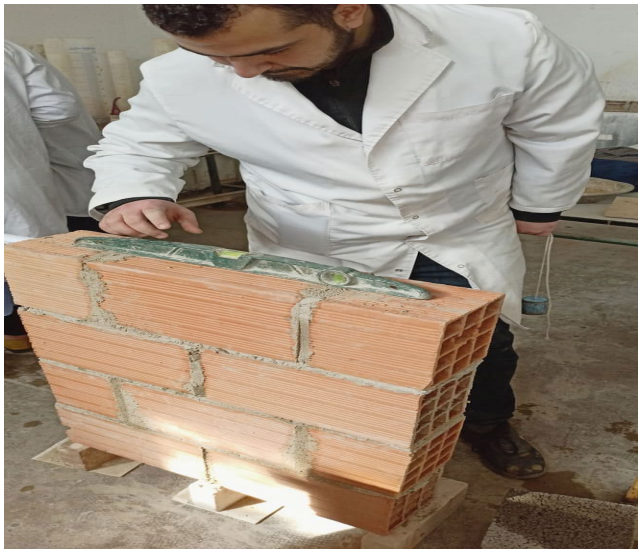

Figure III.1: Some photos of our experience.

The experimental setup entailed the meticulous construction of three brick walls, meticulously engineered to meet specific dimensions of 83 cm x 61.5 cm x 17 cm. These walls served as the focal point of the experiment, meticulously crafted using hollow bricks carefully selected for their structural properties. Each brick was intricately designed with 12 air cavities. The individual bricks, measuring 30 x 20 x 15 cm, were strategically arranged to form the walls, with particular attention paid to ensuring precise alignment and stability. The air cavities within each brick were meticulously crafted in a parallelepiped configuration, each boasting dimensions of 3.9 × 3.9 cm^2. This intricate design not only added to the structural integrity of the bricks but also facilitated controlled airflow within the walls, a crucial aspect of the experimental investigation. In the construction process, mortar played a pivotal role, serving as the binding agent between the bricks. Each brick was meticulously placed and secured using the prepared mortar, with joints meticulously filled to a thickness of 1.5 cm. This meticulous attention to detail in the construction process ensured the structural integrity and stability of the walls, laying the groundwork for the subsequent experimental investigations. The experimental design comprised three distinct scenarios, each characterized by a unique finishing layer applied to the surface of the walls:

Case 1: A 2 cm layer of mortar served as the finishing layer, meticulously applied to the surface of the walls. The application process followed stringent protocols to ensure uniformity and consistency, as depicted in the schematic representation presented in Figure III.2. The reference mortar composition, meticulously formulated, consisted of 1 part cement (C) and 3 parts sand (S), meticulously mixed to achieve a consistent texture and composition. The water-cement ratio (W/C) was carefully maintained at 0.5, ensuring optimal hydration and adhesive properties.

Case 2: In this scenario, a 2 cm layer of diatomite was meticulously applied as the finishing layer. Diatomite, renowned for its insulating properties and environmentally friendly nature, was carefully selected to explore its potential as a finishing material for the walls. The application process was meticulously executed, with precise attention paid to achieving an even distribution of the diatomite layer across the surface, as illustrated in Figure III.3.

Case 3: This scenario introduced a novel approach by applying a composite finishing layer comprised of 2 cm of diatomite infused with paraffin, featuring a melting point of 54°C, as depicted in Figure III.4. This meticulous application ensured uniform distribution and adherence of the composite layer, laying the groundwork for detailed analysis and evaluation of its thermal properties and performance characteristics.

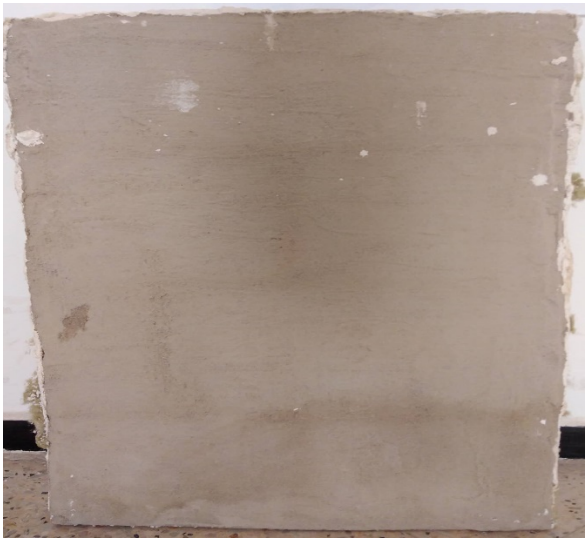

. Figure III.2 Brick wall with a Mortar finishing layer.

Figure III.3: Brick wall with a Diatomite finishing layer.

Figure III.4: Brick wall with a PCHCM finishing layer.

III.2.1 Advanced Instrumentation for Thermal Analysis

The experimental setup was meticulously designed, featuring two compartments accurately crafted from sturdy 1.5 cm thick plywood panels, ensuring structural integrity and stability throughout the experiment. To enhance thermal insulation and maintain optimal environmental conditions within the compartments, the plywood panels were meticulously insulated with an 8 cm thick layer of extruded polystyrene, meticulously applied to all interior surfaces. This insulation arrangement, meticulously depicted in Figure III.6, served as a crucial barrier against external temperature fluctuations, ensuring the internal climate remained consistent and conducive to precise experimental conditions. Compartment 1, with a calculated volume of 0.34 m^3, was specifically outfitted with sophisticated temperature and humidity control mechanisms. This compartment housed a meticulously calibrated heater and humidifier, meticulously positioned to facilitate precise regulation of temperature and humidity levels throughout the duration of the experiment. The humidifier, leveraging ultrasonic wave technology, generated a gentle, cool steam, contributing to the maintenance of optimal humidity levels within the testing chamber. The meticulous control over temperature and humidity was facilitated by the utilization of state-of-the-art instrumentation, notably the ZL-7918A device. This advanced control unit ensured the accurate calibration and maintenance of climatic conditions within the testing chamber, guaranteeing consistency and reliability in experimental procedures. Compartment 2, boasting a volume of 0.64 m^3, served as the observation chamber, housing an array of temperature and humidity sensors meticulously positioned 35 cm away from side 2 of the wall under scrutiny. These sensors, meticulously calibrated and synchronized, provided real-time feedback on environmental conditions within the chamber, enabling precise monitoring and analysis of thermal performance. To complement the sensor array, an infrared camera of the highest caliber, the Testo 890, was strategically positioned on the exit side of compartment 2, meticulously aligned to capture temperature and humidity data on side 2 of the wall, as illustrated in Figure 1. This cutting-edge imaging device, equipped with advanced thermal sensing capabilities, facilitated the non-invasive measurement of surface temperatures and humidity levels, providing invaluable insights into thermal dynamics and moisture distribution across the experimental setup. Moreover, the Testo 890 boasted robust data storage capabilities, meticulously archiving all temperature and humidity-related data captured throughout the experiment. This comprehensive data logging functionality ensured the preservation of experimental records, facilitating thorough analysis and validation of research findings.

The compartment 1 was gradually heated using resistance heaters, controlled by the ZL-7918A temperature and humidity regulation device. Temperatures were precisely set according to the required specifications for the experiment or process at hand. During this phase, the ZL-7918A device played a crucial role in regulating and maintaining temperature parameters in compartment 1,

ensuring uniform and controlled heating. Concurrently, sensors were deployed in compartment 2 to monitor environmental conditions, including temperature and humidity, to ensure their stability and homogeneity. Once temperatures in compartment 2 reached a state of thermal equilibrium, indicating stable conditions, the cooling process in compartment 1 was initiated. Temperatures were adjusted and maintained at 25.5°C, in line with the specific requirements of the experimental protocol or production. Throughout this process, the ZL-7918A device played a central role in ensuring precise and reliable control of environmental conditions, which is crucial for the success of many scientific and industrial applications.

Figure III.5 : Photos on the experimental device.

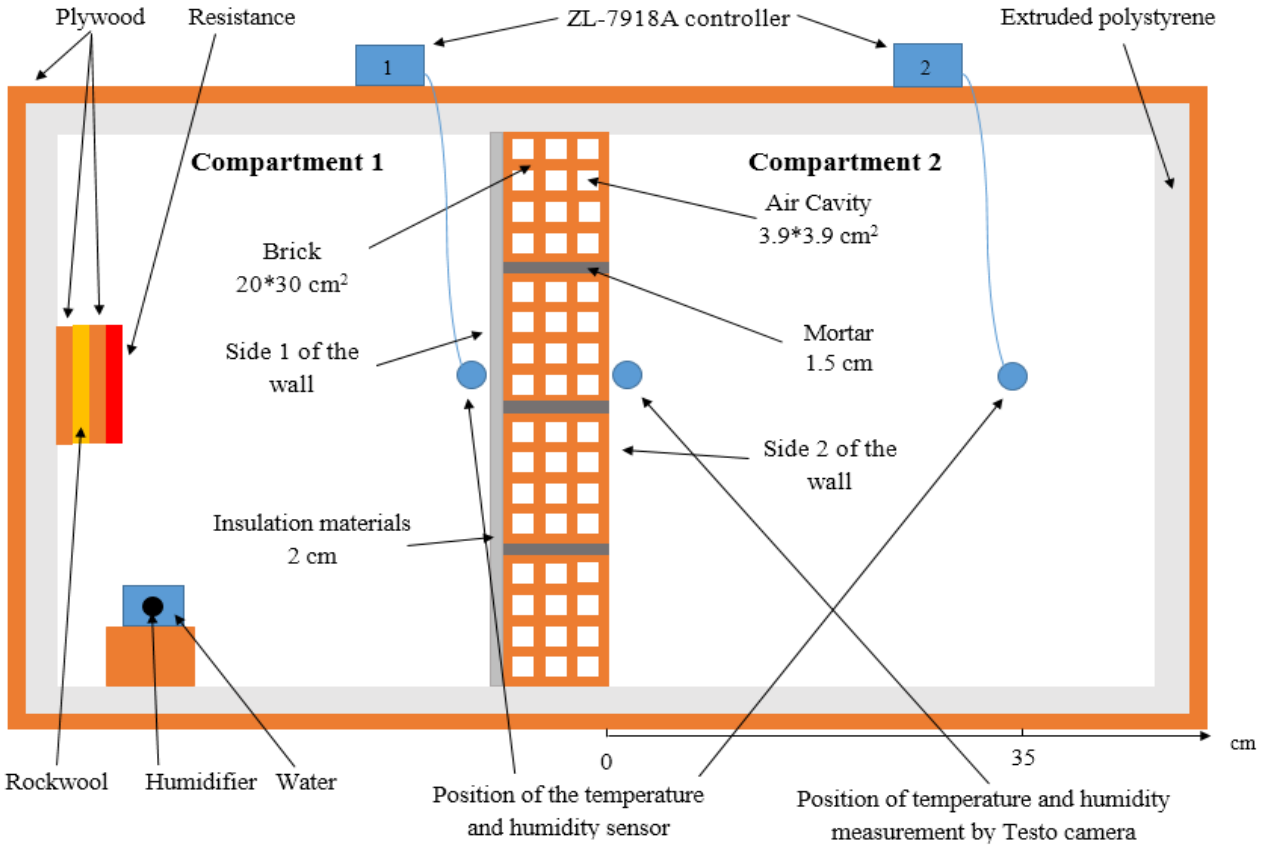

Figure III.6 : Explanatory diagram of the experimental device.

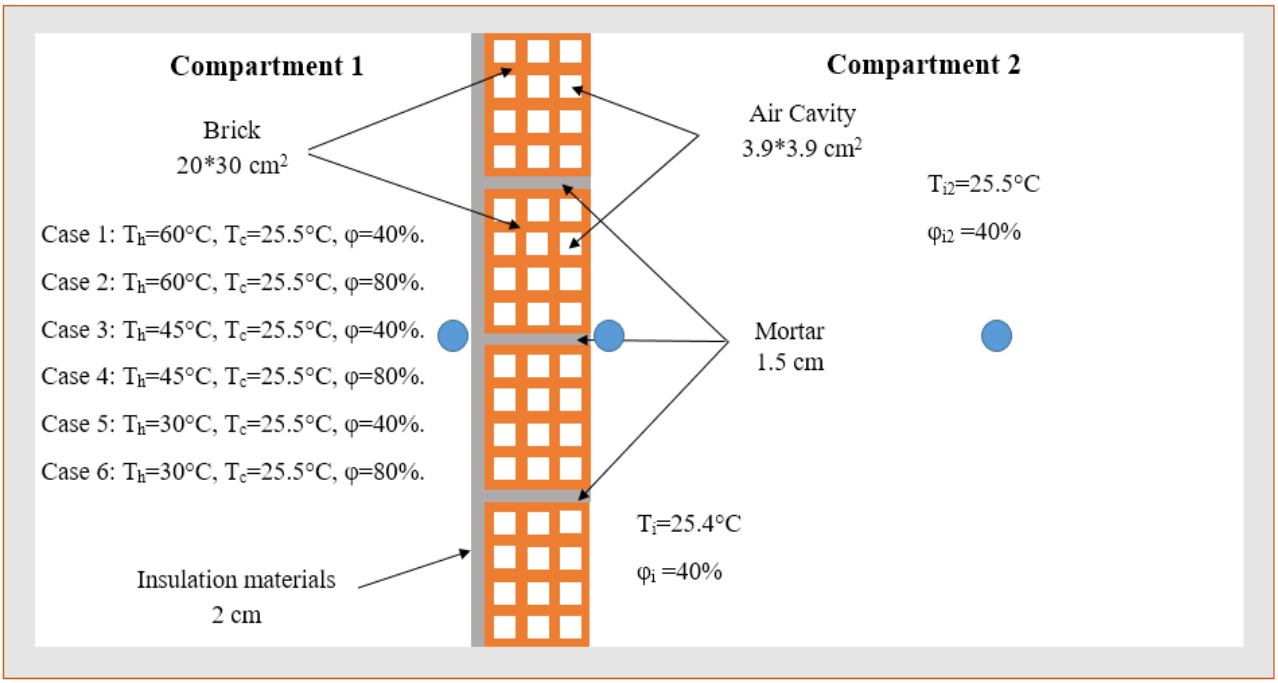

Figure III.7 : Boundary conditions in the experiment.

III.2.2 Materials used to measure and control temperature and humidity

III.2.2.1 ZL-7918A Temperature and Humidity Controller

ZL-7918A is an intelligent, safe, and stable temperature and humidity controller, applicable for controlling climate chambers, warehouses, and more. It has the ability to control lighting, temperature, humidity, auxiliary heating, ventilation, and alarms. It boasts high accuracy with a wide measuring range.

Figure III.8: ZL-7918A controller.

III.2.2.2 Silicone resistor

It consists of two copper wires covered with a layer of silicone that forms a cylindrical shape. The length of this resistance is 4m and its diameter is 5mm. This resistance stands out from others for its response speed, as the temperature does not increase significantly when the required temperature is reached within +2°C and -2°C.

Figure III.9: Silicone resistor.

III.2.2.3 Air humidifier

It is a device for providing humidity. It operates through ultrasonic waves that strike water, causing it to rise in the form of a fine, cool mist.

Figure III.10 : Air humidifier.

III.2.2.4 Testo 890 thermal camera

The Testo 890 camera captures thermal processes in real-time and features a USB 2.0 interface for direct transfer of thermographic recording data to a PC, enabling analysis at any time. To configure video settings, the IRSoft software on a PC is utilized. The camera is highly suited for monitoring temperature changes in various processes. It provides temperature measurements from different points pixel by pixel, making it possible to evaluate thermal changes over time. The camera's recording function allows for the capture of different individual images at defined intervals or after specific events, such as exceeding limit values. Testo places great emphasis on the quality of the detector, which is the heart of all thermal cameras. The Testo 890 camera, with its integrated 640 x 480 pixel detector and high-quality germanium optics, achieves exceptional image quality. The camera's ability to detect a higher number of measurement points in the thermal image allows for more precise identification and analysis of details. Additionally, Testo's Super Resolution technology produces high-resolution thermal images with Megapixel quality (1280 x 960 pixels), enabling precise thermography of even the smallest or most distant measurement objects [93].

Figure III.11: Testo 890.

III.3 Theoretical study, governing equations and COMSOL programming

During our experimentation, we encountered challenges in sourcing certain materials, namely paraffin, and so we turned to numerical modeling to augment our studies. Over the years, there have been numerous research works undertaken, many of which have adopted phenomenological modeling approaches inspired by the pioneering work of AV. Luikov [47]. F. Tariku et al. [53] developed a dynamic model to address the issue of heat, air, and moisture transfer between the envelope and the chamber. M. Qin et al. [94] established a model based on water vapor concentration and temperature, which demonstrated significant agreement with experimental results. In their effort to provide valid data to the heat and moisture transfer model, TZ. Desta et al. [95] investigated the coupled transfer of heat, air, and moisture in a habitat. K. Abahri et al. [96] proposed a simplified, one-dimensional model for evaluating the coupled transfer of heat and moisture in porous building materials, which reduced the initial mathematical problem into a fourth-order equation that was easier to solve. DH. Xu et al. [97] developed a dynamic model that was coupled with heat and moisture transfer and condensation in a porous fabric with low temperature.

Energy and mass balances are expressed in terms of measurable transfer drivers (such as temperature, water content, vapor pressure, and relative humidity) and coefficients that are explicitly linked to the macroscopic properties of the materials (including thermal conductivity, specific heat, water vapor permeability, and diffusion coefficient) that have been determined experimentally. For our numerical study, we utilized a coupled heat and moisture transfer model that was established by Künzel [35]. In this model, we regarded temperature and relative humidity as driving potentials that regulate heat and moisture transfer while ensuring continuity of variables at the interface. The moisture content is shown to be discontinuous in Figure III.12. To solve the differential transfer

equations, we used a numerical simulation program called COMSOL Multiphysics, which is based on the finite element method [12].

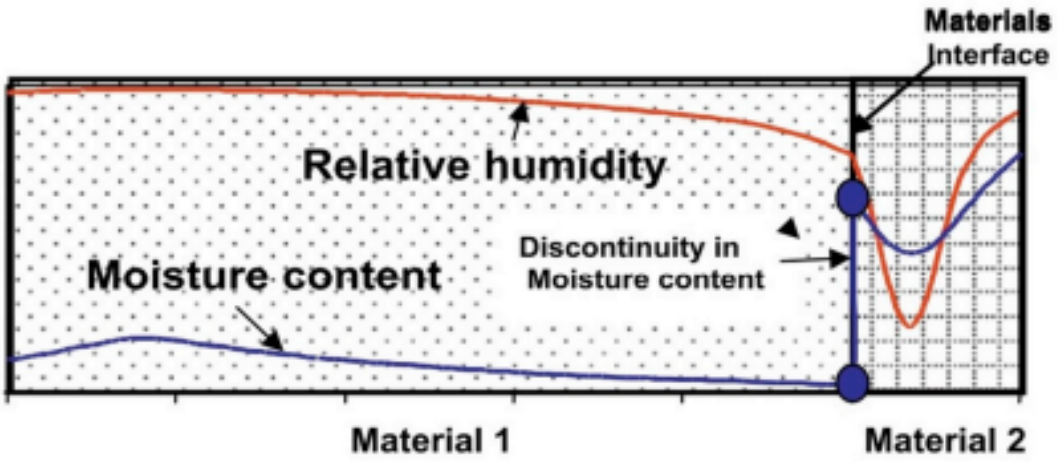

Figure III.12: Example of relative humidity and moisture content profiles at the interface of two different materials [30].

III.3.1 Model assumptions

The following assumptions are taken into account, as stated in the research by HM. Künzel [35]:

- ✓ The effects of chemical reaction, hysteresis, deformation, and gravity are not taken into account;
- ✓ Each material is considered as a homogeneous porous medium;
- ✓ Local thermodynamic equilibrium is verified (at the pore level);
- ✓ The liquid phase is composed only of pure water;
- ✓ Dry air and water vapor are treated as perfect and incompressible gases.

III.3.2 Governance equations of coupled heat and moisture transfer.

The process of heat and moisture transfer in porous materials is typically represented by a set of three partial differential equations. These equations are derived by ensuring that the balance of mass and energy is maintained within a small, infinitesimal volume element.

$$\begin{cases} \frac{\partial \omega}{\partial t} = -div(g_l + g_v) \\ \frac{\partial \omega_a}{\partial t} = -div(g_a) \\ C_p \rho_s \frac{\partial T}{\partial t} = -div(q) \end{cases} \quad \text{(III.1)}$$

III.3.2.1 Multiphase moisture transfer

Moisture transfer occurs in two forms: liquid and water vapor. Liquid water transfer is induced by a capillary pressure gradient, which is obtained by directly applying Darcy's law. Water vapor transport is a diffusion process under a vapor pressure gradient, which is obtained by Fick's law.

$$g_l = -k_l \nabla P_c - k_{fl} \nabla P \tag{III.2}$$

$$g_v = -k_v \nabla P_v - k_{fv} \nabla P \tag{III.3}$$

$$g_m = g_l + g_v = -k_v \nabla P_v - k_f \nabla P - k_l \nabla P_c \tag{III.4}$$

By considering the assumption of a local thermodynamic equilibrium at the pore level between the gas and liquid phase, Kelvin's law is applicable Nilsson [98], thus:

$$P_c = \frac{RT\rho_e}{M} ln\left(\frac{P_v}{P_{vsat}}\right) \tag{III.5}$$

Using Kelvin's law, the capillary pressure gradient is transformed into a combination of water vapor pressure gradient and a temperature gradient with a coefficient that expresses the contribution of a temperature difference in liquid water transfer.

$$\nabla P_c = \left[\frac{RT\rho_e}{MP_v}\right] \nabla P_v + \left[\frac{RT\rho_e}{M}\left(\frac{\partial ln\left(\frac{P_V}{P_{vsat}}\right)}{\partial T}\right) + \frac{R\rho_e}{M} ln\left(\frac{P_v}{P_{vsat}}\right)\right] \nabla T \tag{III.6}$$

$$P_{vsat} = exp\left(23{,}5771 - \frac{4042{,}9}{T-37{,}58}\right) \tag{III.7}$$

Therefore, the density of the mass flux of the liquid phase is written in the form:

$$g_l = -k_l^* \nabla P_v - k_{fl} \nabla P - k_T \nabla T \tag{III.8}$$

In the end, the total mass flux density is expressed as follows:

$$g_m = -k_m \nabla P_v - k_f \nabla P - k_T \nabla T \tag{III.9}$$

$$C_m \rho_s \frac{\partial P_V}{\partial t} = div(k_m \nabla P_v + k_f \nabla P + k_T \nabla T) \tag{III.10}$$

III.3.2.2 Gas phase transfer

Apart from the transfer of liquid water and water vapor under capillary pressure and vapor pressure gradients, there is also the transfer of dry air and water vapor in the porous material through an infiltration process caused by a total pressure gradient ∇P. This gas infiltration phenomenon is represented by Luikov [47] in the following manner:

$$g_a + g_v = -k_f \nabla P \tag{III.11}$$

$$\omega_l + \omega_v = \frac{PM}{RT\rho_S}\varepsilon(1 - S_l) \quad \text{(III.12)}$$

By proceeding with a partial derivation of the equation:

$$d\left(\frac{PM}{RT\rho_S}\varepsilon(1 - S_l)\right) = \left(\frac{M}{RT\rho_S}\varepsilon(1 - S_l)\right)\nabla P \quad \text{(III.13)}$$

The gas phase balance equation:

$$C_a\frac{\partial P}{\partial t} = div\left(k_f\nabla P\right) \quad \text{(III.14)}$$

III.3.2.3 Heat transfer

Heat transfer in porous media occurs in three different forms, as described by Crausse et al.[99]: conduction under a temperature gradient, which is expressed by Fourier's law; sensible heat advection through liquid and water vapor fluxes; and latent heat transfer due to phase change carried by water vapor. Consequently, the density of the heat flux is expressed as follows:

$$q = -\lambda\nabla T + h_l g_m + l_v g_v \quad \text{(III.15)}$$

$$h_l = c_l(T - T_{ref}) \quad \text{(III.16)}$$

By replacing the total mass flux density and water vapor flux density expressed in the previous equations, the final form of the heat flux density is written as follows:

$$q = -(\lambda + h_l k_T)\nabla T - h_l(k_m\nabla P_v + k_f\nabla P) + l_v j_v \quad \text{(III.17)}$$

The final expression for the heat flux, the energy conservation balance equation, becomes:

$$C_p\rho_s\frac{\partial T}{\partial t} = \mathrm{div}(\lambda\nabla T + \alpha\nabla P_v + \gamma\nabla P) + l_v\rho_s C_m\sigma\frac{\partial P_v}{\partial t} \quad \text{(III.18)}$$

We conclude that the last three equations are:

$$\begin{cases} C_m\rho_s\frac{\partial P_V}{\partial t} = div(k_m\nabla P_v + k_f\nabla P + k_T\nabla T) \\ C_a\frac{\partial P}{\partial t} = div\left(k_f\nabla P\right) \\ C_p\rho_s\frac{\partial T}{\partial t} = \mathrm{div}(\boldsymbol{\lambda}\nabla T + \alpha\nabla P_v + \gamma\nabla P) + l_v\rho_s C_m\sigma\frac{\partial P_v}{\partial t} \end{cases} \quad \text{(III.19)}$$

The PCHCM composite was modeled using the coupled heat and moisture transfer model presented above. The PCM was incorporated into the porosity of the diatomite. The volumetric fraction of diatomite was defined as θ_d, and the volumetric fraction of PCM was equal to $(1\text{-}\theta_d)$. Therefore, the effective thermal properties of the medium assuming a parallel configuration are:

$$(\rho\ Cp)_{eff} = \rho_d\ Cp_d\ \theta_d + \rho_{PCM}\ Cp_{PCM}\ (1 - \theta_d) \quad \text{(III.20)}$$

The PCM was modeled using the modified specific heat capacity equation [30]:

$$Cp_{PCM}\begin{cases} Cp_s \;\; if\; T_m < T \\ \left(\frac{Cp_s + Cp_{li}}{2} + \frac{L_{h_v}}{\nabla T}\right) \;\; if\; T_m \le T \le (T_m + 1) \\ Cp_{li} \;\; if\; (T_m + 1) < T \end{cases} \quad \text{(III.21)}$$

III.3.3 Boundary conditions that were adopted to match the experiment

The boundary conditions for humidity for compartment 1 and compartment 2 of the wall are given by equations (III.22) and (III.23), respectively:

$$\left(D_w \cdot \xi + \delta_p \cdot P_{v,s}(T)\right)\nabla\Phi + \delta_p \cdot \Phi \cdot \frac{\partial P_{v,s}(T)}{\partial \mathrm{t}} \cdot \nabla T = \beta_1\left(\Phi_1 \cdot P_{v,s}(T_1) - \Phi \cdot P_{v,s}(T)\right) \quad \text{(III.22)}$$

$$\left(D_w \cdot \xi + \delta_p \cdot P_{v,s}(T)\right)\nabla\Phi + \delta_p \cdot \Phi \cdot \frac{\partial P_{v,s}(T)}{\partial \mathrm{t}} \cdot \nabla T = \beta_2\left(\Phi_2 \cdot P_{v,s}(T_2) - \Phi \cdot P_{v,s}(T)\right) \quad \text{(III.23)}$$

The experimental boundary conditions for the heat flux at the surfaces of compartments 1 and 2 are given by equations (III.24) and (III.25), respectively:

$$\lambda_{eff}\nabla T + h_v \cdot \delta_p \cdot P_{v,s}(T) \cdot \nabla\Phi = h_n \cdot (T_1 - T) + \beta_1 \cdot h_v(\Phi_1 \cdot P_{v,s}(T_1) - \Phi \cdot P_{v,s}(T)) \quad \text{(III.24)}$$

$$\lambda_{eff}\nabla T + h_v \cdot \delta_p \cdot P_{v,s}(T) \cdot \nabla\Phi = h_n \cdot (T_2 - T) + \beta_2 \cdot h_v(\Phi_2 \cdot P_{v,s}(T_2) - \Phi \cdot P_{v,s}(T)) \quad \text{(III.25)}$$

The natural convection heat transfer coefficient can be found in Ref. [100] as:

$$h_n = \begin{cases} \frac{k}{L} \cdot \left(0.68 + \frac{0.67 \cdot Ra_l^{\frac{1}{4}}}{\left(1 + \left(\frac{0.492 \cdot k}{\mu C_p}\right)^{\frac{9}{16}}\right)^{\frac{4}{9}}} \right) \; if\; Ra_l < 10^9 \\ \frac{k}{L} \cdot \left(0.825 + \frac{0.387 \cdot Ra_l^{\frac{1}{6}}}{\left(1 + \left(\frac{0.492 \cdot k}{\mu C_p}\right)^{\frac{9}{16}}\right)^{\frac{8}{27}}} \right)^2 \; if\; Ra_l < 10^9 \end{cases} \quad \text{(III.26)}$$

III.3.4 Boundary conditions adopted for numerical studies

The numerical boundary conditions for the heat flux at the interior and exterior surfaces of the building wall are given by equations (III.27) and (III.28), and for the moisture flux, equations (5) and (6) are used:

$$\lambda_{eff}\nabla T + h_v \cdot \delta_p \cdot P_{v,s}(T).\nabla\Phi = h_{a,int} \cdot \left(T_{a,int} - T\right) + \beta_{s,int} h_v(\Phi_{a,int} \cdot P_{v,s}(T_{a,int}) - \Phi \cdot P_{v,s}(T)) \quad \text{(III.27)}$$

$$\lambda_{eff}\nabla T + h_v \cdot \delta_p \cdot P_{v,s}(T) \cdot \nabla\Phi = h_{a,ext} \cdot (T_{a,ext} - T) + \varepsilon \cdot \sigma \cdot (T_\infty^4 - T_{a,ext}^4) + \beta_{s,ext} h_v (\Phi_{a,ext} \cdot P_{v,s}(T_{a,ext}) - \Phi \cdot P_{v,s}(T)) \quad \text{(III.28)}$$

The convective heat transfer coefficients for wind, indoor air, and sky temperature are found as [30,101]:

$$h_{a,int} = 2.8 + 3 \cdot V_a \quad \text{(III.29)}$$

$$h_{a,ext} = 2.8 + 3 \cdot V_{vent} \quad \text{(III.30)}$$

$$T_\infty = 0.0552 \cdot (T_{a,ext})^{1.5} \quad \text{(III.31)}$$

Where, V_a is the average indoor air velocity, taken as 0.15 [m/s] according to ASHRAE standard as a comfortable ventilation velocity [30].

The convective mass transfer coefficient is derived from the convective heat transfer coefficient by considering the Illig analogy which has been experimentally approved by Schwarz [102]:

$$\beta_s = 7 \cdot 10^{-9}\, h_a \quad \text{(III.32)}$$

The hygrothermal properties of the materials used in the numerical solution are provided in Table III.1, Table III.2, and Table III.3, and illustrated in Figure III.13.

Properties	Diatomite [30,103,104]	Mortar [30,105]	Brick [30]	Air [30]	PCM [106,30]		PCHCM (16%) [30]	
					Liquid	solid	liquid	solid
λ [W/(m.K)]	0.097	1.41	0.682	0.026	0.149	0.21	0.106	0.116
ρ_s [kg/m^3]	400	1863	1600	1.26	912	769	481.9	459.04
C_p [J/(kg. K)]	1436.5	1076.5	840	1006.43	2660	2140	1632.26	1549.06
Melting temperature [°C]	-	-	-	-	54	-	53	-
Latent heat [kJ/kg]	-	-	-	-	238	-	38.08	-

Table III.1: Hygrothermal properties of the materials used.

Properties	PCM1 [30]		PCHCM1 (16% PCM1)		PCM2 [107]		PCHCM2 (8% PCM1, 8% PCM2)	
	liquid	solid	Liquid	solid	liquid	solid	liquid	solid
λ [W/(m.K)]	0.149	0.35	0.106	0.138	0.14	0.18	0.105	0.125
$\boldsymbol{\rho_s}$ [kg/m^3]	775	814	460	466.24	810		462.8	465.92
$\boldsymbol{C_p}$ [J/(kg. K)]	2660	2140	1632.26	1549.06	3800	4000	1723.04	1697.44
Melting temperature [°C]	28.1	-	27	-	22	-	21	-
Latent heat [kJ/kg]	145.9	-	23.34	-	136.2	-	22.568	-

Table III.2: Hygrothermal properties of PCMs.

Properties	Morocco [108]	Turkish [108]	China [30]
λ [W/(m.K)]	0.18	0.23	0.7
$\boldsymbol{\rho_s}$ [kg/m^3]	400	400	666.7
$\boldsymbol{C_p}$ [J/(kg. K)]	1436.5	1436.5	1436.5

Table III.3: Hygrothermal properties of different diatomites.

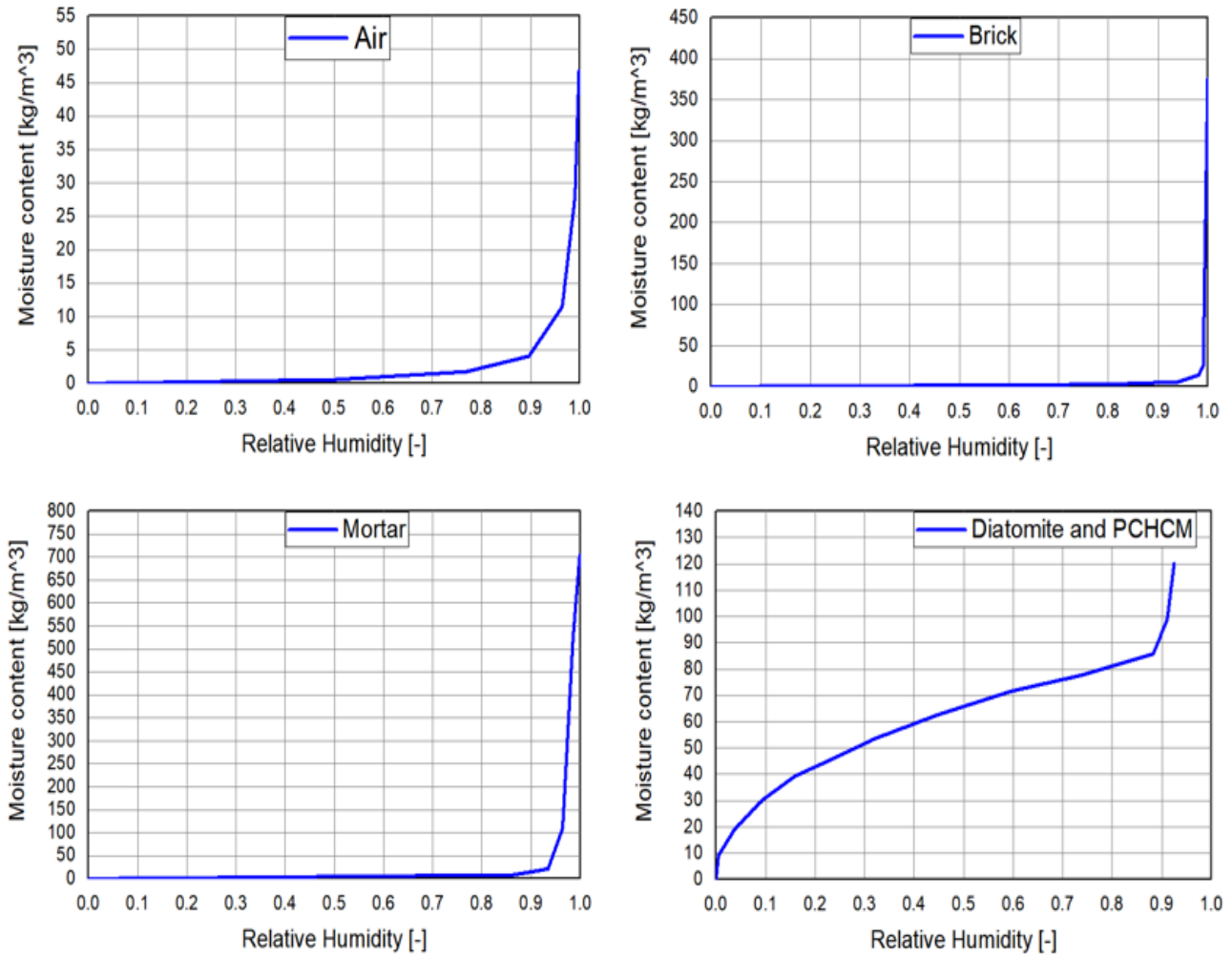

Figure III.13 : Sorption isotherms of the materials constituting the cases studied [12,109].

III.3.5 Numerical resolution

To obtain the temperature and relative humidity profile across a multi-layered wall, the coupled and nonlinear governing equations must be solved simultaneously. COMSOL Multiphysics was chosen as a computational tool to carry out this numerical study, which has become a reliable and proven tool due to its widespread use in the construction field by many researchers. COMSOL Multiphysics provides a library of predefined models to solve known engineering problems, such as convective diffusion, fluid dynamics, coupled heat and mass transfer, and other problems. It also allows the application of modeling techniques based on differential equations, called 'PDE modes,' to solve problems that standard modules may not be able to solve. Using this numerical technique, the developer formulates the PDEs that govern the physical phenomena and solves them using the integrated solver. Another advantage of COMSOL Multiphysics is its system's openness to other design and programming software such as AutoCAD, SolidWorks, Matlab, etc.

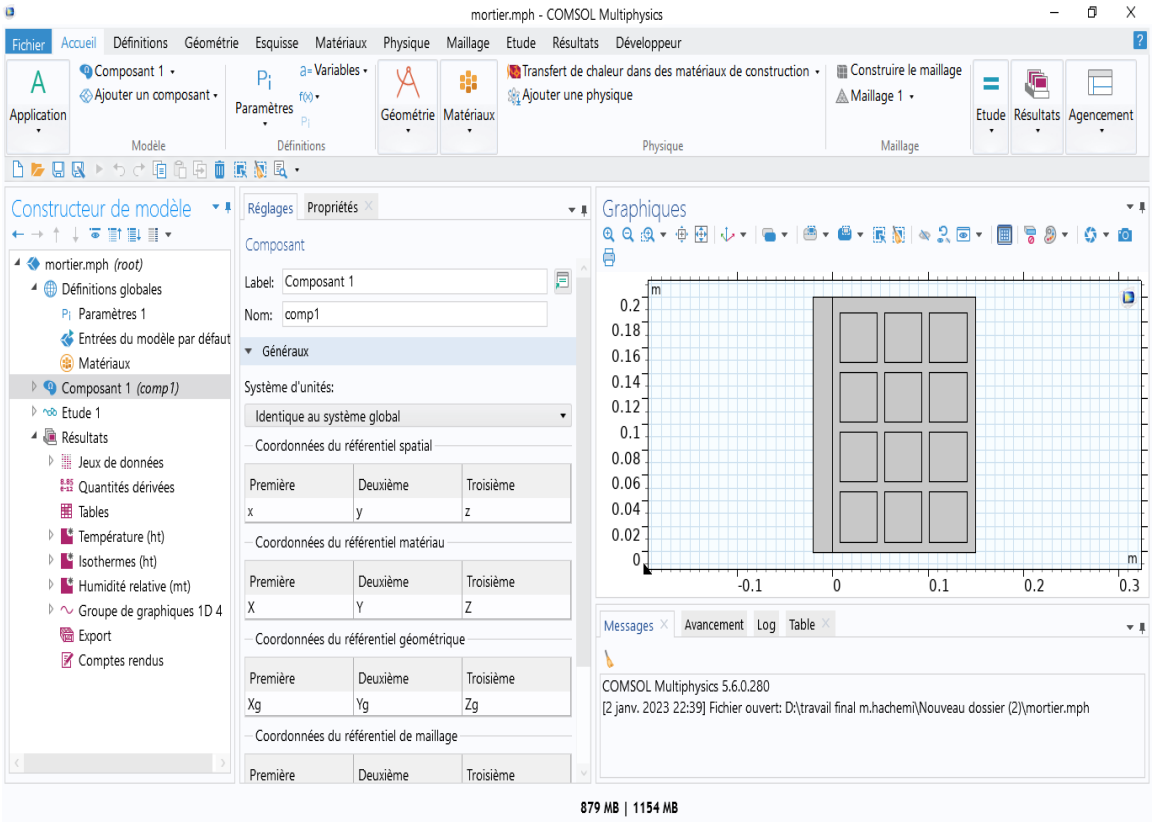

Figure III.14 : COMSOL Multiphysics software interface.

III.3.5.1 Steps of work on Comsol Multiphysics

We open the Comsol Multiphysics program, then the Modeling Assistant, and choose the space physics (2D), then select the physics: heat transfer, then heat and moisture transfer, then building materials, and click (add), then select the study, then the time study (finish). First, we draw the geometric shape, and then enter all the constant and variable information we need, then determine the types of materials present in the geometric shape, in order to enter the thermal properties for each material. Then we determine the type of physics that should be used, create and test the mesh, and finally choose the calculation step.

III.3.5.2 Finite element method

The finite element method is a numerical method for the approximate analysis of differential equations describing physical phenomena of geometry. Since around 1970, it has experienced impressive expansion, which goes hand in hand with the development and increasing power of computers. It has become a daily working tool, for calculation and design, even familiar to the engineer, in fields as diverse as structural analysis, heat transfer, fluid mechanics, electromagnetism, underground flows, combustion, or diffusion of pollutants.

III.3.5.2.1 Main lines of the method

Mesh choice

In 2003, Leung et al. [110] studied the elastic solid vibrations in two dimensions using a Fourier trapezoidal p-element. They found that the Fourier element was more accurate than Gaussian quadrature elements for vibration problems in the plane and was particularly effective for high-frequency vibrations.

- ✓ **Step 1:** Formulation of governing equations and boundary conditions. Most engineering problems are described by partial differential equations associated with boundary conditions defined on a domain and its boundary. The application of FEM requires a rewriting of these equations in integral form. The weak formulation is often used to include boundary conditions.
- ✓ **Step 2:** Division of the domain into subdomains. This step involves discretizing the domain into elements and computing the connectivity of each element as well as the coordinates of its nodes. It thus constitutes the geometric data preparation phase.
- ✓ **Step 3:** Approximation over an element. In each element, the variable such as displacement, pressure, temperature, is approximated by a simple linear, polynomial, or other function. The degree of the interpolation polynomial is related to the number of nodes of the element. The nodal approximation is appropriate. This is where the construction of the element matrices takes place.
- ✓ **Step 4:** Assembly and application of boundary conditions. All element properties must be assembled to form the algebraic system for the nodal values of physical variables. This is where the connectivities calculated in step 2 are used to construct global matrices from element matrices.
- ✓ **Step 5:** Solution of the global system: The global system can be linear or nonlinear. It defines either an equilibrium problem that concerns a stationary or static case or a critical value problem where one needs to determine the eigenvalues and eigenvectors of the system, which generally correspond to the frequencies and eigenmodes of a physical system. A propagation problem that concerns the transient case in which one needs to determine the time variations of physical variables and the propagation of an initial value. Step-by-step integration methods are the most frequent, such as the central finite difference method, Newmark method, Wilson method. These methods must be associated with iteration techniques to handle the nonlinear case. The most famous is the Newton-Raphson method.

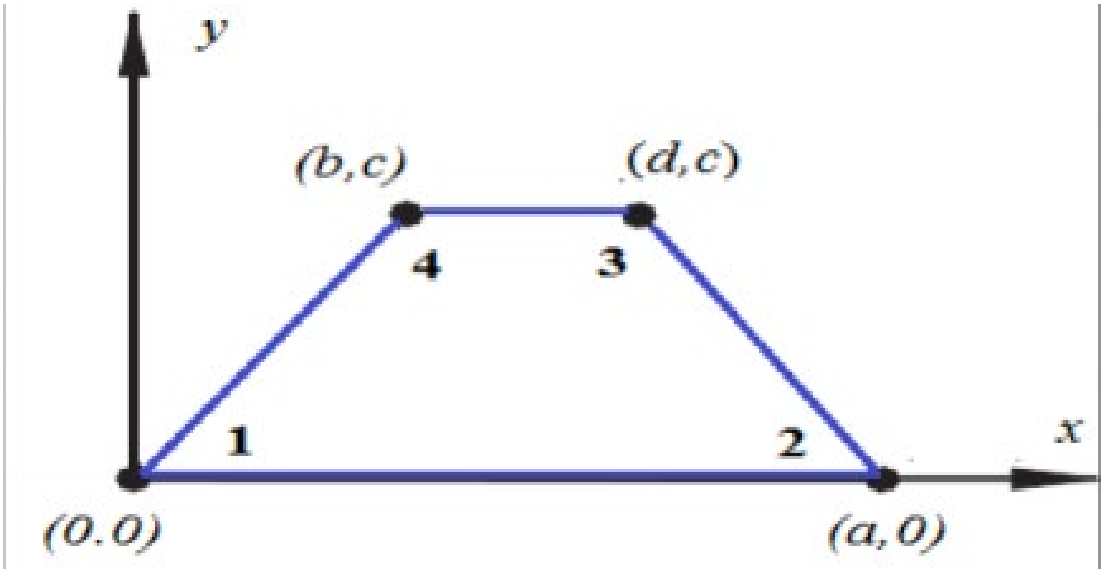

Figure III.15**:** Trapezoidal Fourier of p-element [110].

In 2006, Choo et al. [111] proposed linearly flexible and precise tetragonal triangular plane elements with additional rotational degrees of freedom. They showed that these additional rotations increase the accuracy and quality of the durability of the developed element. A. Houmat's [112] research was devoted to studying the trigonometric version of the finite element method based on the curved quadrilateral element. This factor was developed and applied to the analysis of free vibrations of arbitrarily shaped membrane structures. A. Houmat calculated frequency values for open and closed arcs using curved quadrilateral meshes and demonstrated rapid convergence and high accuracy using this method. These values are very accurate and can be compared to other calculation techniques.

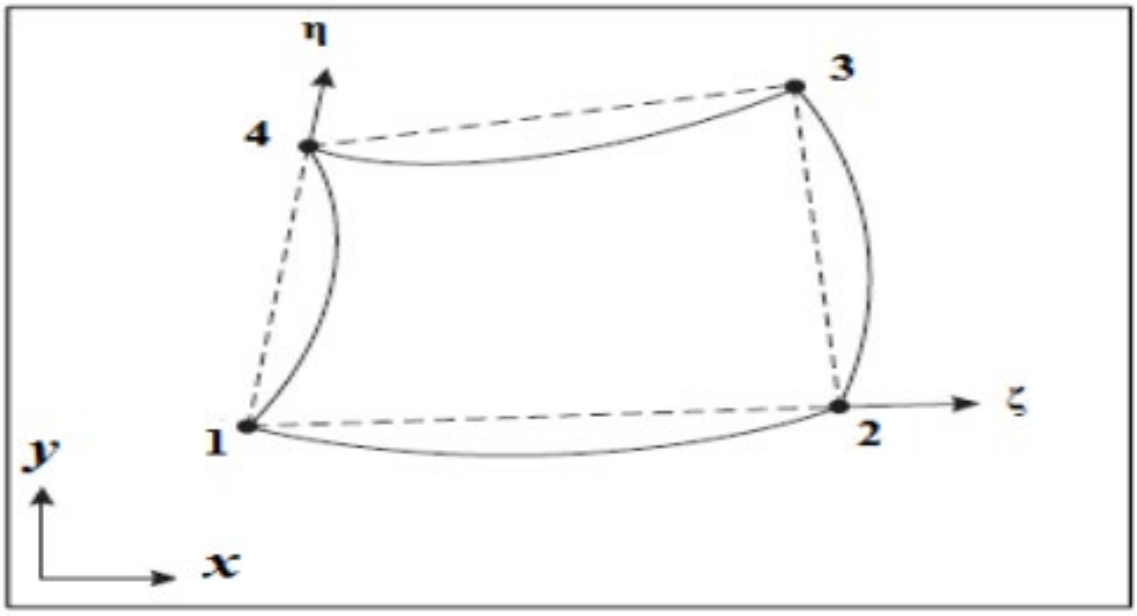

Figure III.16: Curved quadrilateral element [112].

The studies by Darılmaz et al. [113] were devoted to the investigation of a hypothetical 8-node hybrid stress shell element with six degrees of freedom per node, including three translations and three rotations. They examined the performance of the element for different structures, but used it under the condition of static and vibrational analysis of the structure with material properties (isotropic/orthotropic).

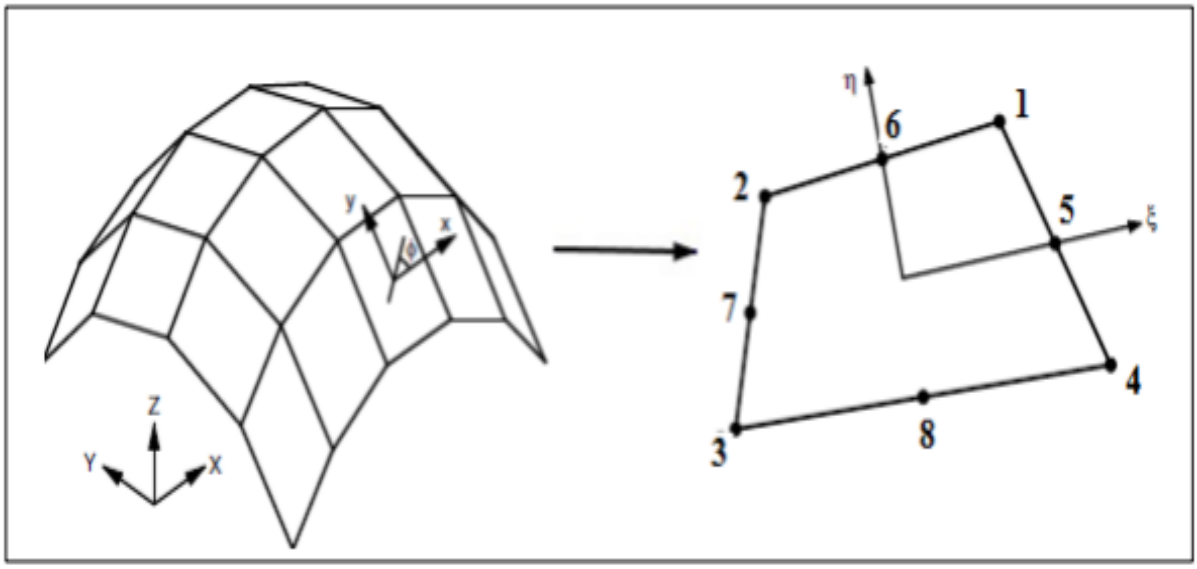

Figure III.17: Quadrilateral shell element with assumed hybrid stress at 8 nodes [113].

In 2009, N. Nguyen-Thanh et al. [114] used the alpha finite element method to analyze free vibrations and structures using meshes with triangular elements.

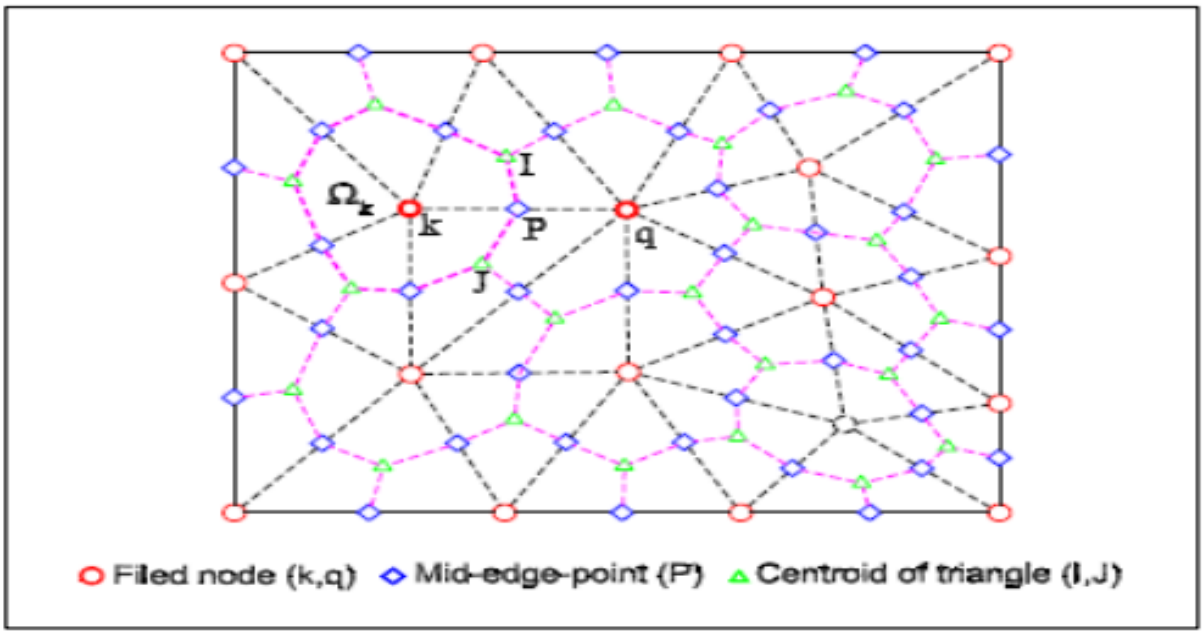

Figure III.18 : Mesh with triangular elements in the alternative alpha finite element method (AαFEM) [114].

The proposed method significantly improves the accuracy of the standard triangular element and provides a super-convergent energy solution for static and dynamic analysis in two-dimensional problems. The following findings were made:

- ✓ The numerical results of AαFEM using triangular elements are always more accurate than those of FEM-T3, and even more accurate than those of FEM-Q4 with the same number of nodes. The convergence rates of the energy norm are asymptotically the same as those of this standard FEM technique.
- ✓ In free vibration and forced vibration analyses, AαFEM is always stable and provides more accurate results than the corresponding FEM-T3 and FEM-Q4 methods.
- ✓ The AαFEM method is easy to implement in a finite element program, and triangular meshes are ideal for complex problem domains.

Conservative form of conservation equations

The customization of the equation can be more easily illustrated by considering that the conservation equation for a general scalar variable ∅ can be expressed as follows:

$$\underbrace{\rho\frac{\partial\theta}{\partial t}}_{I}+\underbrace{\nabla.\rho(V\emptyset)}_{II}=\underbrace{\nabla.(\Gamma^{\emptyset}\nabla\emptyset)}_{III}+\underbrace{S_{\emptyset}}_{IV} \quad \text{(III.33)}$$

I. Transient term.

II. Advection transport term of ∅.

III. Diffusion term of ∅.

IV. Source term.

The general differential equation for an unsteady, incompressible 2D flow is as follows:

$$\rho\left(\frac{\partial\emptyset}{\partial t}+\frac{\Delta\emptyset}{\Delta x}+\frac{\Delta\emptyset}{\Delta y}+\right)=\frac{\partial}{\partial x}\left(\gamma\omega\frac{\partial\emptyset}{\partial x}\right)+\frac{\partial}{\partial y}\left(\gamma\omega\frac{\partial\emptyset}{\partial y}\right)+S\emptyset \quad \text{(III.34)}$$

III.3.6 Initial and Boundary Conditions

III.3.6.1 Boundary conditions for numerical validation

The boundary conditions considered for comparative analysis with experimental setups are presented in Figure III.19. In compartment 1, the temperature is regulated at T_h = 60°C under heating and T_c = 25.5°C under cooling, and the relative humidity is fixed at ϕ_1= 40%. In compartment 2, the temperature and humidity were measured 35cm from the side 2 of the wall. The heat and mass transfer coefficients are calculated using relations 14 and 15, respectively.

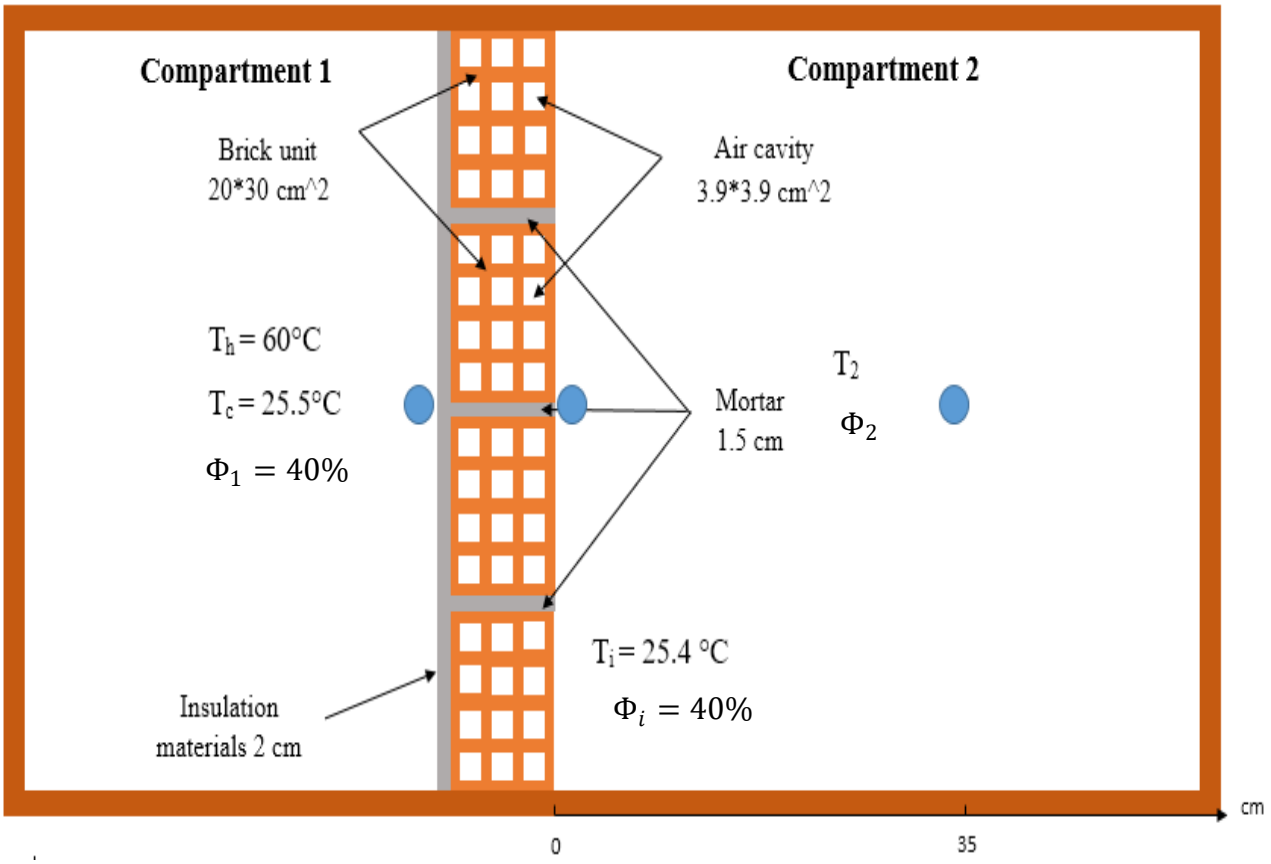

Figure III.19: Axonometric view of a typical hollow brick wall with boundary conditions for validation.

III.3.6.2 Boundary conditions for extension analysis

Considering the climatic conditions of Tlemcen and Hassi Messaoud, which were selected for numerical study and represented in figures III.21 and figure III.22, respectively. The outer surface of the wall is simultaneously subjected to a time-dependent influence: T_{ext} (t), ϕ_{ext} (t), V_{vent} (t), solar radiation with an absorption capacity for the mortar of ε = 0.87 [30]. The mass transfer coefficient is calculated using formula (15). The time-dependent external variables (air temperature, relative humidity, air velocity) are drawn from typical daily meteorological data. For the city of Tlemcen, case 1 corresponds to hot and humid days from August 13 to 16, 2021, and case 2 corresponds to cold and humid days from December 28 to 31, 2021. For the city of Hassi Messaoud, case 1 corresponds to hot and dry days from August 13 to 16, 2021, and case 2 corresponds to cold and dry days from December 28 to 31, 2021) [115].

On the inner surface of the wall, an imposed relative humidity of ϕ_{int}= 50%, and air contact temperature T_{int} = 25 °C, with a heat transfer coefficient of h_{int} = 3.25 W/(m^2 ×K). The initial temperature and initial relative humidity are respectively set to T_{ini} = 25 °C and ϕ_{ini} = 50 %.

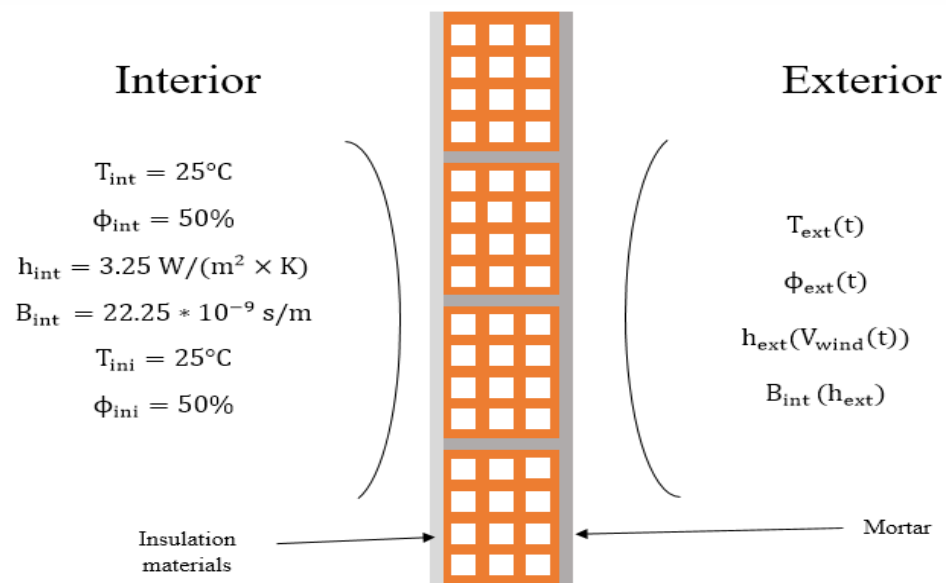

Figure III.20: Axonometric view of a typical hollow brick wall with this numerical boundary condition

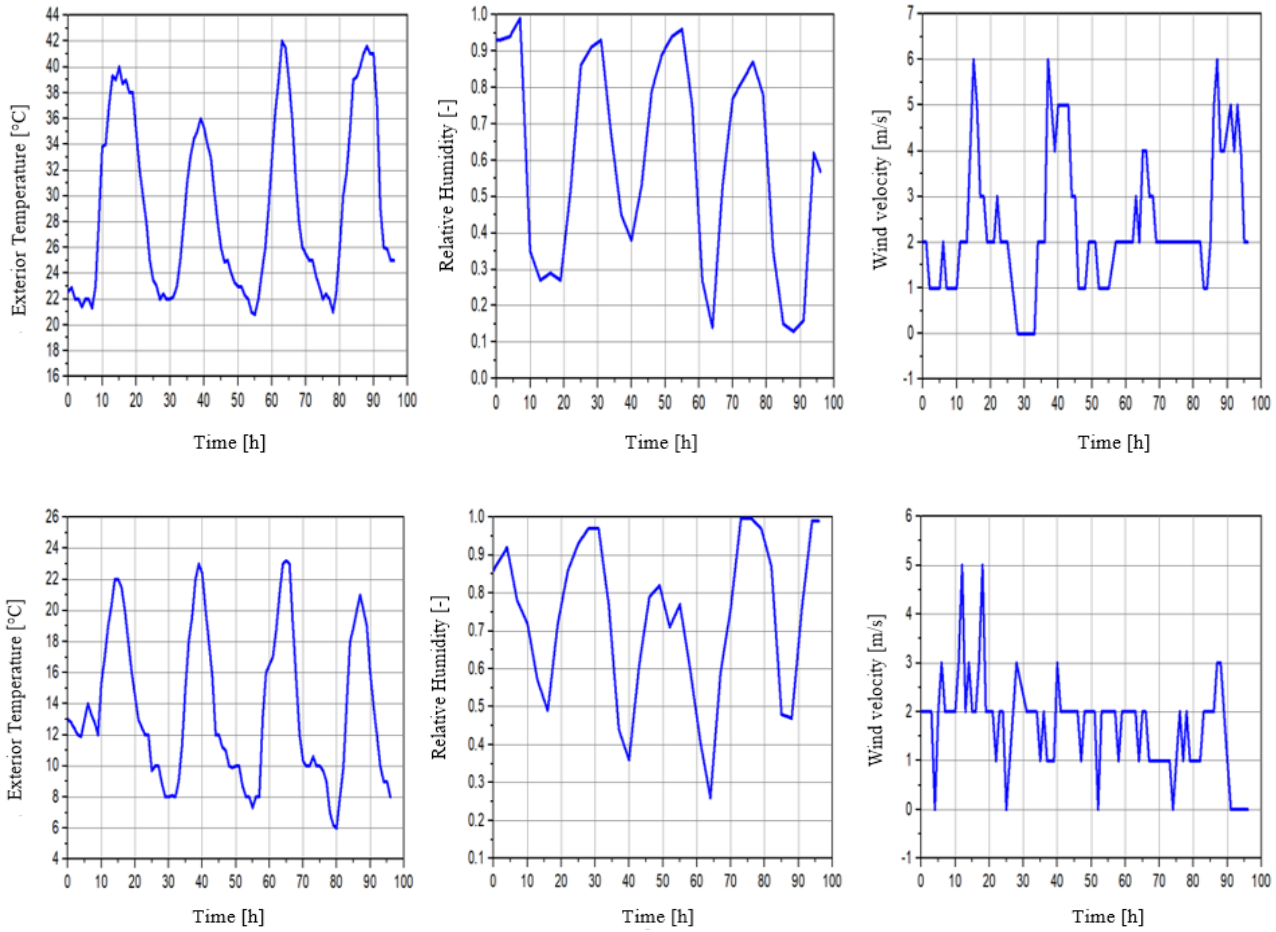

Figure III.21 : Variation of outdoor temperature, relative humidity, and air velocity used in simulations for (a) hot climate (August 13-16, 2021) and (b) cold climate (December 28-31, 2021) in Tlemcen [115].

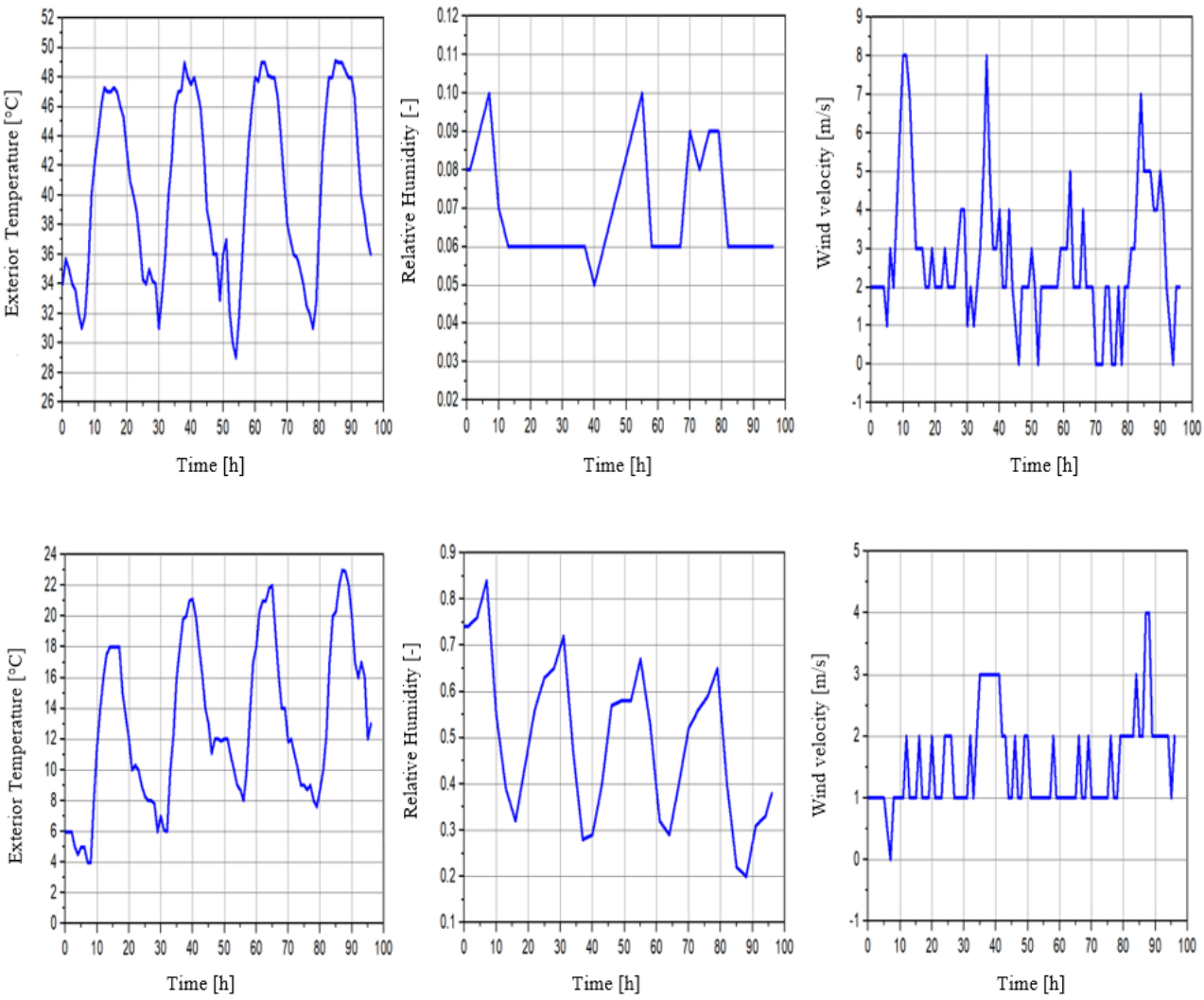

Figure III.22 : Variations in outdoor temperature, relative humidity, and air velocity used in simulations for (a) hot weather conditions (July 01-04, 2021) and (b) cold weather conditions (December 22-25, 2021) in Hassi Messaoud [115].

III.4 Conclusion

This chapter presents an experimental study conducted at the University of Tlemcen laboratory to investigate the hygrothermal behavior of diatomite and PCHCM. To carry out this experimental study, we used a phenomenological mathematical modeling of heat and moisture transfer in construction materials based on the work of HM. Künzel [12]. This model is widely used in the construction field. We considered temperature and relative humidity as key factors in hygrothermal transfer to ensure continuity of this transfer between different material layers.

Chapter IV

Results and Discussions

IV.1 Introduction

The fourth chapter is devoted to discussing the results obtained from the experiments and using the COMSOL Multiphysics software. The work focuses on three cases:

- ✓ The first case analyzes the effect of diatomite, PCHCM, and mortar on the hygrothermal performance of a hollow brick wall through experimental studies.
- ✓ The second case is dedicated to numerical validation using the COMSOL Multiphysics simulation software. The experimental results at a temperature of 60°C and a humidity of 40% were used for numerical validation.
- ✓ The third case is devoted to proposed numerical studies.

IV.2 Results and discussion

IV.2.1 Experimental analysis

In this case, the effects of humidity and temperature on walls with different finishing layers (mortar, diatomite, and PCHCM) were studied by considering a given temperature and humidity in compartment 1. During discharge, a temperature of 25.5°C is maintained, while humidity of 40% and 80% is considered for two distinct cases, as shown in Table IV.1.

We measure humidity and temperature in compartment 2 at two positions.

	Heating Temperature	Cooling Temperature	Relative Humidity
Case 1	30°C	25.5°C	40%
	30°C	25.5°C	80%
Case 2	45°C	25.5°C	40%
	45°C	25.5°C	80%
Case 3	60°C	25.5°C	40%
	60°C	25.5°C	80%

Table IV.1 : Boundary condition for compartment 1.

Case 1 :

Based on the results obtained in Figure IV.1 and Figure IV.2, it can be observed that thermal insulation is improved when diatomite is used alone. However, this thermal insulation decreases relatively when paraffin is added to diatomite. This result can be explained by the fact that the

temperature of the load was lower compared to the phase change temperature. Therefore, the phase change process does not contribute to lowering the interior temperature.

The increase in temperature in compartment 2 and side 2 is primarily attributed to heat transfer through the wall by conduction. The relative humidity increases in compartment 2 and on side 2 primarily during the charging phase due to heat transfer across the wall. This phenomenon is influenced by the interaction between temperature and the air's ability to absorb moisture. Initially, relative humidity rises due to warm, moist air. When warm air contacts cold surfaces, water vapor is released into the air, raising relative humidity. As the temperature continues to rise, the warmth of the air in the compartments enhances its moisture-absorbing capacity. However, without an additional moisture source, this increased capacity doesn't translate into actual humidity increase. Consequently, the relative humidity decreases in compartment 2. When heating stops, the temperature in compartment 2 gradually decreases due to heat loss. Relative humidity rises in compartment 2 and on side 2 of the wall, where the temperature decrease can reduce the air's ability to absorb moisture, potentially leading to increased relative saturation.

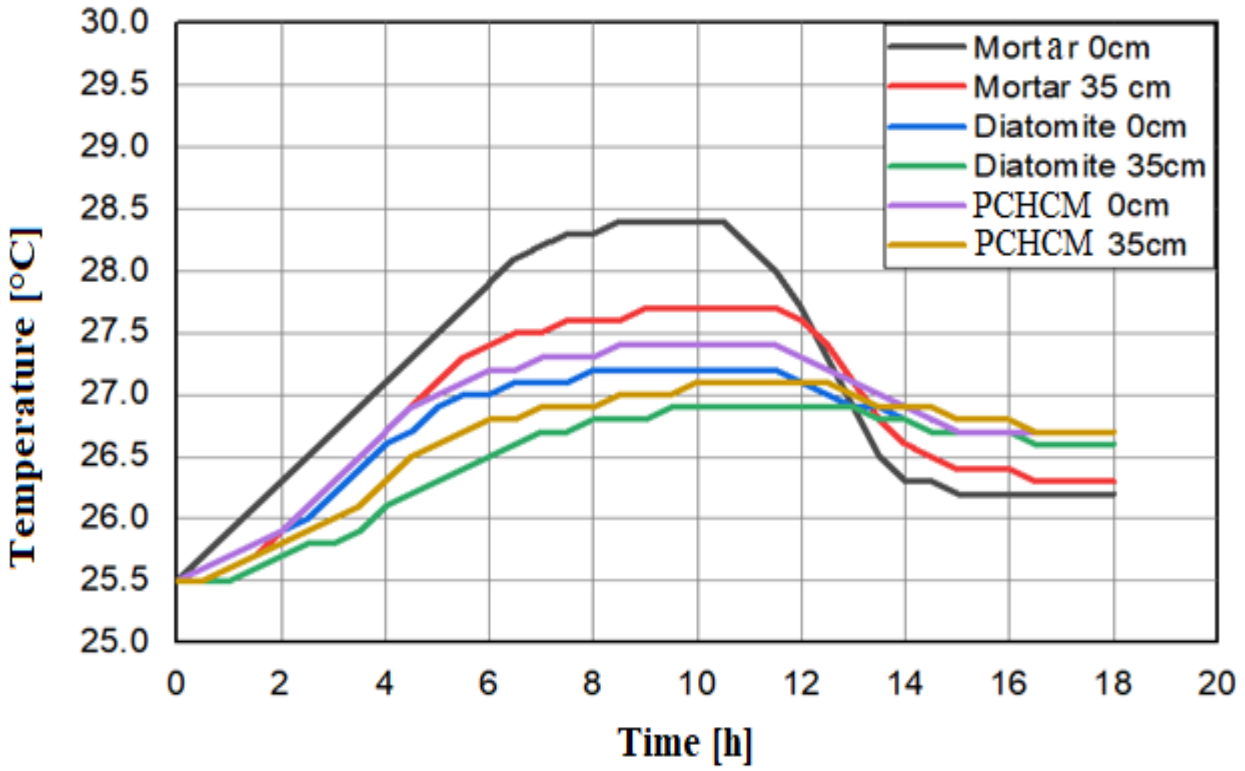

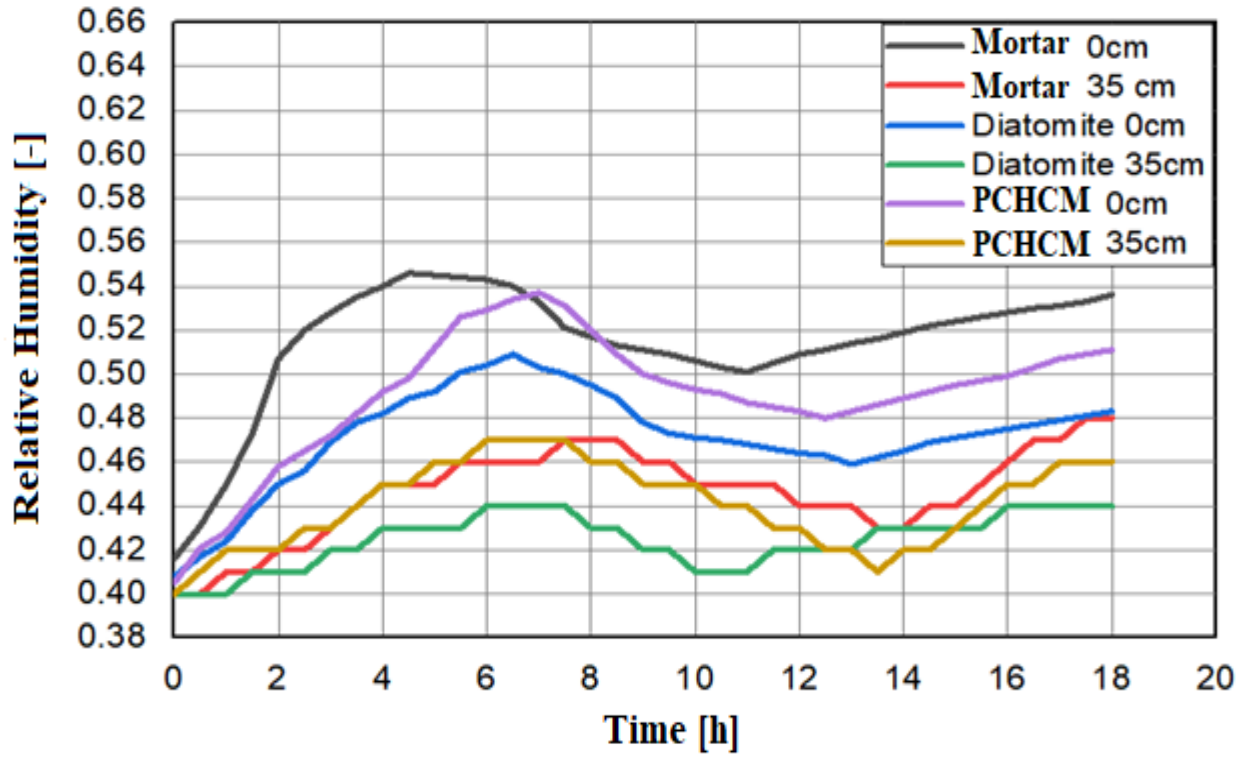

Figure IV.1 : Experimental Results from Compartment 2 for the Boundary Condition of Compartment 1 at T_h= 30°C and Φ_1=40%.

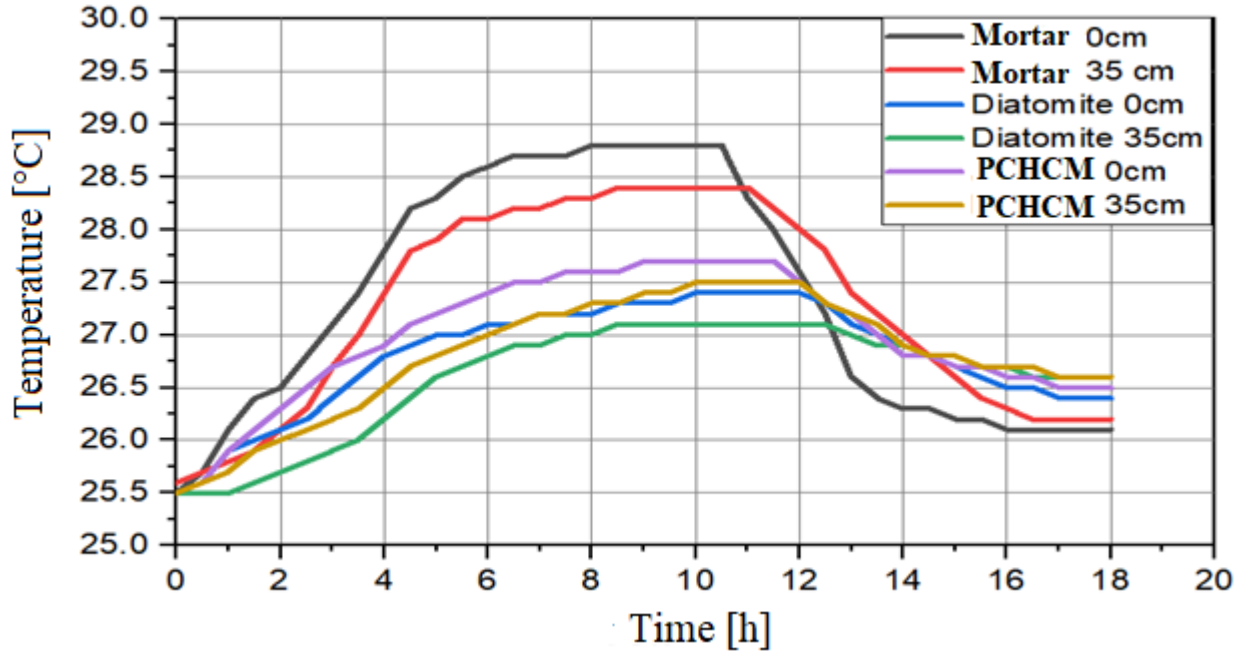

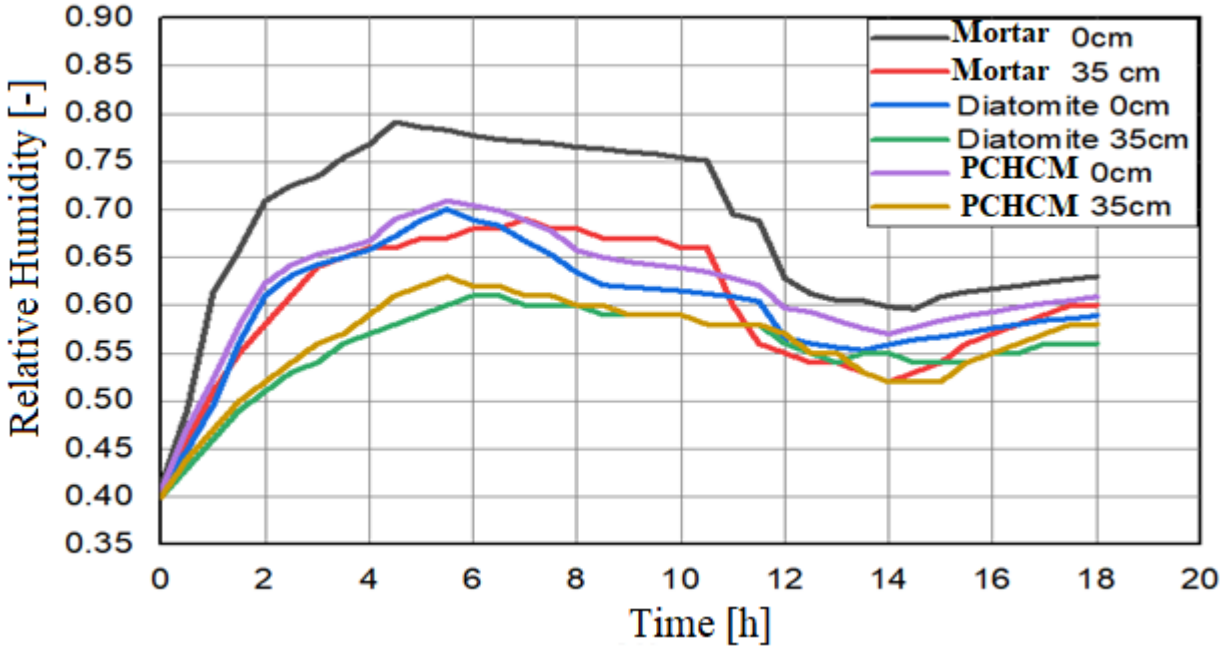

Figure IV.2 : Experimental Results from Compartment 2 for the Boundary Condition of Compartment 1 at T_h= 30°C and Φ_1=80%.

Cas 02:

In Case 2, the experiment was conducted by elevating the temperature to 45°C, while maintaining consistent humidity levels as observed in Case 1 (at 40% and 80%). However, despite these efforts, the anticipated phase change material (PCM) effect failed to manifest due to the failure to attain the required melting temperature (T_{fusion} = 54°C). The PCM's expected role in stabilizing temperature was rendered ineffective within the porous medium of diatomite. It's important to note that even with the humidity factor, typically assumed to aid in temperature moderation, it didn't fulfill this function as expected due to the PCM's presence.

In the instance of the experiment conducted at 80% humidity, the resultant temperature within Compartment 2 measured 31°C when observed at a distance of 35 cm from the wall, specifically in the case of utilizing the diatomite finishing layer. This finding highlights the pronounced influence of moisture evaporation. A comparative analysis between the walls treated solely with diatomite and those integrated with PCM reveals a marginal temperature difference, with the latter registering a slightly higher temperature of 31.5°C. However, this discrepancy in temperature is somewhat mitigated when the humidity levels are reduced to 40%.

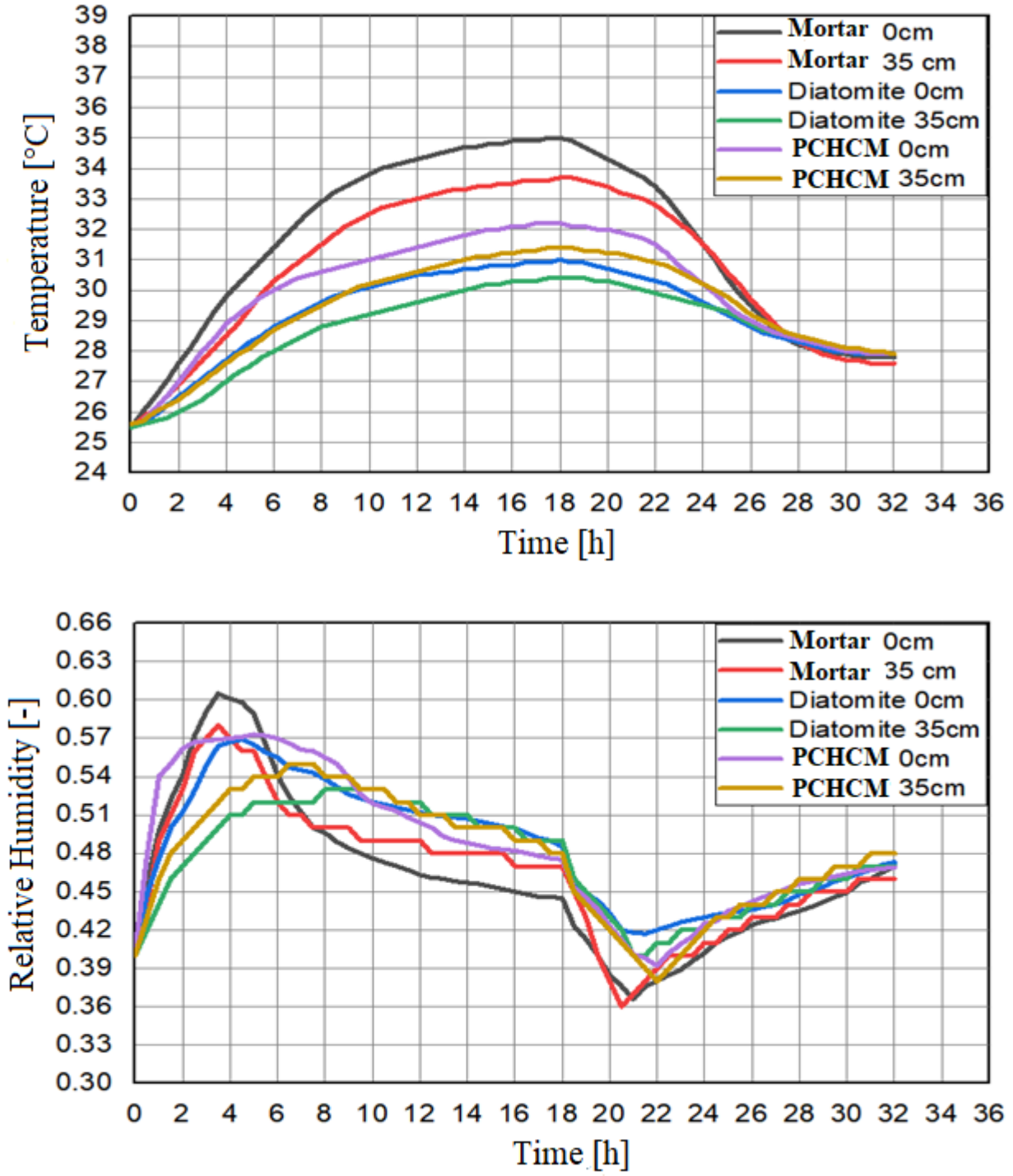

Figure IV.3: Experimental Results from Compartment 2 for the Boundary Condition of Compartment 1 at T_h= 45°C and Φ_1=40%.

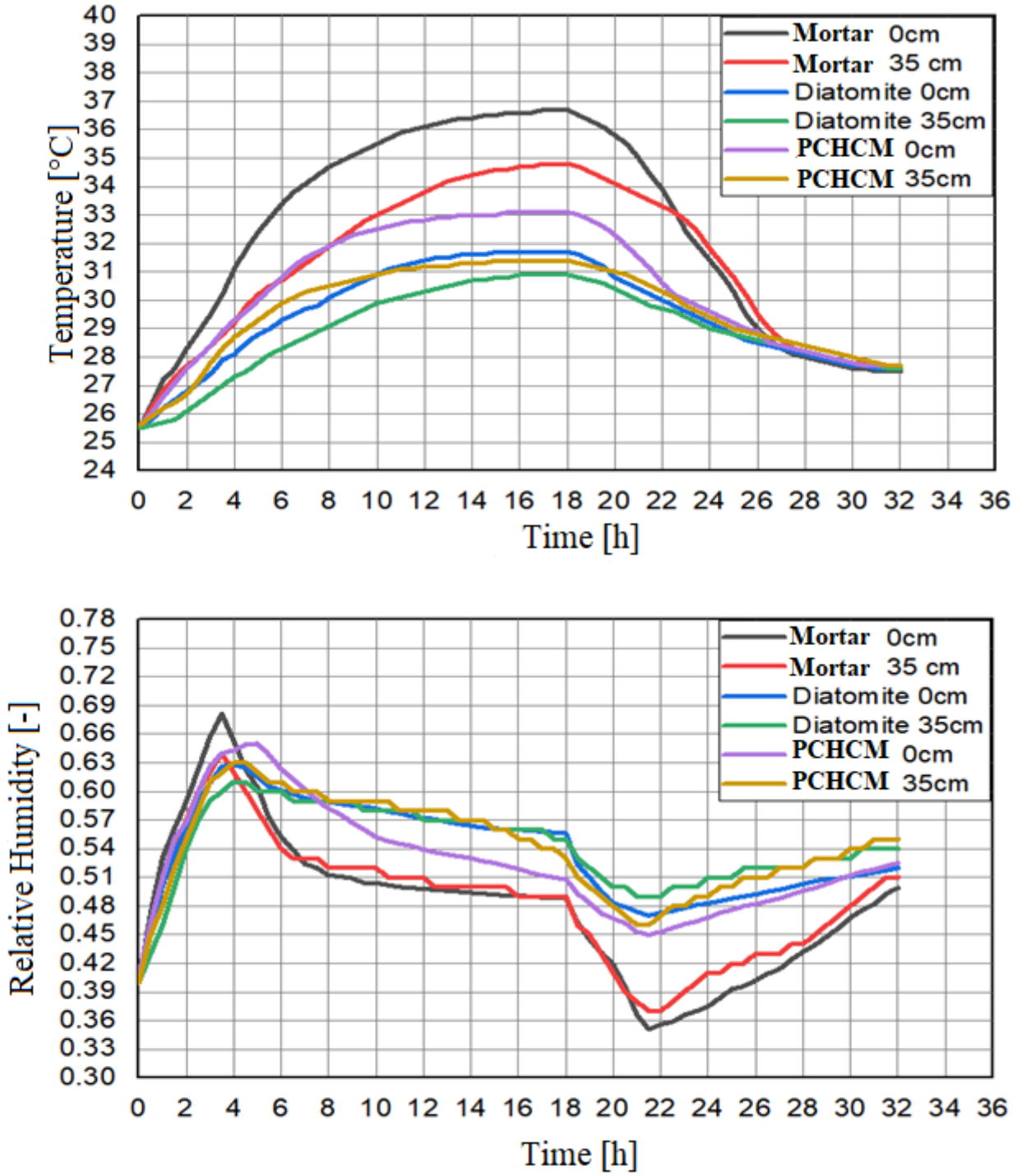

Figure IV.4 : Experimental Results from Compartment 2 for the Boundary Condition of Compartment 1 at T_h= 45°C and Φ_1=80%.

Cas 03

In this Case 03, the process of thermal charging and discharging was studied for different wall types. It is important to mention that the heating temperature is 60°C, which is higher than the given melting temperature of PCHCM (54°C). Results show that the temperature in Compartment 2 during thermal charging at Φ_1=40% is lower for PCHCM compared to diatomite (33°C vs 33.8°C at time=20h). However, the reverse phenomena were observed during the discharging process, where the

temperature of Compartment 2 reached 32°C for PCHCM compared to 30.5°C at time=28h for diatomite. This particular result can be explained by the phase-change effect of the PCM material. Both walls (diatomite and PCHCM) give comparable results for Φ_1=80%. In fact, the measured temperatures for both walls were 34.5°C and 34°C, respectively, at time=20h during a charging process and 30°C and 31°C at t=28h.

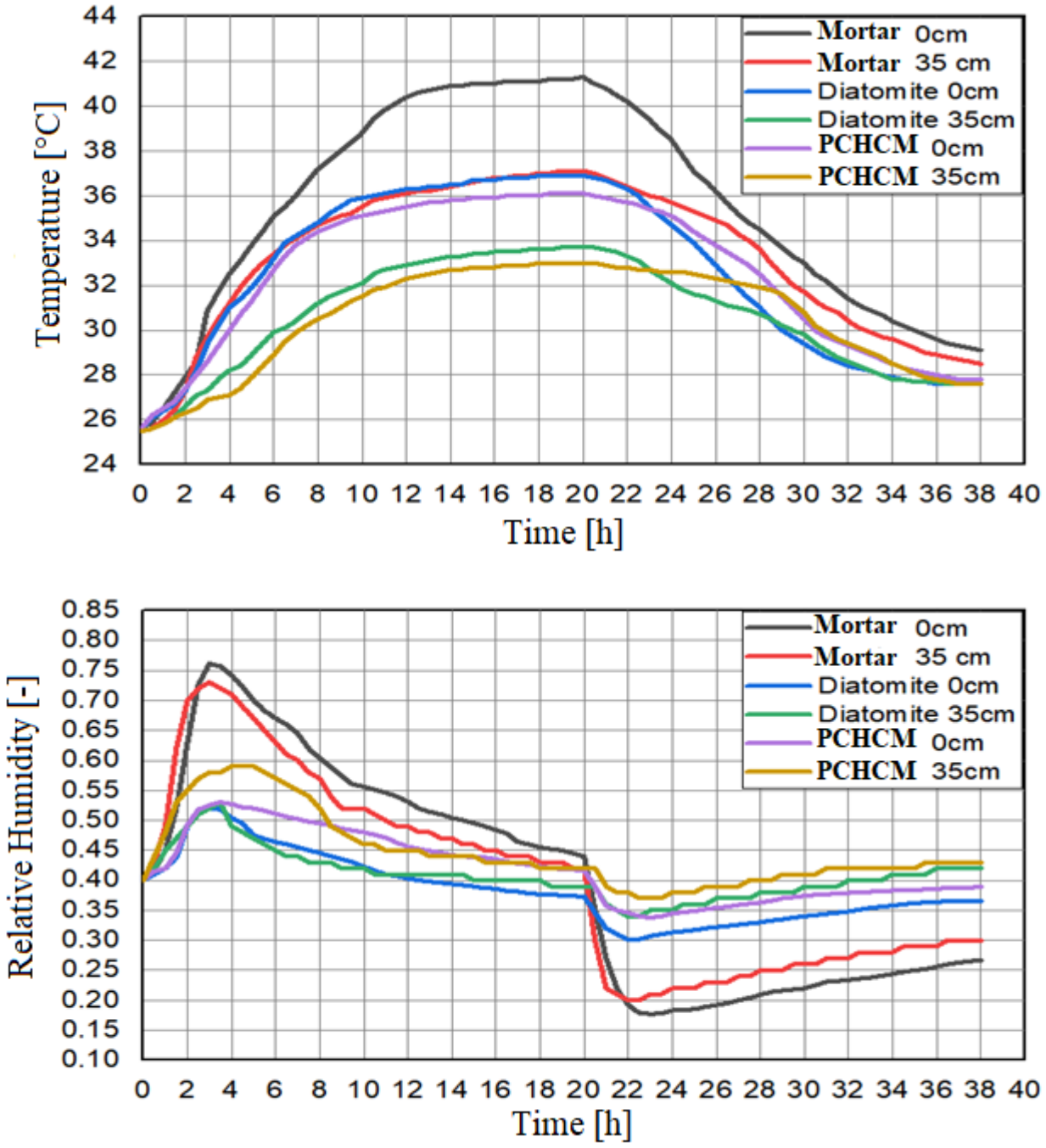

Figure IV.5: Experimental Results from Compartment 2 for the Boundary Condition of Compartment 1 at T_h= 60°C and Φ_1=40%.

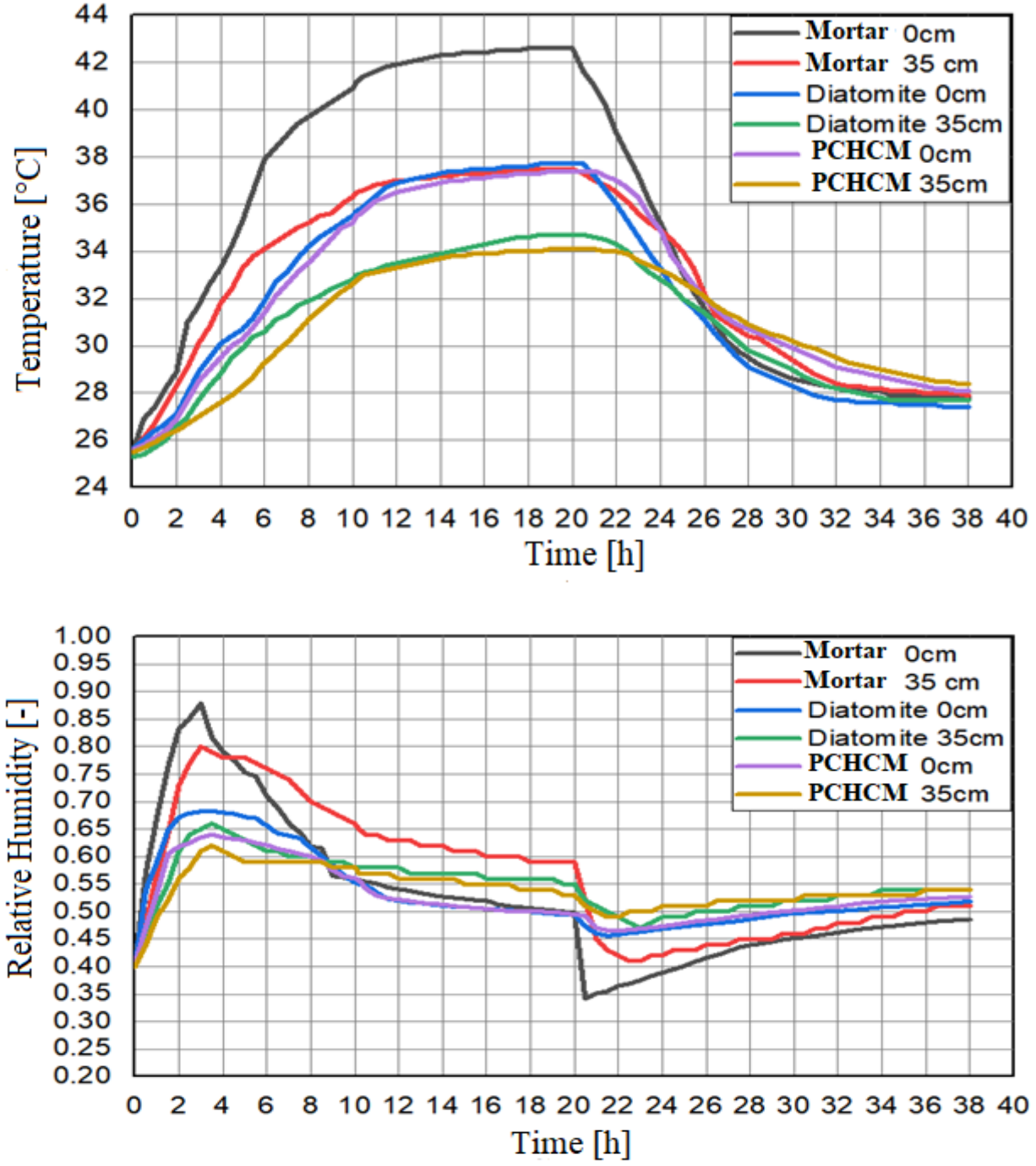

Figure IV.6: Experimental Results from Compartment 2 for the Boundary Condition of Compartment 1 at T_h= 60°C and Φ_1=80%.

IV.2.2 Numerical analysis

IV.2.2.1 Mesh test

Before using the numerical model, it is important to conduct a study on the mesh independence. To this end, we analyzed three mesh grids corresponding to a domain element count of 5998, 10448, and 22494 in triangular form. Temperature and relative humidity on the surface 2 of the mortar finishing layer were chosen for comparison.

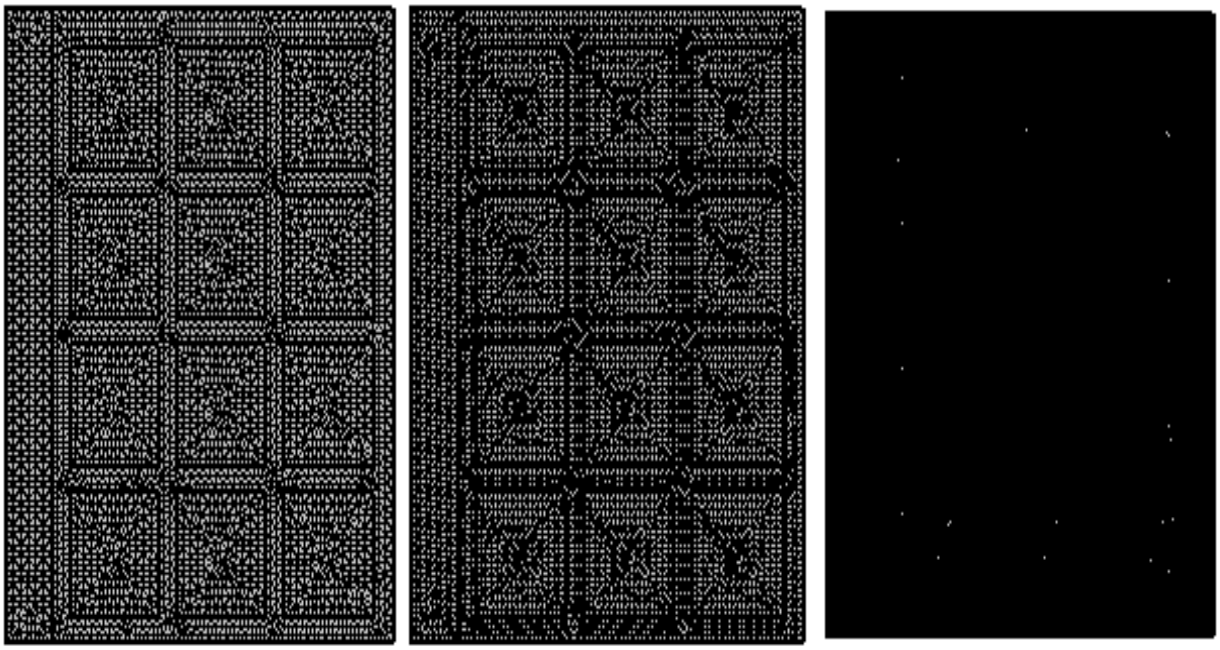

5998 domain elements 10448 domain elements 22494 domain elements

Figure IV.7 : Meshes chosen for our study.

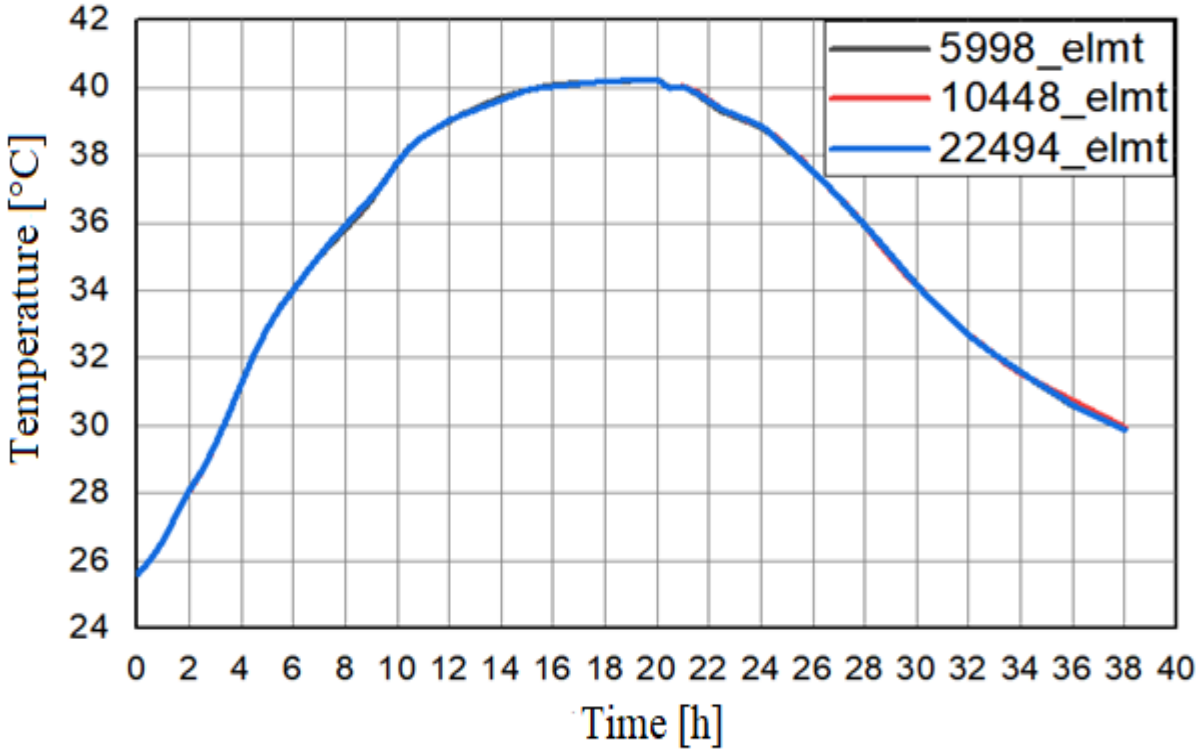

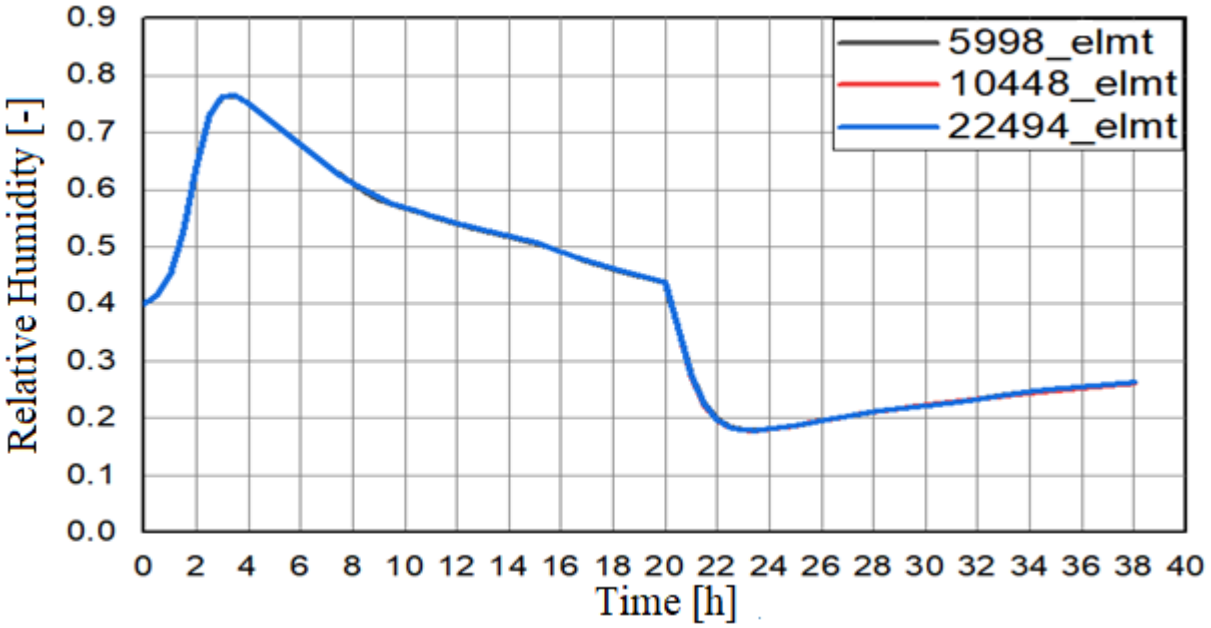

Figure IV.8 : Influence of the number of domain elements on the results.

We observe that the differences obtained for the three analyzed grids are relatively small. Therefore, we have chosen the grid consisting of 5998 domain elements for our simulation as it provides a good balance of computation time. The time step used is Δt = 30 min for all configurations.

IV.2.2.2 Experimental and Numerical comparison

In this section, we compared experimental work conducted over 38 hours under T_h=60°C and Φ_1=40% conditions to a numerical simulation developed using a software based on the finite element method

Case 01 : Brick wall with a Mortar finishing layer.

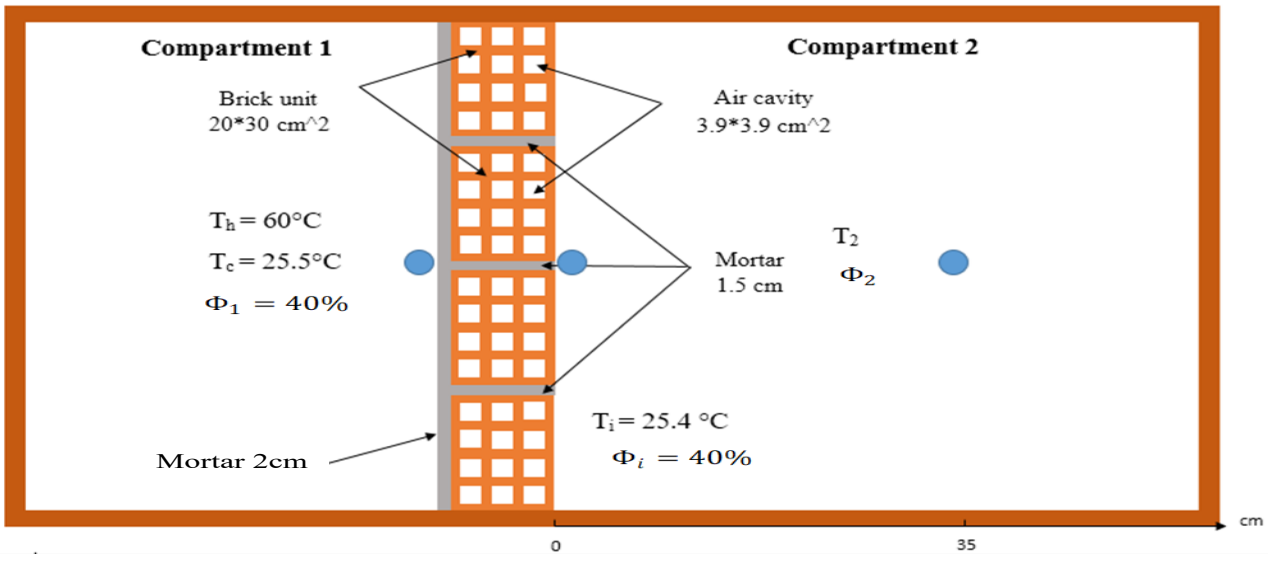

Figure IV.9: Brick wall with a Mortar finishing layer.

According to Figure IV.10, we can conclude that the experimental and numerical simulation results show good agreement. In fact, the temperature and relative humidity difference between the two results does not exceed respectively 2.5% and 2.7% during charging and 3.5% and 3.6% during discharging. It should be noted that the maximum temperature was reached at t=20h and the maximum humidity was observed at t=3h.

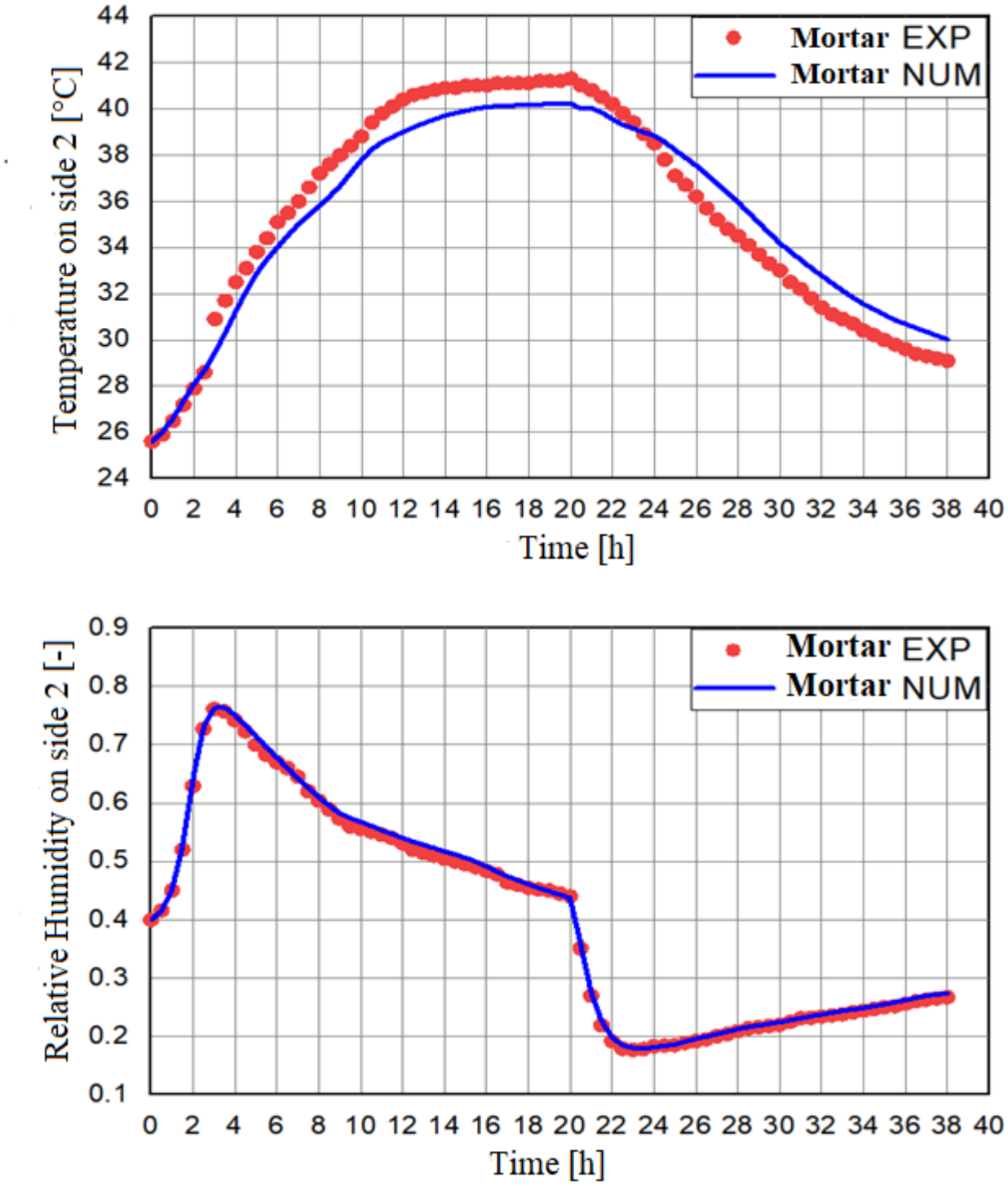

Figure IV.10: Results obtained with a Mortar finishing layer.

Cas 02 : Brick wall with a Diatomite finishing layer.

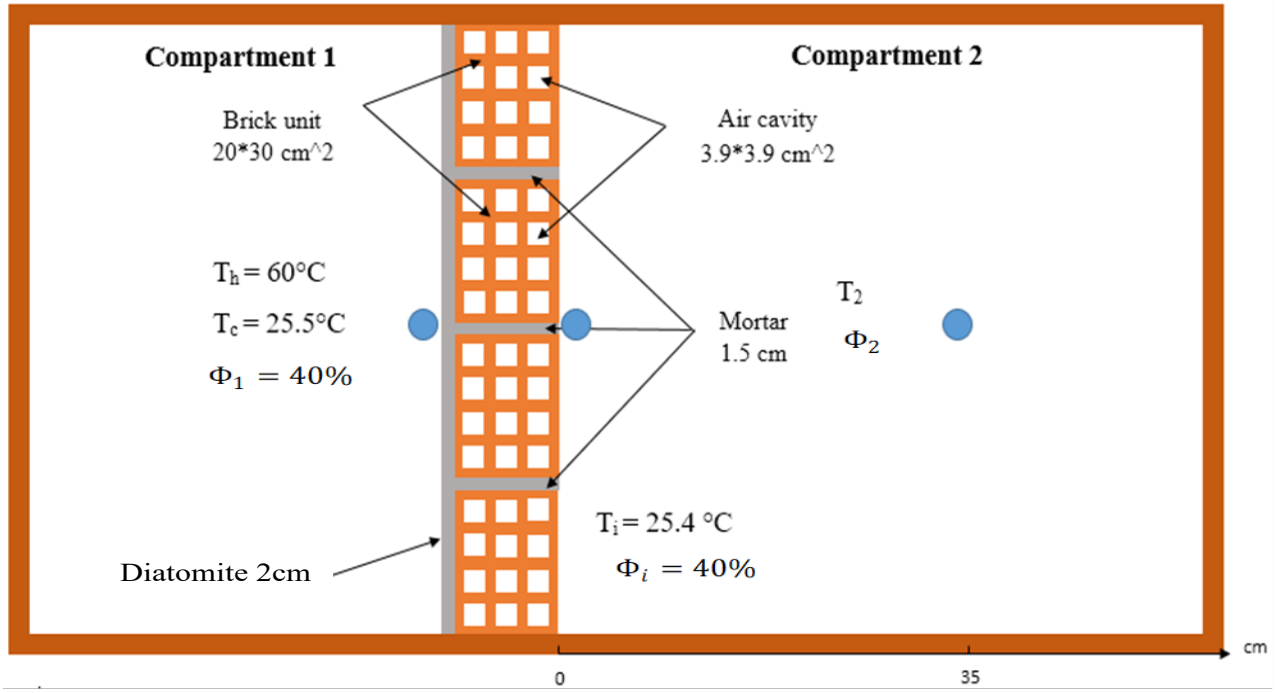

Figure IV.11: Brick wall with a Diatomite finishing layer.

In this second validation analysis, the mortar is replaced by diatomite for the finishing of the exterior walls. According to figure IV.12, there is a good agreement between the experimental and numerical results. The relative error does not exceed 3.5% for temperature and 3.7% for humidity during the charging process. During the thermal discharge, the relative error is 4.3% for temperature and 4.4% for humidity.

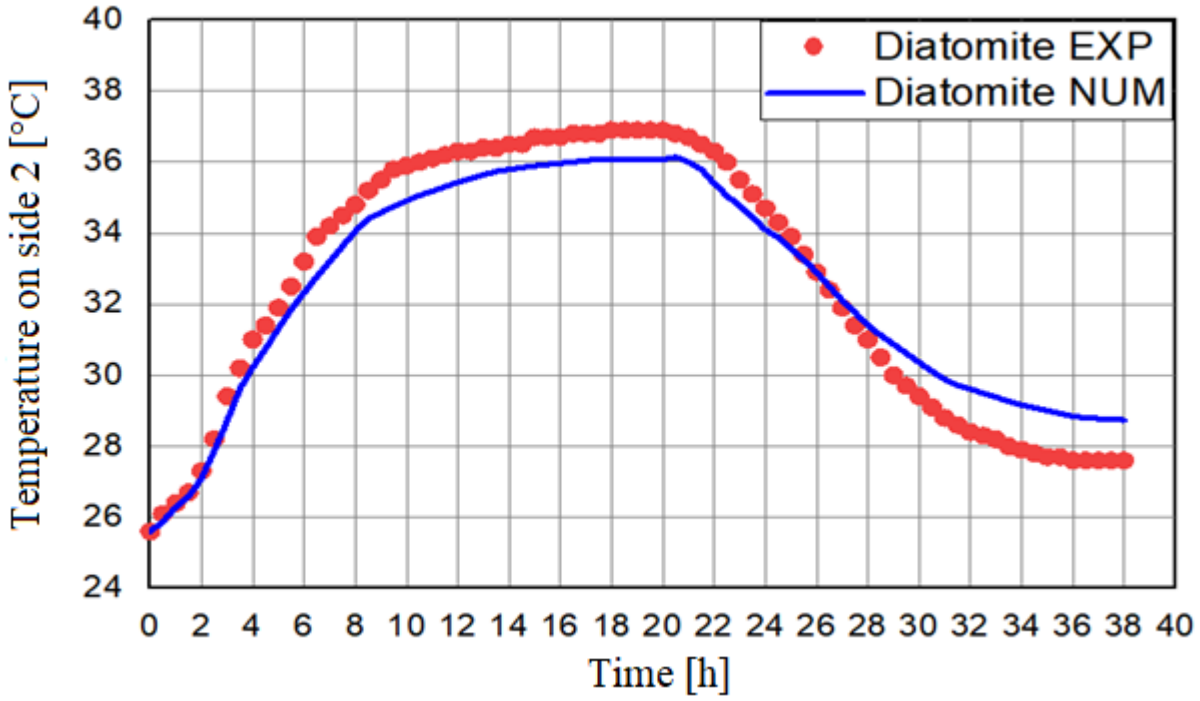

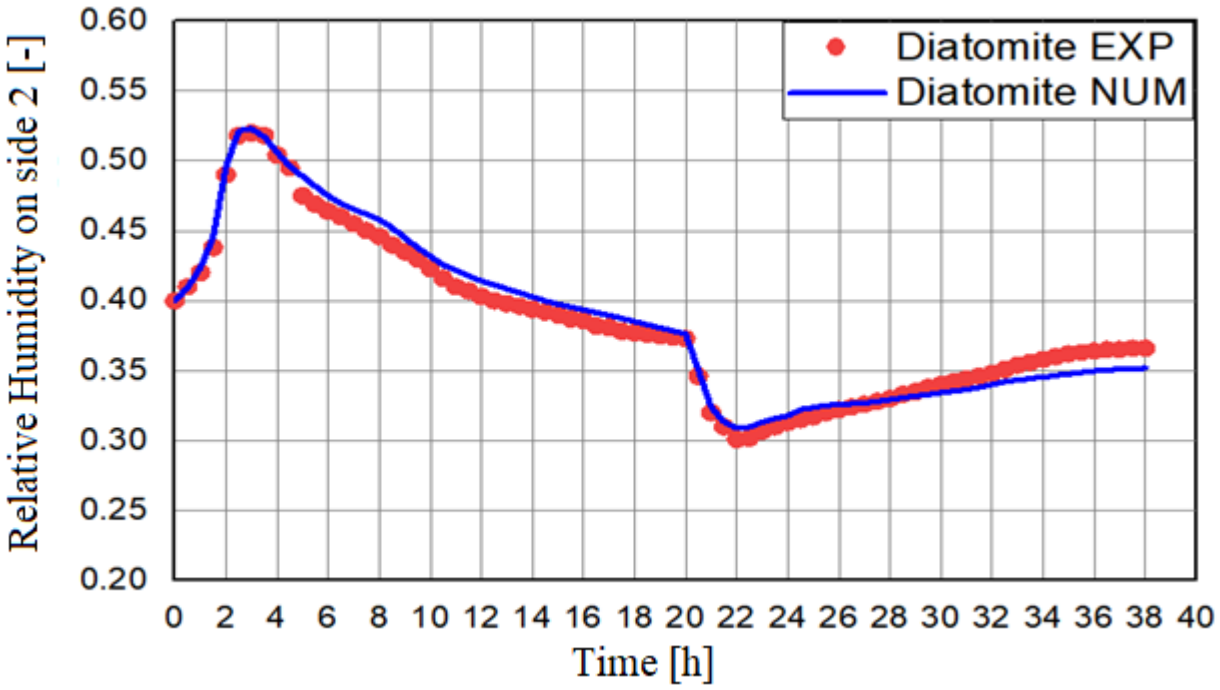

Figure IV.12 : Results obtained with a Diatomite finishing layer.

Cas 03 : Brick wall with a PCHCM finishing layer.

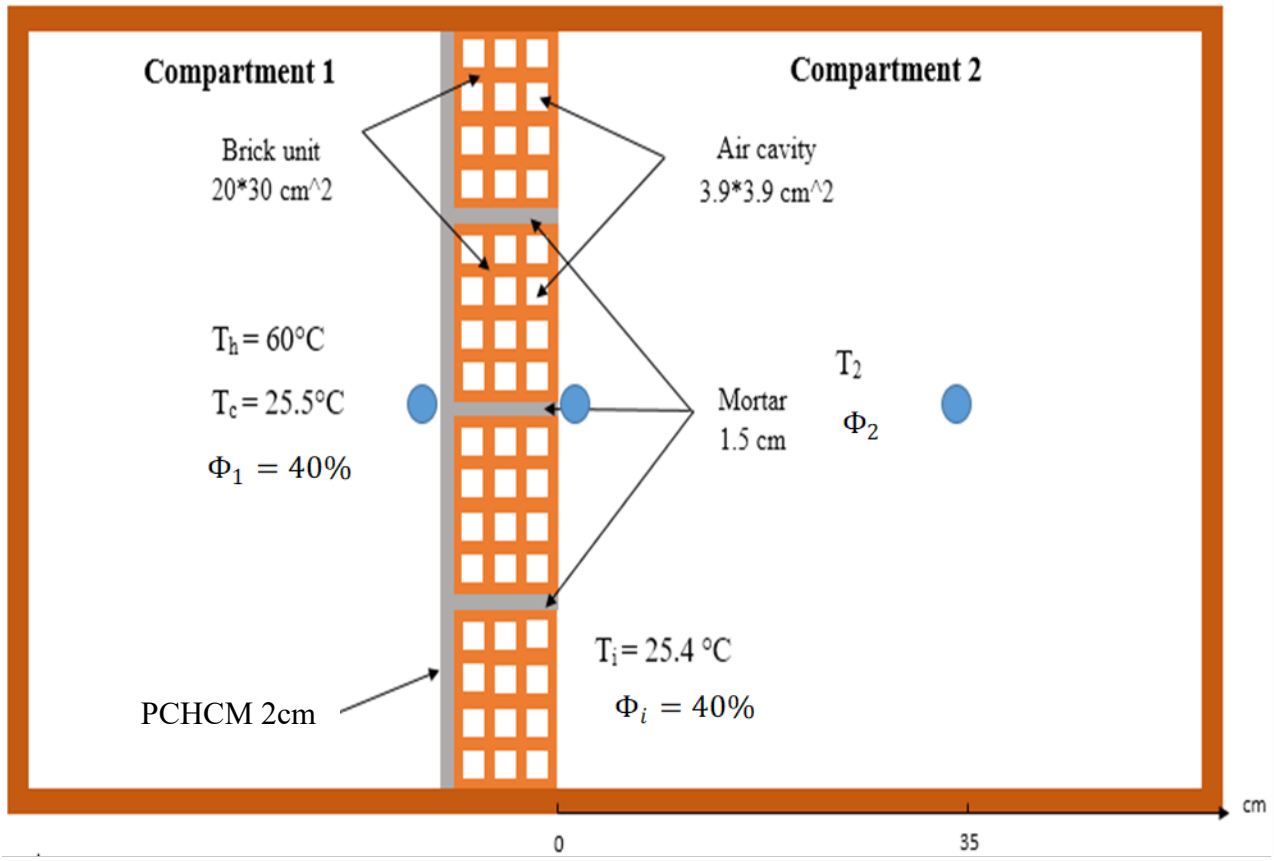

Figure IV.13 : Brick wall with a PCHCM finishing layer.

In this third validation analysis, the PCHCM material was used as insulation for the external wall. As demonstrated in Figure IV.13, the numerical and experimental results show a very good agreement, with the maximum relative error not exceeding 4.5% in all cases. This confirms the accuracy of the numerical simulation in predicting the thermal and humidity behavior of the wall system with PCHCM insulation.

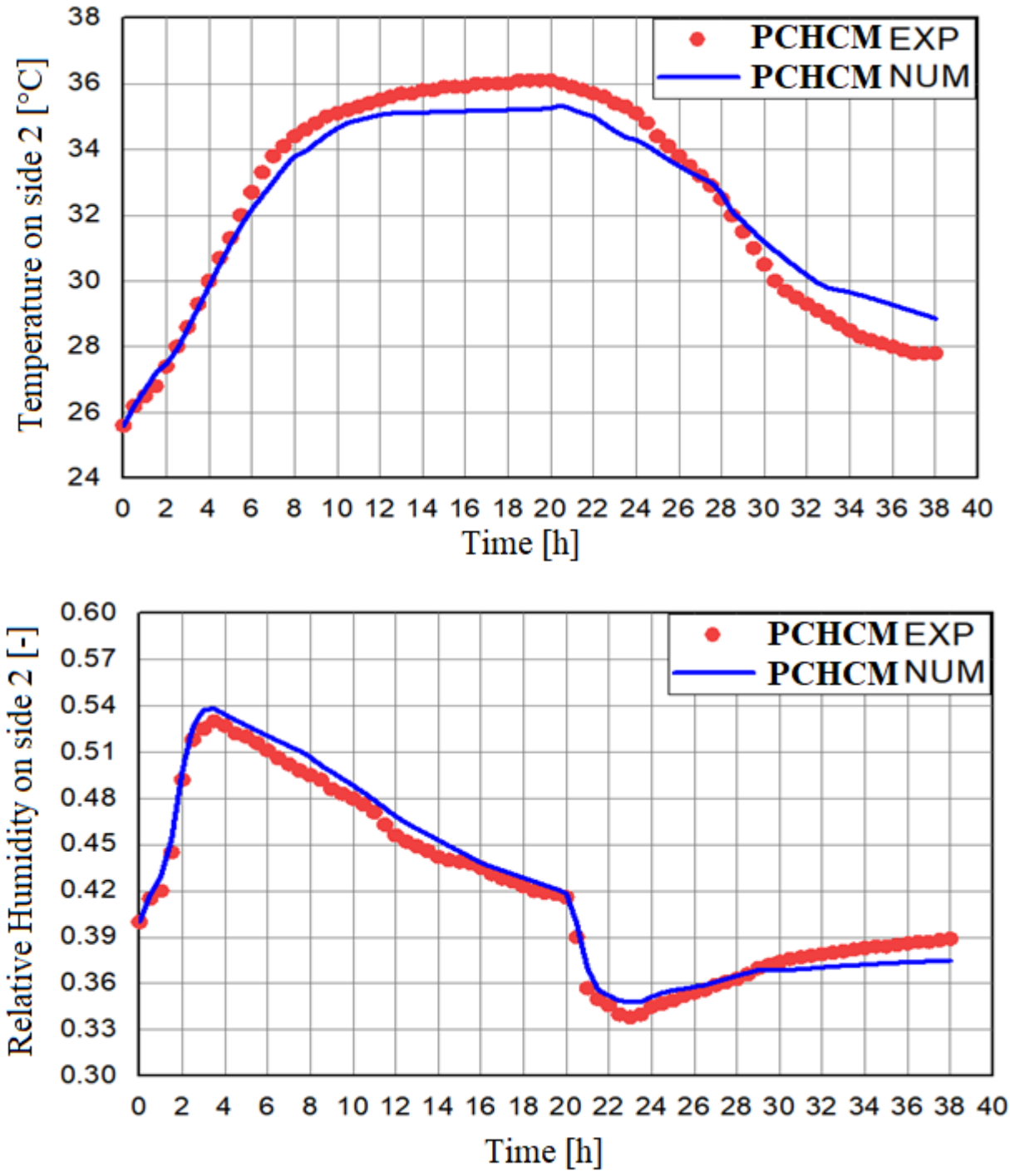

Figure IV.14 : Results obtained with a PCHCM finishing layer.

IV.2.2.3 Impact of Ambient Conditions in Algerian Cities on Different Layers of Wall Finishes.

In this section, a thorough analysis is presented considering different operating conditions related to different seasons, since the validation process has been successfully completed. Two cases corresponding to the summer and winter periods are simulated through relevant boundary conditions of two Algerian cities. Then, a comparative analysis is conducted for diatomite and two PCHCM materials. In this section, the insulation was placed on the inside of the wall, as shown in Figure III.6, because there are no significant temperature changes inside.

Tlemcen

Study of insulators in the summer period

In this first case, thermal performances are studied under high humidity and high temperature conditions corresponding to the summer period in the Tlemcen region. Specifically, this analysis is conducted for building walls using three different finishing layers: diatomite, PCHCM1 based on a single PCM, and PCHCM2 based on two different PCMs with two different melting points (T1 and T2). These layers are placed inside the wall. Figure IV.15 shows remarkable results when using diatomite, PCHCM1, and PCHCM2. Indeed, the hygrothermal effect on the temperature of the internal wall is significantly improved in the case of PCHCM1. The average temperature considered for the summer period is higher than the phase change temperatures (>27) and (>21). As a result, a quantity of latent heat is absorbed by the two PCMs, reducing the ambient temperature during the day. However, this energy is released during the night, as the temperature during this period is lower than 21°C. On the other hand, the indoor relative humidity profiles of diatomite, PCHCM1, and PCHCM2 are respectively maintained within a comfort humidity range of 40% to 60%.

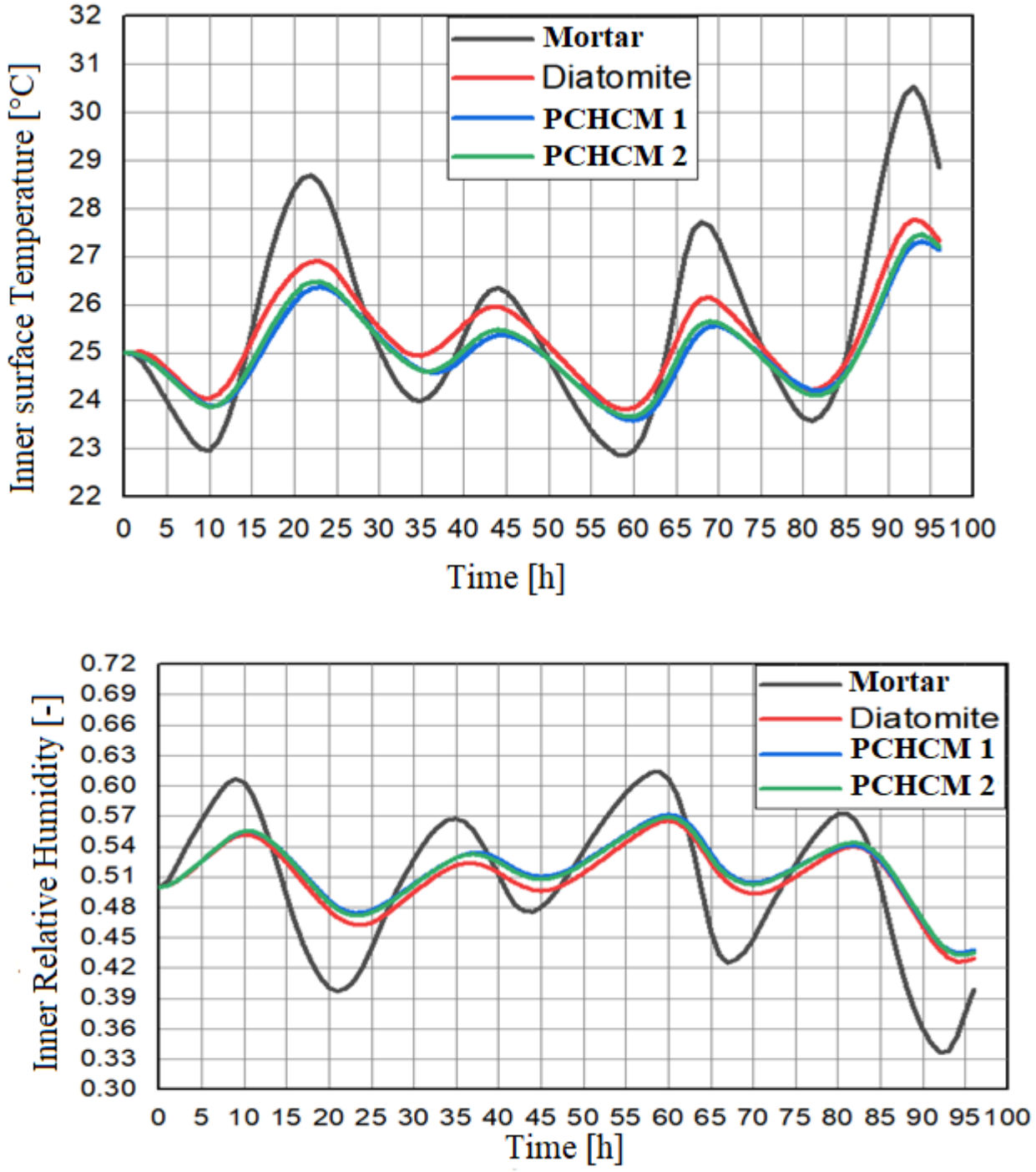

Figure IV.15 : Variation of Temperature and Relative Humidity at the Interior Surface (August 13-16, 2021) in Tlemcen.

Study of insulators in the winter period

In this second case, thermal performance is studied under low temperature and high humidity conditions corresponding to the winter period in the Tlemcen region. The same three different finishing layers - diatomite, PCHCM1 based on a single PCM, and PCHCM2 - are used. Figure IV.16 shows a partial effect on the interior temperature as the ambient temperature considered during this

period oscillates between 21°C and 27°C. PCM1 has no effect on temperature stabilization, whereas PCHCM2 is better suited when the temperature is below 27°C.

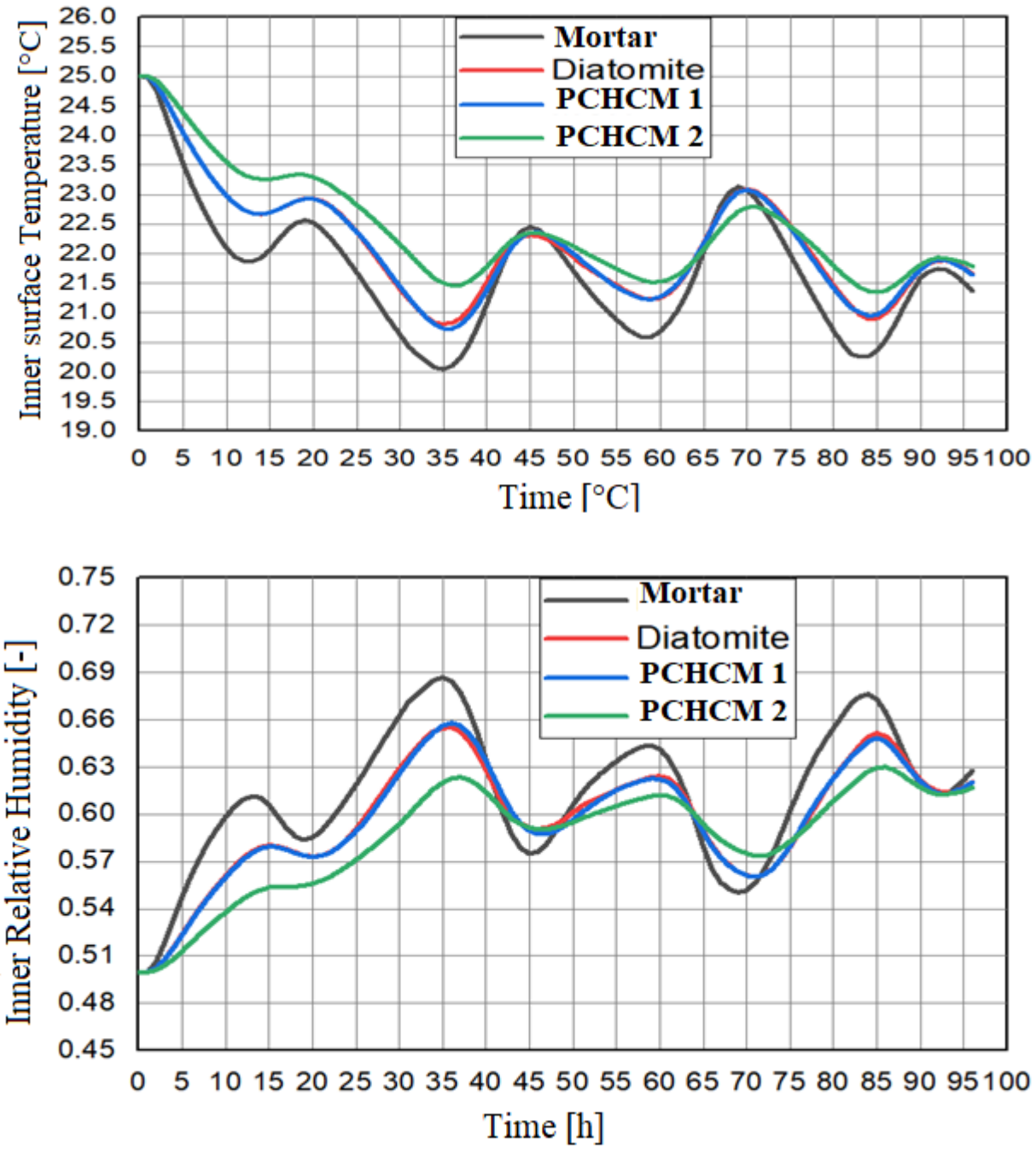

Figure IV.16 : Variation of temperature and relative humidity at the interior surface (December 28-31, 2021) in Tlemcen.

Hassi Messaoud

Study of insulators in the summer period

In the third case, we studied the improvement of thermal performance in a hot and dry climate (Hassi Messaoud) on a building wall using the same different finishing layers (diatomite, PCHCM1, and PCHCM2) placed inside the wall. Figure IV.17 shows that the use of diatomite, PCHCM1, and

PCHCM2 has a remarkable effect on improving the thermal performance on the inner wall surface. The temperatures we selected from these days are significant and higher than the phase change temperatures (>27) and (>21). The results showed that PCM1 is the only one that gives us a significant effect because PCM2 is still in a liquid state, and as the external temperature is very high compared to its melting point, its presence has a negative effect.

The relative humidity is very low during all 4 days, not exceeding 11%, which promotes reverse dehumidification (from the inside to the outside). It can be seen that insulation with PCHCM1 can reduce dehumidification towards the outside and, at the same time, stabilize the relative humidity at the inner surface.

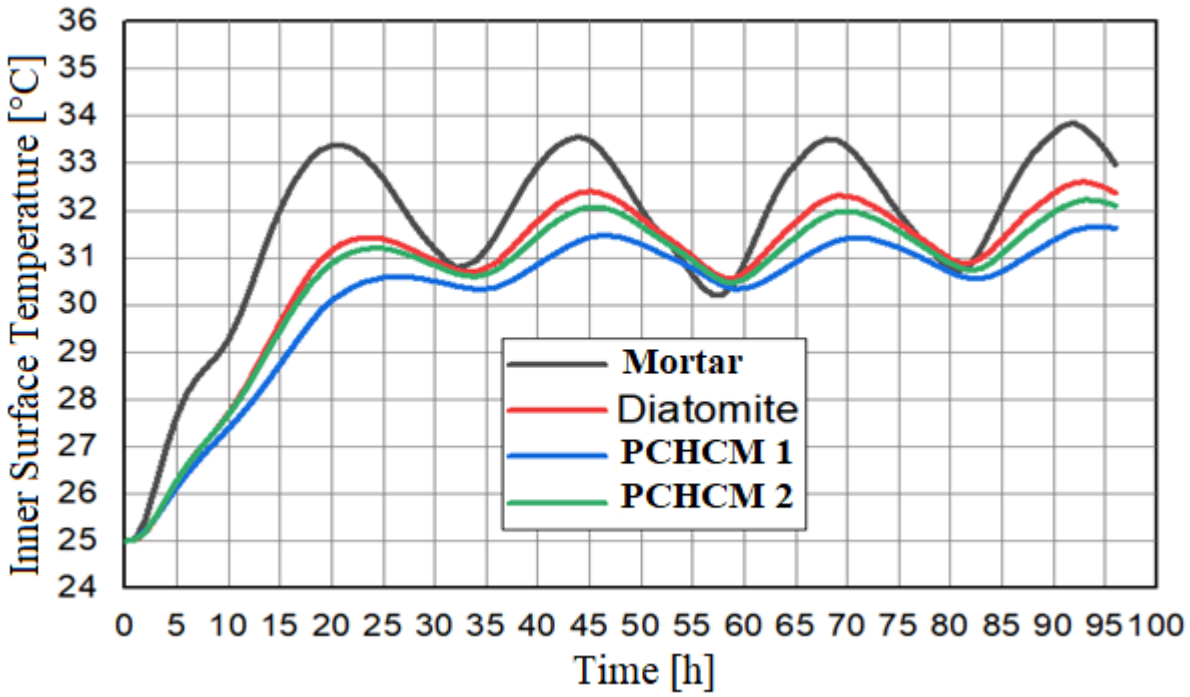

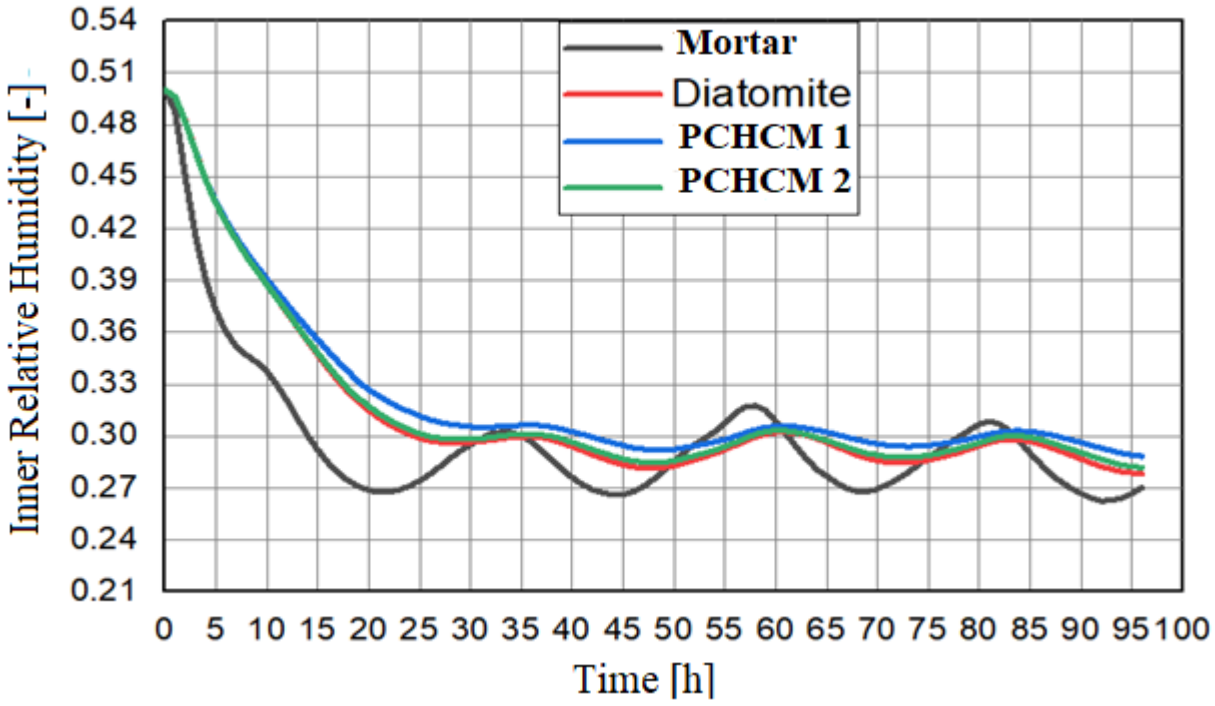

Figure IV.17 : Variation of temperature and relative humidity on the interior surface (July 1-4, 2021) in Hassi Messaoud.

Study of insulators in the winter period

In this second case, thermal performances were studied at low temperatures and moderate humidity corresponding to the winter period in the Hassi Messaoud region. Figure IV.18 shows a partial effect on the internal temperature for diatomite and PCHCM1, as the ambient temperature during this period is below 23°C, so PCM1 will not affect temperature stability. As for PCHCM2, a significant effect is observed compared to the others, as the melting temperature of PCM1 is lower than that of the ambient temperature.

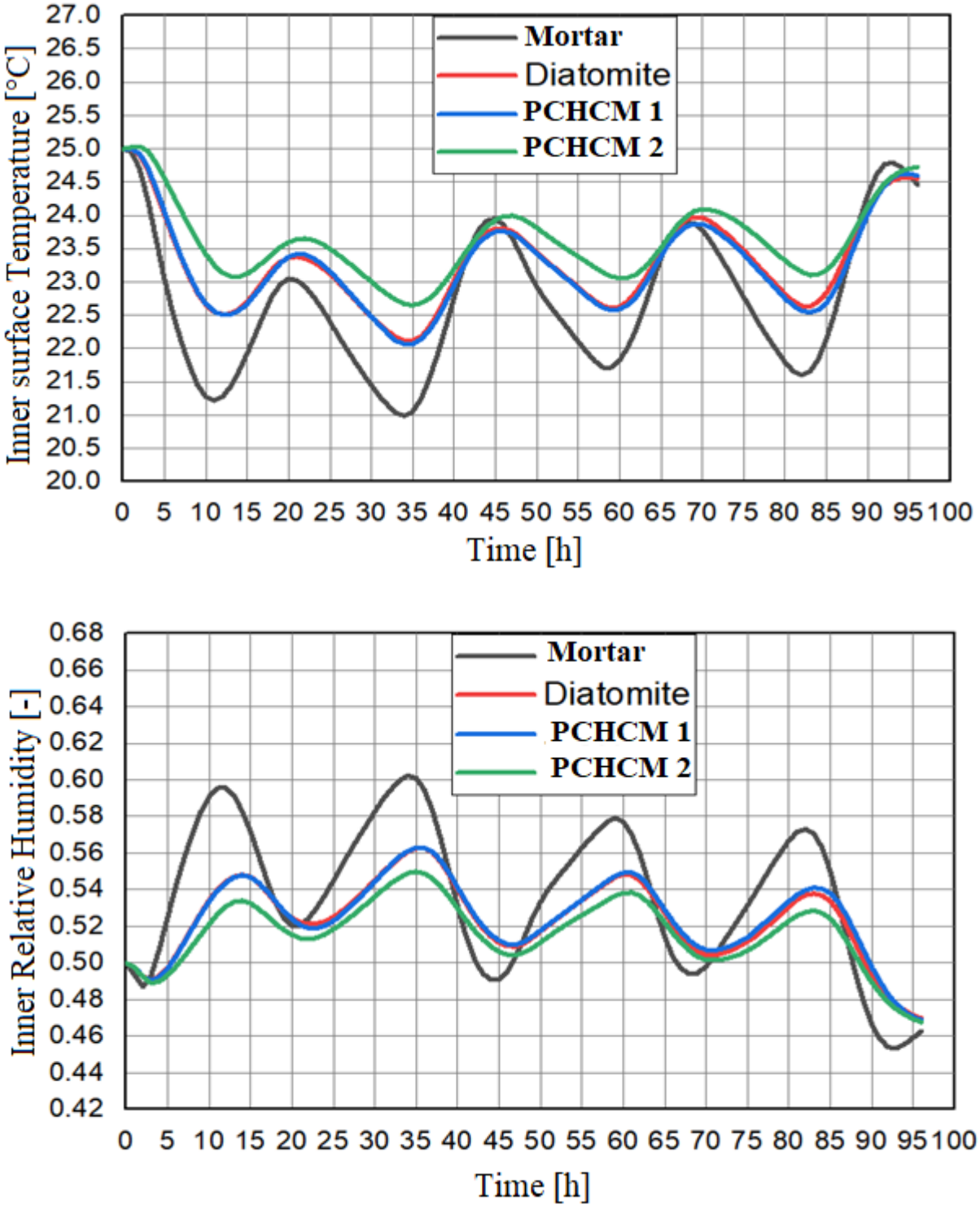

Figure IV.18 : Variation of temperature and relative humidity at the interior surface (July 1-4, 2021) in Hassi Messaoud.

IV.2.2.4 Comparison of different diatomites

We chose the climate of Hassi Messaoud to make a numerical comparison between some existing diatomites in the world (Algerian, Moroccan, Turkish and Chinese diatomites).

The numerical comparison presented in Figure IV.19 between different diatomites shows that Algerian diatomite is among the best for thermal insulation of buildings due to its low thermal conductivity and high porosity.

Study of insulators in the summer period

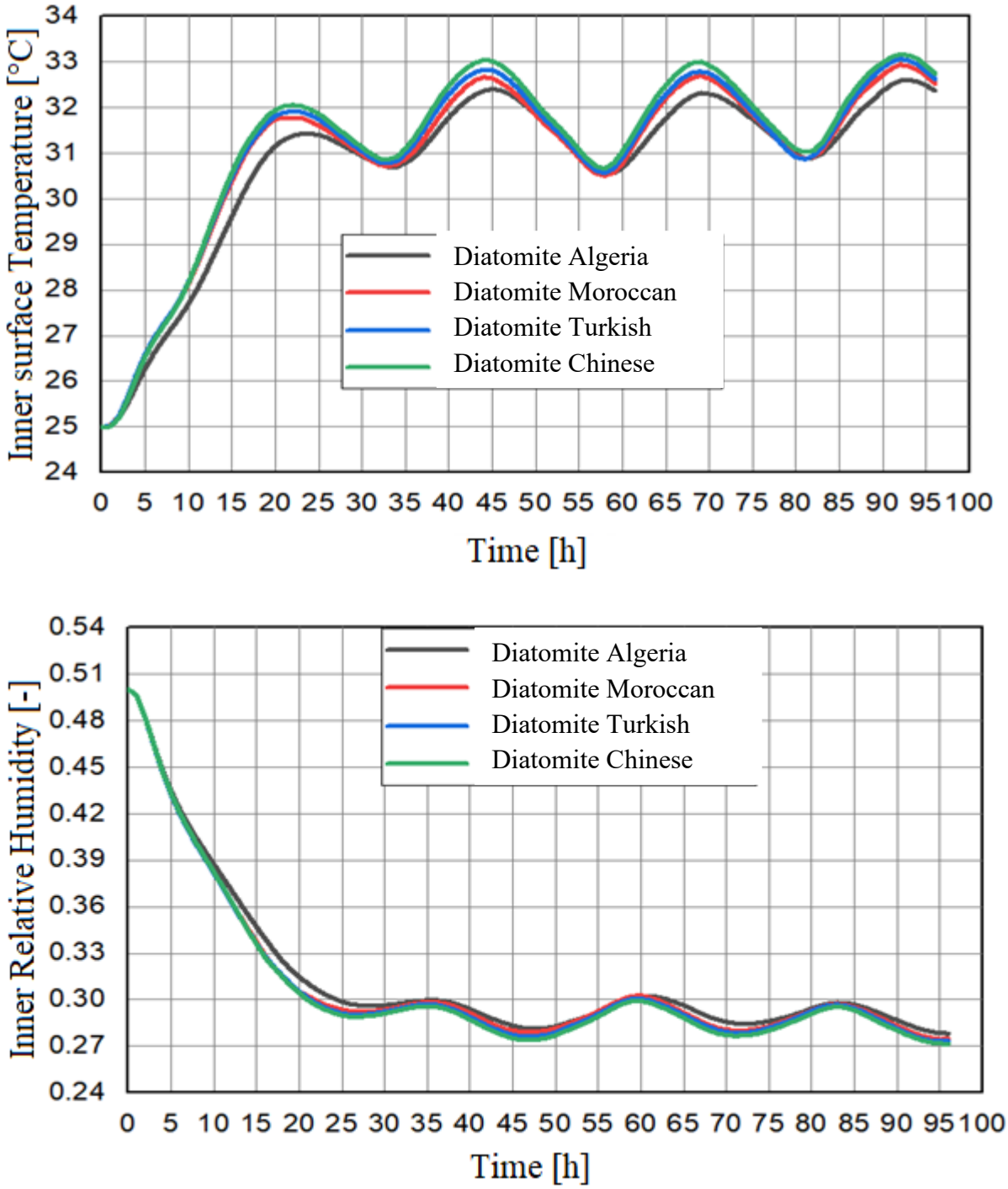

Figure IV.19: Comparison of the different diatomites in the hot season.

Study of insulators in the winter period

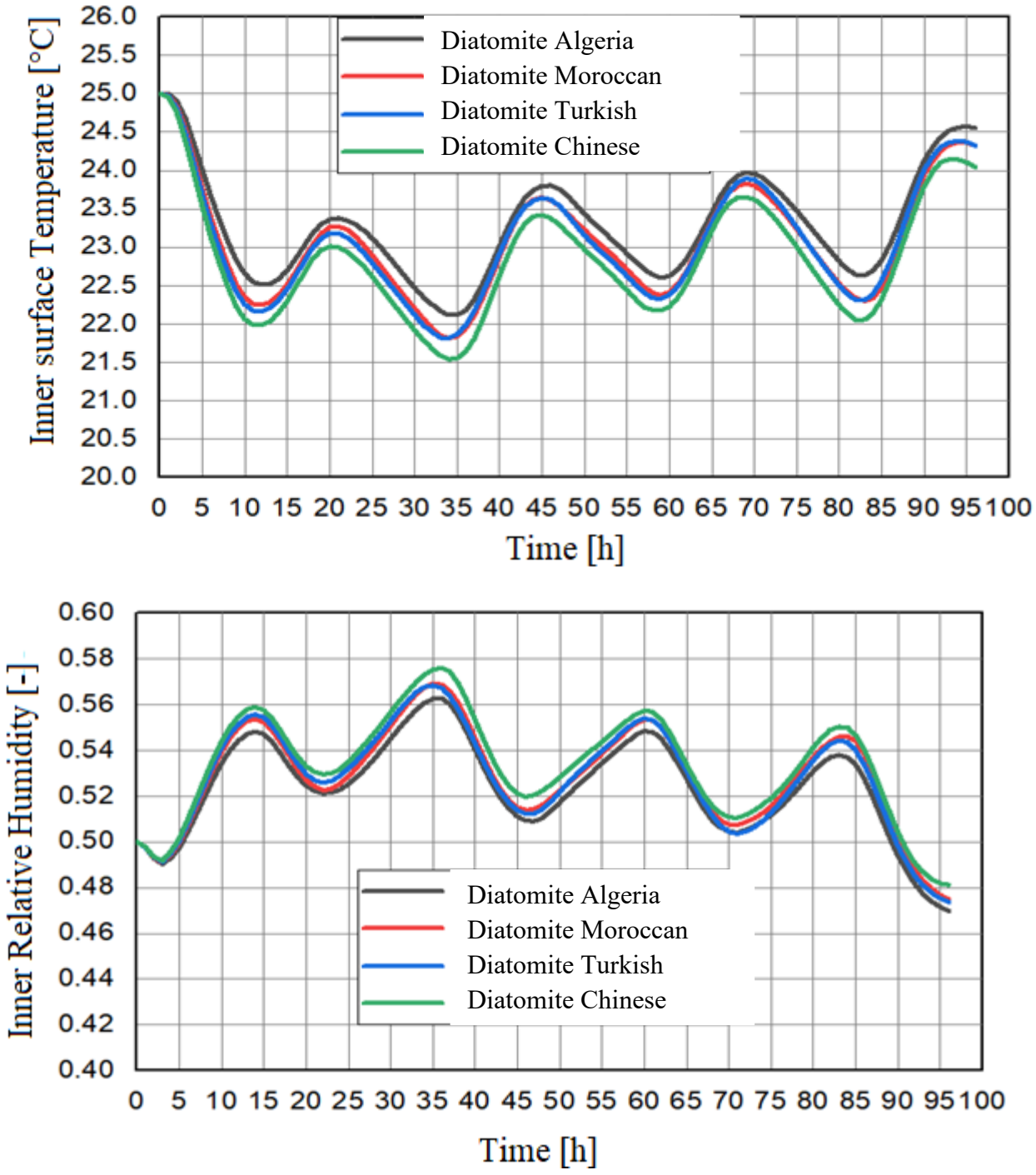

Figure IV.20: Comparison of the different diatomites in the cold season.

IV.3 Conclusion

In this chapter, we have attempted to highlight the importance of using Algerian diatomite alone and reinforced with phase change materials (PCMs) as an innovative passive material for thermal insulation of buildings in Algeria.

Firstly, the effect of replacing mortar with diatomite and then with PCHCM (a PCM with a fusion temperature of 54°C) on heat and moisture transfer was compared and analyzed. The results showed

that PCHCM has a greater ability to reduce internal temperature and relative humidity fluctuations if the ambient temperature is higher than the fusion temperature, and if the ambient temperature is lower than the fusion temperature, diatomite alone gives better results.

Next, a Comsol Multiphysics simulation program was used to extend the research. The simulation results were verified from the experiments we conducted. The results showed that the relative error did not exceed 4.6%.

Then, two Algerian provinces were studied by numerical simulation. Diatomite and PCHCM1, containing one PCM, and PCHCM2, containing two different PCMs, were used as finishing layers for the brick wall. The results showed that the use of PCHCM2 gives better results than PCHCM1 throughout the year.

Finally, we compared Algerian diatomite with some diatomite found in several other countries. The results indicated that Algerian diatomite is better than many diatomites found in the world.

General Conclusion

General conclusion

In recent years, the global population has surged, leading to a sharp increase in the demand for natural gas. This demand is driven by its diverse applications, from domestic heating to industrial processes and power generation. However, this surge presents a significant challenge as natural gas is finite and non-renewable. Continued exploitation may lead to depletion, highlighting the urgent need for alternative energy sources and conservation strategies. Amidst this backdrop, the construction sector emerges as a major energy consumer and greenhouse gas emitter. Buildings, both residential and commercial, contribute significantly to global energy consumption, mainly for heating, cooling, and lighting. Tackling energy inefficiencies in buildings is crucial for sustainable development and combating climate change impacts. Thus, this thesis aims to explore innovative approaches to reduce energy consumption in buildings, with a focus on improving thermal insulation. Traditional insulation materials, like mortar, though effective to some extent, often fall short, especially in regions with extreme weather conditions. To address this, the study investigates the potential of diatomite, a naturally occurring sedimentary rock known for its excellent insulating properties, and its reinforced variants incorporating PCM. Experimental analyses, conducted on a meticulously designed test bench, compared diatomite, mortar, and PCM (with a melting temperature set at 54°C). Results showed PCM's superior performance, especially under low relative humidity and temperatures exceeding the melting point. A numerical model, validated against experimental data, further supported these findings with negligible relative errors. A comprehensive assessment compared diatomite with two PCM variants, showing notable efficacy, particularly in areas with significant temperature fluctuations between seasons. Additionally, a comparative analysis of diatomite sources globally highlighted the exceptional quality of Algerian diatomite, positioning it as a premier choice for construction applications. The integration of diatomite with PCM variants emerged as a compelling alternative to traditional mortar, promising substantial enhancements in thermal insulation. Results demonstrated diatomite's capacity to mitigate temperature and humidity fluctuations, resulting in a commendable 22% reduction in total heat flux. Furthermore, the incorporation of PCM with dual variants yielded even more promising results, reducing total heat flux by 27% in summer and 20% in winter, making it a formidable solution for year-round insulation needs.

Moving forward, further exploration is warranted, including comprehensive mechanical studies and the manufacturing and commercialization of diatomite plates within the Algerian market. This would facilitate widespread adoption and realization of its transformative potential within the construction industry. Beyond immediate research objectives, the thesis emphasizes the importance of

interdisciplinary collaboration and knowledge exchange in driving innovation and addressing complex societal challenges.

Reference

[1] M. Economidou, V. Todeschi a,b, P. Bertoldi a et al, Review of 50 years of EU energy efficiency policies for buildings, Energy & Buildings, 225 (2020) 110322.

[2] Fraine, Y., Seladji, C., Aït-Mokhtar, A., "Effect of microencapsulation phase change material and diatomite composite filling on hygrothermal performance of sintered hollow bricks," Building and Environment, vol. 154, pp. 145–154, 2019, https://doi.org/10.1016/j.buildenv.2019.02.036.

[3] Kharchi, R., "Energy efficiency in buildings," Research and Development, 2019, https://www.cder.dz/vlib/bulletin/pdf/bulletin_028_05.pdf.

[4] Benmostefa, O.F.; Belhadi, S., "The energy audit in the building and technical-economic evaluation of energy efficiency solutions: Case of the structures of the university of Tlemcen," master's thesis, University of Abu Bekr Belkaid Tlemcen, June 2019, chapter 3, page 48, http://dspace.univ-tlemcen.dz/bitstream/112/14994/1/Ms.Gm.Benmostefa%2bBelhadi.pdf.

[5] Chen, Z., Su, D., Qin, M., Fang, G., "Preparation and characteristics of composite phase change material (CPCM) with SiO 2 and diatomite as endothermal-hydroscopic material," Energy and Buildings, vol. 86, pp. 1–6, 2015, https://dx.doi.org/10.1016/j.enbuild.2014.10.013.

[6] Ismail, R.M., Megahed, N.A., Eltarabily, S., "A conceptual framework for phase change material integration in building components," Indoor and Built Environment, 2023, https://doi.org/10.1177/1420326X231153924.

[7] Pasupathy, A., Velraj, R., Seeniraj, R.V., "Phase change material-based building architecture for thermal management in residential and commercial establishments," Renewable and Sustainable Energy Reviews, vol. 12, pp. 39–64, 2008, https://doi.org/10.1016/j.rser.2006.05.010.

[8] Zhang, Z., Ci, Z., Zhang, T., "Heat-Storage Performance Optimization for Packed Bed Using Cascaded PCMs Capsules," International Journal of Thermophysics, vol. 42, p. 72, 2021, https://doi.org/10.1007/s10765-021-02828-7.

[9] Lee, K.O., Medina, M.A., Raith, E., Sun, X., "Assessing the integration of a thin phase change material (PCM) layer in a residential building wall for heat transfer reduction and management," Applied Energy, vol. 137, pp. 699–706, 2015, https://doi.org/10.1016/j.apenergy.2014.09.003.

[10] Yu, J., Yang, Q., Ye, H., Luo, Y., Huang, J., Xu, X., et al., "Thermal performance evaluation and optimal design of building roof with outer-layer shape-stabilized PCM," Renewable Energy, vol. 145, pp. 2538-2549, 2020, https://doi.org/10.1016/j.renene.2019.08.026.

[11] Tamboli, A., Sohoni, V.S., "A study on recent advances in phase change material and its experimental assessments in masonry construction technology," Journal of Building Rehabilitation, vol. 7, p. 91, 2022, https://doi.org/10.1007/s41024-022-00229-3.

[12] Kim, T., Ahn, S., Leigh, S.-B., "Energy consumption analysis of a residential building with phase change materials under various cooling and heating conditions," Indoor and Built Environment, vol. 23, 2013, https://doi.org/10.1177/1420326X13481990.

[13] Vu, D.H., Wang, K.S., Bac, B.H., Nam, B.X., "Humidity control materials prepared from diatomite and volcanic ash," Construction and Building Materials, vol. 38, pp. 1066–1072, 2013, https://doi.org/10.1016/j.conbuildmat.2012.09.040.

[14] Trabelsi, A., Belarbi, R., Turcry, P., Aït-Mokhtar, A., "Water vapour desorption variability of in situ concrete and effects on drying simulations," Magazine of Concrete Research, vol. 63, no. 5, pp. 333–342, 2011, https://doi.org/10.1680/macr.9.00161.

[15] Yang, M., Kong, F., He, X., "Moisture buffering effect of hygroscopic materials under wall moisture transfer," Indoor and Built Environment, vol. 31, 2020, https://doi.org/10.1177/1420326X20975835.

[16] Zhou, B., Chen, Z., "Experimental study on the hygrothermal performance of zeolite-based humidity control building materials," International Journal of Heat and Technology, vol. 34, no. 3, pp. 407–414, 2016, https://doi.org/10.18280/ijht.340309.

[17] Zheng, J., Shi, J., Ma, Q., Dai, X., Chen, Z., "Experimental study on humidity control performance of diatomite-based building materials," Applied Thermal Engineering, vol. 114, pp. 450–456, 2017, https://doi.org/10.1016/j.applthermaleng.2016.11.203.

[18] Bouguerra, A., Amiri, O., Aït-Mokhtar, A., Diop, M.B., "Water sorptivity and pore structure of wood-cementitious composites," Magazine of Concrete Research, vol. 54, no. 2, pp. 103–112, 2002, https://doi.org/10.1680/macr.2002.54.2.103.

[19] S. Karaman, A. Karaipekli, A. Sari, A. Biçer, Polyethylene glycol (PEG)/diatomite composite as a novel form-stable phase change material for thermal energy storage, Solar Energy Materials and Solar Cells. 95 (2011) 1647–1653.

[20] J.L. Shang, Z.F. Zong, H. Zhang, Synthesis and analysis of new humidity-controlling composite materials, International Journal of Minerals, Metallurgy, and Materials. 24 (5) (2017) 594.

[21] M. Qin, Z. Chen, Synthesis and characteristics of composite phase change humidity control materials, Energy Procedia. 139 (2017) 493–498.

[22] Z. Wu, M. Qin, Z. Chen, Phase change humidity control material and its application in buildings, Procedia Engineering. 205 (2017) 1011–1018.

[23] M. Hasan, T. Saidi, M. Jamil, M. F. Fadillah; The resistance of high strength concrete with diatomaceous earth exposed to high temperatures. AIP Conf. Proc. 30 January 2023; 2613 (1): 030002. https://doi.org/10.1063/5.0119356

[24] M. Abdel Wahab, I. Abdel Latif, M. Kohail, A. Almasry, The use of Wollastonite to enhance the mechanical properties of mortar mixes, Construct. Build. Mater. 152 (2017) 304–309. https://doi.org/10.1016/j.conbuildmat.2017.07.005

[25] A. Ergün, Effects of the usage of diatomite and waste marble powder as partial replacement of cement on the mechanical properties of concrete, Construction and Building Materials (25) 2011, 806-812, https://doi.org/10.1016/j.conbuildmat.2010.07.002

[26] Hamidi, Y., Aketouane, Z., Malha, M., Bruneau, D., Bah, A., Goiffon, R., Integrating PCM into hollow brick walls: toward energy conservation in Mediterranean regions, Energy and Buildings 248 (2021) 111214, https://doi.org/10.1016/j.enbuild.2021.111214.

[27] Abbas, H.M., Jalil, J.M., Ahmed, S.T., Experimental and numerical investigation of PCM capsules as insulation materials inserted into a hollow brick wall, Energy and Buildings 246 (2021), 111127, https://doi.org/10.1016/j.enbuild.2021.111127.

[28] MY. Ferroukhi, Modelling of thermo-hydro-aerodynamic transfers in building envelopes: assessment of disorders caused by humidity. PhD thesis in civil engineering, University of La Rochelle. NNT: 2015LAROS027, 2015.

[29] H. Hens, Final report, volume 1: Task 1: Modelling, IEA Annex 24 Hamtie, 1996.

[30] Y. Fraine, Study and analysis of heat and moisture transfer with phase change in porous building materials, PhD thesis in mechanical engineering, University of Tlemcen. 2020.

[31] National energy balance, 2018, http://www.energy.gov.dz

[32] Rousseau, M.. (2003). Heat, Air and Moisture Strategies for Managing Condensation in Walls. Natl. Res. Counc. Can. NRCC-46734

[33] Julien Berger. Contribution to hygrothermal modeling of buildings: application of model reduction methods. Civil engineering. University of Grenoble, 2014. French. ffNNT: 2014GRENA028ff.

[34] Fares BENNAI, Study of the mechanisms of coupled heat and humidity transfers in porous construction materials in the unsaturated regime, doctoral thesis in civil engineering, University of Rochelle and University of A. Mira de Bejaia. 2017.

[35] Kunzel, H.M., Simultaneous Heat and Moisture Transport in Building Components. One- and Two Dimensional Calculation Using Simple Parameters, Dissertation university Stuttgart, Germany, 1995 (ISBN 3-8167-4103-7).

[36] Philip, J., and De Vries, D. (1957). Moisture movement in porous material under temperature gradients. Trans. Am. Geophys. Union 2, 222–232.

[37] Jerman, M., and Černý, R. (2012). Effect of moisture content on heat and moisture transport and storage properties of thermal insulation materials. Energy and Buildings. 53, 39–46.

[38] E. Sanchez-Palencia, Einstein-like approximation for homogenization with small concentration. I–elliptic problems. Nonlinear Analysis, Theory, Methods and Applications, 1985, 9, 1243–1254.

[39] C. Moyne, M. Murad, A two-scale model for coupled electro-chemo-mechanical phenomena and onsager's reciprocity relations in expansive clays : I homogenization analysis. Transport in Porous Media, 2006, 62, 333–380.

[40] T. Lemaire, C. Moyne, D. Stemmelen, Modelling of electro-osmosis in clayey materials including pH effects. Physics and Chemistry of the Earth, Parts A/B/C, 2007, 32, 441–452.

[41] W. Mchirgui, Modeling of water transfers in partially saturated porous media by periodic homogenization - Application to cementitious materials, doctoral thesis in civil engineering, University of Rochelle, 2012.

[42] Bouddour, A., Auriault, J.., and Mhamdi-Alaoui, M. (1998). Heat and mass transfer in wet porous media in presence of evaporation-condensation. International Journal of Heat and Mass Transfer. 41, 2263–2277.

[43] Lewandowska, J., and Laurent, J. (2001). Homogenization modelling and parametric study of moisture transfer in an unsaturated heteregeneous porous medium. Transport Porous Media 45, 321–345.

[44] S. Maghous, Z. Saada, L. Dormieux, J. Canou, JC. Dupla, A model for in situ grouting with account for particle filtration. Computers and Geotechnics, 2007, 34, 164–174.

[45] J. Sanahuja, L. Dormieux, G, Chanvillard, Modelling elasticity of a hydrating cement paste. Cement and Concrete Research, 2007, 37, 1427–1439.

[46] Q. Zhu, D. Kondo, J. Shao, Homogenization-based analysis of anisotropic damage in brittle materials with unilateral effect and interactions between microcracks. International journal for numerical and analytical methods in geomechanics, 2009, 33, 749–772.

[47] Luikov, A.V. (1966). Heat and mass transfer in capillary porous bodies. Pergamon Lond.

[48] CR. Pedersen, Prediction of moisture transfer in building constructions. Building and Environment, 1992, 3, pp. 387–397.

[49] H. Janssen, B. Blocken, J. Carmeliet, Conservative modelling of the moisture and heat transfer in building components under atmospheric excitation. Heat and Mass Transfer, 2007a, 50, 1128–1140.

[50] VP. De Freitas, V. Abrantes, P. Crausse, Moisture migration in building walls— Analysis of the interface phenomena. Building and Environment, 1996, 31, 99–108.

[51] M. Qin, R. Belarbi, A. Aït-Mokhtar, LO. Nilsson, Coupled heat and moisture transfer in multi-layer building materials. Construction and Building Materials, 2009a, 967– 975.

[52] Y. Ait Oumeziane, Evaluation of the hygrothermal performances of a wall by digital simulation: application to hemp concrete walls, Doctoral thesis, INSA DE Rennes, 2013.

[53] F. Tariku, K. Kumaran, P. Pazio, Transient model for coupled heat, air and moisture transfer through multilayered porous media. International Journal of Heat and Mass Transfer, 2010a, 53, 3035–3044.

[54] R. Prommas, Theoretical and experimental study of heat and mass transfer mechanism during convective drying of multi-layered porous packed bed. International Communications in Heat and Mass Transfer, 2011, 38, 900 905.

[55] I. Dincer, M.A. Rosen, Cold storage by latent heat. Ed. Technical Engineer, 2002

[56] Souad Khedache, development of new composites for improving the thermal inertia of construction materials, doctoral thesis in Mechanical, Structural and Energy Engineering, Mouloud Mammeri University of Tizi-Ouzou.

[57] A. Abhat, "Low temperature latent heat thermal energy storage: Heat storage materials", Sol. Energy, vol. 30, no. 4, pp. 313-332, 1983.

[58] Sharma Someshower Dutt, Kitano Hiroaki, Sagara Kazunobu, « Phase Change Materials for Low Temperature Solar Thermal Applications », Res. Rep. Fac. Eng. Mie Univ., Vol. 29, pp : 31-64, 2004.

[59] Wang, X., Zhang, Y., Xiao, W. et al. Review on thermal performance of phase change energy storage building envelope. Chin. Sci. Bull. 54, 920–928 (2009). https://doi.org/10.1007/s11434-009-0120-8

[60] D. Feldman, D. Banu, D. Hawes, and E. Ghanbari, “Obtaining an energy storing building material by direct incorporation of an organic phase change material in gypsum wallboard,” Solar Energy Materials, vol. 22, no. 2, pp. 231–242, Jul. 1991.

[61] T.-C. Ling and C.-S. Poon, “Use of phase change materials for thermal energy storage in concrete: An overview,” Construction and Building Materials, vol. 46, pp. 55–62, Sep. 2013.

[62] T. Lee, D. W. Hawes, D. Banu, and D. Feldman, “Control aspects of latent heat storage and recovery in concrete,” Solar Energy Materials and Solar Cells, vol. 62, no. 3, pp. 217–237, May 2000.

[63] D. W. Hawes, D. Banu, and D. Feldman, “Latent heat storage in concrete,” Solar Energy Materials, vol. 19, no. 3, pp. 335–348, Nov. 1989.

[64] D. Zhang, J. Zhou, K. Wu, “Study of phase-changing energy storage composite material and its power peak regulation function,” pp. 27–30, 2003.

[65] L. F. Cabeza, A. Castell, C. Barreneche, A. de Gracia, and A. I. Fernández, “Materials used as PCM in thermal energy storage in buildings: A review,” Renewable and Sustainable Energy Reviews, vol. 15, no. 3, pp. 1675–1695, Apr. 2011.

[66] Zhengxuan Liu, Zhun (Jerry) Yu, Tingting Yang, Di Qin, Shuisheng Li, Guoqiang Zhang, Fariborz Haghighat, Mahmood Mastani Joybari, A review on macro-encapsulated phase change

material for building envelope applications, Building and Environment, Volume 144, 2018, https://doi.org/10.1016/j.buildenv.2018.08.030.

[67] A. Marani, Moncef L. Nehd. Integrating phase change materials in construction materials: Critical review. Construction and Building Materials, 217 (2019) 36-49.

[68] H. MERADI et al., Caractérisation de diatomite d'origine Algérienne pour l'isolation thermique, IC-WNDT-MI'14, Annaba, novembre 2014.

[69] R. Amri; Influence of heat treatment time on the different properties of kieselguhr used in filtration; Master's thesis, department of metallurgy and materials engineering, University of Annaba, 2004.

[70] H. Meradi, LH. Atout, A. Balaska, The valorization of natural resources: case of diatomite from the DE SIG region, 3rd international conference on welding, NDT and the materials and alloys industry (IC-WNDT-MI'12) Oran du 26 -28 Nov 2012.

[71] J. Zheng, J. Shi, Q. Ma, X. Dai, Z. Chen, Experimental study on humidity control performance of diatomite-based building materials, Applied Thermal Engineering 114 (2017) 450–456

[72] B. Hamdi and S. Hamdi, Thermal Properties of Algerian Diatomite, Study of the Possibility to Its Use in the Thermal Insulation, International Congress on Energy Efficiency and Energy Related Materials (ENEFM2013), Proceedings, Antalya, Turkey, 9-12 October 2013.

[73] SAFA MESSEAOUDA, Study of the retention and elimination capacity of metal cations by natural adsorbents, doctoral thesis, Specialty: Natural and Life Sciences, Mascara, 2015.

[74] Frederic L. and Kadey J.R. (1983). Industrial Minerals and Rocks. American Institute of Mining, Metallurgical and Petroleum Engineers, New York.

[75] Aruntas H.Y., Albayrak M. and Tokyay H.A. (1998). Investigation of diatomite properties from Ankara-Kizilcahamam and Cankiri-Cerkes regions. Turk. J. Eng. Environ. Sci., 22: 337-343.

[76] Arik H. (2003). Synthesis of Si N by the carbo-thermal reduction and nitridation of diatomite. 3 4 J. Eur. Ceramic Soc., 23: 2005-2014.

[77] Ladda M., Atthawan B. and Cherdsak U. (2008). The use of diatomite to remove color and turbidity in sugar industry. Kasetsart J. (Nat. Sci.) 42 : 107 – 116.

[78] Van Buren J. P. (1984). Hue in bottied apple juice. in: AppZe Juice Worhhop. Downing, D.L. Ed. Special Report New York State Agriculturai Experiment Station, Geneva, New York, USA, 54: 18- 24

[79] Abrantes F., Lopes C., Mix A. and Pisias N. (2007). Diatoms in Southeast Pacific surface sediments reflect environmental properties. Quaternary Sci. Rev., 26: 155- 169

[80] Vizinet J., De Reviers (1995). The uses of diatoms. Life and Environment. Communication at the 3rd conference of the Association of French-speaking Diatomists, Banyuls, Sept. 1994

[81] Stoermer E.F. et Smol J.P.(1999). The diatoms: applications for the environmental and earth sciences." Cambridge Univ. Press, pp. 469.

[82] Gueho E., Pesando D. and Barelli M. (1977). Antifungal properties of a diatomite Chaetoceros lauderiralfs, Journal of Mycopathologia, Springer, V60, pp.105-107.

[83] Ludes B., Coste M. (1996). Diatoms and forensic medicine. International Medical Editions. Tec & Doc, Lavoisier and EM Inter, Cachan, 258 p.

[84] Druart J.C., Kofman S. and Malicier D. (1997). The pig, a model for the study of diatoms in the diagnosis of human drowning: first results. Symposium of the Assoc. French-speaking Diatomists, V18(1), pp. 82-83, Strasbourg.

[85] Vizinet J., De Reviers (1995). The uses of diatoms. Life and Environment. Communication at the 3rd conference of the Association of French-speaking Diatomists, Banyuls, Sept. 1994.

[86] https://www.rsrefractorygroup.com/diatomite-insulation-brick/ 02/09/2022.

[87] https://www.etsy.com/fr/listing/1118829258/misona-diatomite-tapis-de-bain?ga_order=most_relevant&ga_search_type=all&ga_view_type=gallery&ga_search_query=diatomite&ref=sr_gallery-1-3&pro=1 02/09/2022.

[88] https://www.pool-and-co.fr/produit/acti-diatomite-5kg/ 02/09/2022.

[89] https://www.biotanic-culture.com/insecticide-fongicide/615-diatomite-terre-de-diatomee-500gr.html 02/09/2022.

[90] O.HADJADJ-AOUL, "Study of chromatographic column support based on local Algerian materials" State Doctorate Thesis, ENP, 2000.

[91] S. Benayache, S. Alleg, A. Mebrek, J. J. Suñol, Thermal and microstructural properties of paraffin/diatomite composite, Vacuum 157 (2018) 136–144.

[92] J. Zheng, J. Shi, Q. Ma, X. Dai, Z. Chen, Experimental study on humidity control performance of diatomite-based building materials, Applied Thermal Engineering 114 (2017) 450–456

[93] Thermal camera for professionals, https://www.pei-france.com/uploads/tx_etim/Doc_testo_890_2012_FR.pdf.

[94] M. Qin, A. Aït-Mokhtar, R. Belarbi, Two-dimensional hygrothermal transfer in porous building materials, Applied Thermal Engineering, 30 (2010) 2555-2562.

[95] TZ. Desta, J. Langmans, S. Roels, et al, Experimental data set for validation of heat, air and moisture transport models of building envelopes, Building and Environment, 46 (2011) 1038-1046.

[96] K. Abahri, R. Belarbi, A. Trabelsi, Contribution to analytical and numerical study of combined heat and moisture transfers in porous building materials, Building and Environment, 46 (2011) pp1354-1360.

[97] DH. Xu, MB. Ge, HL. Zhang, Numerical solution of a dynamic model of heat and moisture transfer in porous fabric under low temperature, International Journal of Heat and Mass Transfer, 61(2013) pp149-157.

[98] LO. Nilsson, Moisture mechanics in building materials and building components, PhD course, Lund Institute of Technology, Sweden, 2003.

[99] Crausse, P., Laurent, J., & Perrin, B. (1996). Influence of hysteresis phenomena on the water properties of porous materials. Revue Générale de Thermique, 35(410), 95–106. https://doi.org/10.1016/s0035-3159(96)80002-x

[100] F.P. Incropera, D.P. DeWitt, T.L. Bergman et A. S. Lavine, Fundamentals of Heat and Mass Transfer, chapitre 9 : Free Convection, page 571, John Wiley & Sons, 2006.

[101] AIN. Korti, Numerical heat flux simulations on double-pass solar collector with PCM spheres media, International Journal of Air-Conditioning and Refrigeration 24 (2) (2016) 13.

[102] Schwarz, B.: Die Wärme- und Stoffüber-tragung an Außenwandoberflächen (Heat and material transfer in outdoor wall surfaces). Diss. Universität Stuttgart 1971.

[103] Technical sheet of the Algerian diatom (the city of sig) October 2008.

[104] B. Hamdi and S. Hamdi, Thermal properties of Algerian diatomite, study of the possibility of its use in thermal insulation, International Congress on Energy Efficiency and Energy Related Materials (ENEFM2013) pp 27–32 .

[105] E. Sassine, Z. Younsi, Y. Cherif, E. Antczak, Frequency domain regression method for predicting the thermal behavior of brick walls of existing buildings, Applied Thermal Engineering (2016).

[106] Sharma Someshower Dutt, Kitano Hiroaki, Sagara Kazunobu, “Phase Change Materials for Low Temperature Solar Thermal Applications,” Res. Rep. Fac. Eng. Mie Univ., Vol. 29, pp: 31-64, 2004.

[107] W. Dongxia, R. Mourad, E. Mohammed, D. Rabah, B.Rachid, L. Bin, “Experimental investigation into the hygrothermal behavior of a new multilayer building envelope integrating PCM with a biosourced material” , building and Environment Volume 201, August 15, 2021, 107995.

[108] B. Hamdi and S. Hamdi, Thermal properties of Algerian diatomite, study of the possibility of its use in thermal insulation, International Congress on Energy Efficiency and Energy-related Materials (ENEFM2013) pp 27–32.

[109] Mathieu Bendouma. External thermal insulation systems: experimental and numerical studies of heat and humidity transfers. Thermal [physics.class-ph]. University of South Brittany, 2018. French.

[110] https://www.infoclimat.fr/observations-meteo/archives/1er/juillet/2021/hassi-messaoud/60581.html

[111] A.Y.T. LEUNG, ZHU BIN, JIANJIN ZHENG, HAO YANG « Analytic trapezoidal Fourier p-element for vibrating plane problems »Journal of Sound and Vibration. City University of Hong Kong, Tatchee Avenue, HKSAR, China, (2003).

[112] Y.S.CHOO, N.C.BYUNG, C.LEE « Quadrilateral and triangular plane elements with rotational degrees of freedom based on the hybrid Trefftz method »Korea Advanced Institute of Science and Technology, Korea,(2006).

[113] A.HOUMAT .Article « Free vibration analysis of arbitrarily shaped membranes using the trigonometric p-version of the finite-element method » Faculty of Engineering, University of Tlemcen, B.P. 230, Tlemcen 13000, Algeria(2006)

[114] KUTLU DARILMAZ et DE NAHIT KUMBASAR. « An 8-node assumed stress hybrid element for analysis of shells » Department of Civil Engineering, Istanbul Technical University, 34469 Maslak, Istanbul, Turkey, 2006.

[115] N. NGUYEN-THANHA, TIMON RABCZUKA, H. NGUYEN-XUANBE, STÉPHANE PA BORDASC, D. « An alternative alpha finite element method (AαFEM) for free and forced structural vibration using triangular meshes »Journal of Computational and Applied Mathematics 2009.